

**Prediction of Mean Flow Data  
for Adiabatic 2-D Compressible  
Turbulent Boundary Layers**

*F. Motallebi*





706273

# Prediction of Mean Flow Data for Adiabatic 2-D Compressible Turbulent Boundary Layers

Bibliotheek TU Delft



C 3021884

2392  
341  
6

# Series 01: Aerodynamics

01



# **Prediction of Mean Flow Data for Adiabatic 2-D Compressible Turbulent Boundary Layers**

*F. Motallebi*



Delft University Press / 1997

*Published and distributed by:*

Delft University Press  
Mekelweg 4  
2628 CD Delft  
The Netherlands  
Telephone +31 (0)15 278 32 54  
Fax +31 (0)15 278 16 61  
e-mail: DUP@DUP.TUDelft.NL

*by order of:*

Faculty of Aerospace Engineering  
Delft University of Technology  
Kluyverweg 1  
P.O. Box 5058  
2600 GB Delft  
The Netherlands  
Telephone +31 (0)15 278 14 55  
Fax +31 (0)15 278 18 22  
e-mail: Secretariaat@LR.TUDelft.NL  
website: <http://www.lr.tudelft.nl/>



*Cover: Aerospace Design Studio, 66.5 x 45.5 cm, by:  
Fer Hakkaart, Dullenbakkersteeg 3, 2312 HP Leiden, The Netherlands  
Tel. +31 (0)71 512 67 25*

90-407-1564-5

Copyright © 1997 by Faculty of Aerospace Engineering

All rights reserved.

No part of the material protected by this copyright notice may be reproduced or utilized in any form or by any means, electronic or mechanical, including photocopying, recording or by any information storage and retrieval system, without written permission from the publisher: Delft University Press.

Printed in The Netherlands

## CONTENT

Nomenclature	1
1. Abstract	3
2. Introduction	4
2.1 The Mean Velocity Profile	4
2.2 The Integral Length Scale $\Delta^+$	5
3. Skin Friction and Velocity Algorithm	6
4. Discussion and Comparison with Experimental Data	7
4.1 Subsonic Data	7
4.2 Transonic and Low Supersonic Data	8
4.3 High Supersonic Data	9
4.4 Boundary Layer Shape Parameter	10
5. Concluding Remarks	11
6. References	12
Tables	14
Figures	



### Nomenclature

$\alpha$	= parameter in van Driest transformation, Eq. 3-1
$A^+$	= damping factor, Eq. 5
$b$	= parameter in van Driest transformation, Eq. 3-2
$c$	= intercept for law of the wall ( $=5.1$ )
$C_f$	= skin friction coefficient , $2\tau_w/\rho_\infty u_\infty^2$
$H$	= shape parameter, $\delta^+/\theta$
$k$	= slope for law of the wall ( $=0.41$ )
$M$	= Mach number
$r$	= temperature recovery factor ( $=0.89$ )
$Re_\Delta$	= Reynolds number based on integral length scale $\Delta^+, u_\tau \Delta^+ / v_w$
$Re_\theta$	= momentum thickness Reynolds number based on the boundary layer edge condition , $u_\infty \rho_\infty \theta / \mu_\infty$
$Re_{\theta w}$	= momentum thickness Reynolds number , $u_\infty \rho_\infty \theta / \mu_w$
$T$	= temperature
$u$	= streamwise velocity
$u^+$	$= u^+ / u_\tau$
$u_\tau$	= friction velocity, $\sqrt{\tau_w / \rho_w}$
$w(y/\delta)$	= wake function, $1 - \cos[\pi(y/\delta)]$
$y$	= coordinate normal to the streamwise direction
$y^+$	$= y u_\tau / v_w$
$Z_1$	$= Re_\theta / 425 - 1$ , Eq. 4-1
$\gamma$	= ratio of specific heats ( $=1.4$ for air)
$\delta$	= boundary layer thickness
$\Delta C_f$	= percent error in skin friction coefficient, $(1 - C_{f,cal} / C_{f,exp}) \times 100$
$\Delta H$	= percent error in shape parameter, $(1 - H_{cal} / H_{exp}) \times 100$

$\delta^*$	= boundary layer displacement thickness
$\Delta^*$	= integral length scale, i.e. area beneath turbulent defect law plot, $\delta \int_0^1 [(u_\delta^* - u^*) / u_\tau] d(y/\delta)$
$\theta$	= boundary layer momentum thickness
$\mu$	= absolute viscosity
$\nu$	= kinematic viscosity
$\pi$	= pi number
$\Pi$	= wake parameter, see Eq.4
$\rho$	= density
$\tau$	= local shear stress
$\eta$	= $y/\delta$

#### Subscripts and Superscripts

$cal$	=calculated
$exp$	= experimental
$ir$	=inner region of a turbulent boundary layer
$w$	= wall or evaluated based on wall parameters
$\delta$	= boundary layer edge
*	= transformed condition

## 1. Abstract

The report presents an algorithm for the prediction of mean flow data (i.e. skin friction, velocity profile and shape parameter) for adiabatic two-dimensional compressible turbulent boundary layers at zero pressure gradient. The transformed law of the wall, law of the wake, the van Driest model for the complete inner region and a correlation between the Reynolds number based on the boundary layer integral length scale ( $Re_{\Delta}$ ) and the Reynolds number based on the boundary layer momentum thickness ( $Re_{\theta w}$ ) were used to predict the skin friction coefficient, velocity profile and the shape parameter of the boundary layer. In most cases, for subsonic flows with  $Re_{\theta}$  less than about  $1.6 \times 10^5$ , and for transonic-low supersonic flows, the present method provides better results for the prediction of skin friction coefficient than that of Huang et al. At high supersonic flows, both methods are less accurate in the prediction of skin friction coefficient, and no preference can be given to either methods. In addition, regardless to the flow Mach number, the calculation of percent error in the prediction of skin friction coefficient by both methods, shows no significant dependence on  $Re_{\theta}$ . It has been also shown that while the present method and that of Huang et al satisfactorily predict the velocity profile for subsonic flows (i.e.  $M_{\delta} < 1.0$ ) with no apparent Reynolds number effect, their accuracy at transonic and supersonic speeds is Reynolds number dependent. This suggests that at least for high speed flows the expression used for the transformed mean velocity profile (i.e. Coles and van Driest formulations) does not sufficiently represent all the physical aspects of the mean flow distribution in a turbulent boundary layer. Extra information or perhaps a better physical approach to the formulation of the mean structure of compressible turbulent boundary layers even when they are formed under zero pressure gradient and in a adiabatic thermal condition, is required in order to achieve complete (physical and mathematical) convergence when it is applied in any prediction method. Also it is shown that for a given flow Mach number the percent error in the prediction of shape parameter depends on the expression by which the mean velocity profile is defined and as expected is not sensitive to the Reynolds number based on momentum thickness of the boundary layer.

## 2. Introduction

### 2.1 The Mean Velocity Profile

Prandtl<sup>1</sup> proposed that for incompressible turbulent boundary layer flows over smooth surfaces, the velocity profile outside the viscous sub-layer and in the logarithmic region can be described by the so called law of the wall correlation :

$$\frac{u}{u_\tau} = \frac{1}{k} \ln \frac{yu_\tau}{\nu_w} + c \quad (1)$$

Although this correlation was developed from incompressible experiments, Fernholz and Finley<sup>2</sup> suggested that they are applicable to compressible flows provided that the density variation through the boundary layer is taken into account and among the available techniques the van Driest<sup>3,4</sup> method has been shown to give the best agreement with the well known incompressible expressions over a wide range of Mach and Reynolds numbers on both adiabatic and cooled walls. Using the form of van Driest transformation and incorporating the concept of temperature recovery factor  $r$ , the combined wall-wake formulation of the mean transformed velocity profile (i.e. outside the laminar sub-layer) is given by<sup>5,6</sup> :

$$\frac{u^*}{u_\tau} = \frac{1}{k} \ln \frac{yu_\tau}{\nu_w} + c + 2 \frac{\Pi}{k} \sin^2 \left( \eta \frac{\pi}{2} \right) \quad (2)$$

where :

$$u^* = \frac{u_b}{b} \sin^{-1} \left[ \frac{2b^2 \left( \frac{u}{u_b} \right) - \alpha}{(\alpha^2 + 4b^2)^{\frac{1}{2}}} \right] \quad (3)$$

in which :

$$\alpha = \frac{T_b}{T_w} \left( 1 + r \frac{\gamma - 1}{2} M_b^2 \right) - 1 \quad (3-1)$$

$$b^2 = r \frac{\gamma - 1}{2} M_b^2 \frac{T_b}{T_w} \quad (3-2)$$

$\Pi$  is the wake parameter which can be calculated from the following equation as suggested by Cebeci and Smith<sup>7</sup> :

$$\Pi = 0.55 [ 1 - \exp(-0.243 z_1^{0.5} - 0.298 z_1) ] \quad (4)$$

in which:

$$z_1 = Re_b / 425 - 1 \quad (4-1)$$

The two constants of the law of the wall were taken as  $k = 0.41$  and  $c = 5.1^6$ . The exclusion of viscous sub-layer in Eq.2 cannot have a serious implication for subsonic turbulent boundary layers but may cause problems when dealing with high speed turbulent boundary layers<sup>8</sup> as it can occupy a substantial portion of the boundary thickness. For this reason any mean velocity profile formulation for high speed turbulent boundary layers should include the viscous sub-layer. However as it will be shown later for high Reynolds flows and regardless of the flow Mach number any model for the mean velocity profile of turbulent boundary layers should include the viscous sub-layer. Such a model for the complete inner region (i.e. viscous sub-layer plus log-region) is due to van Driest<sup>9</sup>:

$$\left(\frac{u^*}{u_\tau}\right)_{ir} = \int_0^{y^*} \frac{2}{1 + \sqrt{1 + 4k^2(y^*)^2[1 - \exp(-y^*/A^*)]^2}} dy^* \quad (5)$$

which can be numerically solved with  $u^*(0) = 0$  for  $u^*(y^*)$ , where  $A^*$  is a damping factor. van Driest<sup>9</sup> tried various values and found that  $A^* = 26$  with  $k = 0.4$  produces an excellent representation of his experimental data. However in this paper  $A^* = 25.3$  as recommended by Huang et al<sup>8</sup> has been used (with  $k = 0.41$  and  $c = 5.1$ ). Therefore the mean velocity profile across the total thickness of the boundary layer can be given by:

$$\frac{u^*}{u_\tau} = \left(\frac{u^*}{u_\tau}\right)_{ir} + \frac{\Pi}{k} w\left(\frac{y}{\delta}\right) \quad (6)$$

## 2.2 The Integral Length Scale $\Delta^*$

Fernholz and Finley<sup>2</sup> suggested that for compressible flows the relation between  $Re_{\Delta^*}$  and  $Re_{\theta_w}$  is independent of flow Mach number and is as follows:

$$\ln Re_{\Delta^*} = \ln Re_{\theta_w} + 0.04 \quad (7)$$

Note that in reference 5 the coefficient of  $\ln(Re_{\theta_w})$  in Eq.7 has been incorrectly given as 0.964<sup>10</sup>. However experimental data<sup>11,12</sup> from a large number of boundary layer traverses over the Mach number range of 0.3 to 0.85 in this laboratory and also independent experimental data<sup>13,14,15</sup> for the Mach number range of between low subsonic to supersonic, suggests that in contrast to the conclusion of Fernholz and Finley<sup>2</sup>, Eq.7 is valid only for high supersonic flows (i.e.  $M_\infty > 2.0$ ) and such a relationship between the two Reynolds numbers is Mach number dependent and for subsonic and transonic-low supersonic flows should be as follows:

-  $M_\delta < 1.0$  :

$$\ln Re_{\Delta^*} = 0.958 \ln Re_{\theta w} + 0.684 \quad (8)$$

-  $1.0 \leq M_\delta \leq 2.0$  :

$$\ln Re_{\Delta^*} = 0.964 \ln Re_{\theta w} + 0.5394 \quad (9)$$

Note that while the velocity profile (Eq.2 or 6) is sufficient for the calculation of  $\Delta^*$  and  $\theta$ , for the evaluation of  $Re_{\Delta^*}$ , the friction velocity must be known. This has led to the use of the above correlations for the prediction of skin friction and hence the velocity profile as is discussed in the following section.

Of course a continuous description of  $Re_{\Delta^*}$  as a function of Mach number and Reynolds number (i.e.  $Re_{\Delta^*} = f(M_\delta, Re_{\theta w})$ ) which could cover the whole Mach number range would have been much preferred. But due to the lack of sufficient experimental data particularly in the high subsonic-transonic range, at this stage it was not possible to arrive at such relationship.

### 3. Skin Friction and Velocity Profile Algorithm

The corner-stone of the present method is to use the correlation between the  $Re_{\Delta^*}$  and  $Re_{\theta w}$  in conjunction with an analytical expression for the mean velocity profile (i.e. Eq.2 or 6) in order to predict the skin friction and mean velocity profile. For subsonic, transonic and low supersonic flows the author's correlation (Eqs.8 or 9) is used. The method is extended to high supersonic flows by using Eq.7 instead of Eqs.8 or 9. Therefore for a given flow condition (i.e. known  $M_\delta$  and freestream total pressure and temperature) the following iterative procedure is used:

- 1- Give the value of  $\theta$ .
- 2- Assume  $\delta$  (an value of  $\delta = 10\theta$  may be used as an initial guess)
- 3- Assume  $u_\tau$ .
- 4- Recalculate  $u_\tau$  by using Eqs.2 and 8 for subsonic flows ( $M_\delta < 1.0$ ), Eqs.6 and 9 for transonic and low supersonic flows ( $1.0 \leq M_\delta \leq 2.0$ ) and Eqs.6 and 7 for supersonic flows ( $M_\delta > 2.0$ ). In the recalculation of  $u_\tau$ , one of the Eqs. 7, 8 or 9 depending on the value of  $M_\delta$  must be satisfied.
- 5- Use the calculated  $u_\tau$  to recalculate the boundary layer velocity profile (i.e.  $u/u_\delta$ ) and hence the boundary layer momentum thickness by using the appropriate transformed velocity profiles (Eqs. 2 or 6) and the inverse of the van Driest transformation (i.e. inverse of Eq.3).

- 6- If the calculated momentum thickness is equal to the value in step 1, then move to step 7. Otherwise change the boundary layer thickness  $\delta$ , and repeat the procedure from step 3.
- 7- Construct the velocity profile by using the predicted  $C_f$ ,  $\delta$  and Eq.2 for subsonic flows ( i.e.  $M_\infty < 1.0$  ) or Eq.6 for flows with  $M_\infty \geq 1.0$  .

Numerical calculation of integral quantities of the boundary layer was performed in double precision mode by applying the trapezium rule. The step size in each integration was decreased until further reduction had no influence in the numerical result of the integral. The number of iteration in the above procedure was generally less than 10 to 20 depending on the Mach number of the flow. In all cases the accuracy in the calculation of boundary layer momentum thickness was less than 0.01 mm.

This method differs from the Huang et al <sup>8</sup> method in two ways. Firstly instead of using the inverse of Eq. 3 as a criteria for the prediction of skin friction, Eqs.7 to 9 depending upon the flow Mach number were used. Secondly for subsonic flows the combined law of the wall and the law of the wake (i.e. Eq.6) was applied for describing the velocity profile. Also for comparison purposes the Huang et al method was modified by using Eq.2 instead of Eq.6 in their algorithm (i.e. excluding the viscous sub-layer).

#### 4. Discussion and Comparison with Experimental Data

##### 4.1 Subsonic Data

For this Mach number range, data from the works of Winter and Gaudet <sup>13</sup> , Gaudet <sup>14</sup> and Collins et al <sup>15</sup> for the flow Mach number range of about 0.2 to 0.97 were used in order to evaluate the accuracy of the present method and a number of the existing theories for the prediction of skin friction, shape parameter and velocity profile. The Reynolds number based on the boundary layer momentum thickness encountered in these experiments ranged from about  $20 \times 10^3$  to  $300 \times 10^3$ . The percent error in the skin friction coefficient (i.e.  $\Delta C_f = (1 - C_{f,cal}/C_{f,exp}) \times 100$  , by different methods <sup>8,16,17,18,19</sup> and modified Huang et al is given in table 1. Some of the data are also plotted in Figures 1 to 6. As can be seen for all the data examined here the van Driest II <sup>16</sup> and Spalding & Chi <sup>17</sup> methods provide the most accurate skin friction coefficient as compared with the experimental data, and in particular for  $Re_\theta < 40000$  ,  $\Delta C_f$  is practically zero (see Figs.4 to 6). The present method as compared with Huang et al method <sup>8</sup> and the modified Huang method generally provides better accuracy (up to 1 %) except for  $Re_\theta > 1.6 \times 10^5$  (Fig. 1 & 2). It is believed that for this Mach number range as the momentum Reynolds number is increased the role of viscous laminar sub-layer

becomes more important and its exclusion from the theoretical velocity profile has adverse effect on the prediction of skin friction coefficient. For low Reynolds number subsonic flows, i.e.  $Re_0$  less than about  $1.6 \times 10^5$ , the exclusion of the viscous sub-layer in the Huang et al method<sup>8</sup> does not have serious effects on the prediction of skin friction (see table 1), but it significantly decreased the computation time. For a selected number of the experimental data, Figs. 7 to 13 show the predicted velocity profiles in semi-logarithmic and normal coordinates for a range of Mach number between 0.2 and 0.97. As can be seen from these figures, in all cases, the agreement between the predicted velocity profile by the present method, Huang et al<sup>8</sup> and modified Huang et al and the experimental data is very satisfactory. Near the wall the Huang et al<sup>8</sup> method which includes the viscous sub-layer for the mean velocity profile, differs from the present and the modified Huang et al methods (Figs. 7a to 13a). Of course, this difference between the analytical profiles cannot be observed when they are plotted in normal forms (Figs. 7b to 13b). The effect of Reynolds number on the prediction of velocity profile can be seen in Figs. 11 to 13, for  $M_\delta = 0.79$  and  $Re_0$  between  $81 \times 10^3$  to about  $160 \times 10^3$ . As can be seen there exists no significant Reynolds number effect on the predicted velocity profile.

#### 4.2 Transonic and Low Supersonic Data ( $1.0 < M_\delta < 2.0$ ).

At this Mach number range, again the van Driest II<sup>16</sup> and Spalding & Chi<sup>17</sup> methods provide the most accurate result for the prediction of skin friction coefficient. See table 2 and figures 14 and 15. For a given flow Mach number, the high Reynolds number experiment of Winter and Gaudet<sup>13</sup>, and the low Reynolds number experiment of Collins et al<sup>15</sup> show that the percent error in the prediction of skin friction coefficient by the present method, that of Huang et al<sup>8</sup> and modified Huang et al method is practically constant. This suggests that the accuracy for the prediction of skin friction coefficient by these three algorithms is not very sensitive to the Reynolds number based on the momentum thickness. Some of the experimental data for velocity profiles together with the theoretical curves are presented in Figures 16 and 23, for  $M_\delta = 1.39$  and  $Re_0$  between  $17.9 \times 10^3$  to  $128 \times 10^3$ . As can be expected near the wall the modified Huang et al departs from the other two methods. In contrast to the behaviour of the percent error in the prediction of skin friction coefficient, there exists a strong Reynolds number influence on the prediction of velocity profiles by the present method and that of Huang et al<sup>8</sup> (Figs. 19 to 23). At the lower range of Reynolds number both methods fail to correctly predict the velocity profiles, but as the Reynolds number increases the

difference between the predicted velocity profiles and the experimental data decreases. This behaviour cannot be explained by the presumption that the law of the wall and the van Driest formulation are universal functions, independent of Reynolds number and streamwise location. One should also note that for the set of experimental data examined here, the wake parameter  $\Pi$  is practically constant and could not have any influence on this behaviour (the wake parameter depends strongly on  $Re_0$  only for small Reynolds numbers).

#### 4.3 High Supersonic Data ( $M_\infty > 2.0$ ).

At this range of Mach number, there is no clear advantage in the prediction of skin friction coefficient by the present method, Huang et al method<sup>8</sup>, modified Huang method and the method of van Driest II<sup>16</sup>, and no preference can be given to either methods (see table 3 and Figs.24 to 26). The velocity profile as calculated by the present method and that of Huang et al<sup>8</sup> provide similar results (Figs.27 to 33). The effect of Reynolds number on the predicted velocity profile can be seen in figures 27 to 29 and figures 30 to 33. Experimental data in Figs.27 to 29 are taken from Stalmach<sup>23</sup> at  $M_\infty = 3.684$  and  $Re_0$  between 2114 and 10500. Second set of data (Figs. 30 to 33) are from Winter and Gaudet<sup>13</sup> at  $M_\infty = 2.19$  and  $Re_0$  between 14640 and 88907. These two set of data have been selected intentionally because they represent two set of boundary layer flows, one with some post-transitional behaviour and suffering from small scale effect and the other one representing a fully developed and thick turbulent boundary layer. The experimental data from Stalmach (profile 5802301) shows transitional behaviour and in general his data suffer from the small physical scale. In contrast the second set of data from Winter and Gaudet provide a reliable set of measurements for fully developed thick turbulent boundary layers. In despite of these differences, both set of data show similar trend to the variation of Reynolds number, which rules out that the small scale effect or post transitional characteristics of a turbulent boundary layers has anything to do with this observed behaviour. That is, similar to the transonic and low supersonic flows (Fig 19a), both methods underestimate the velocity profiles at lower range of Reynolds number. It is important to note that although the wake parameter  $\Pi$  in the Stalmachs' experiment<sup>23</sup> varies from 0.4464 to 0.5499 (low Reynolds number effect), it does not compensate for the effect of Reynolds number on the whole predicted velocity profile. This dependence on the Reynolds number which is observed in the prediction of the velocity profile and not in the percent error for the prediction of skin friction coefficient, suggest that at least for  $M_\infty \geq 1.0$  the analytical expression used for the mean vel-

ocity profile of turbulent boundary layers (i.e. Eq.2 or Eq.6) does not properly represent the full physical aspects of the mean flow distribution of a turbulent boundary layer. The strong Reynolds number effect observed here, also questions the presumption of the universality of the commonly used expressions (Eqs. 2 or 6) for the wall bounded turbulent flows which has been also discussed in length by Gad-el-Hak et al<sup>20,21</sup>.

#### 4.4 Boundary Layer Shape Parameter

Typical results for the boundary layer shape parameter as calculated by present method, Huang et al<sup>8</sup> method and that of Modified Huang for a range of flow Mach number is presented in Figs.34 to 44. All the three methods predict the boundary layer shape parameter to within  $\pm 2\%$  of its experimental values. As expected for a given flow Mach number the calculated  $H$  is not sensitive to the variation of Reynolds number but it is sensitive to the boundary layer velocity distribution. That is for subsonic flows the present method and the modified Huang et al methods produce the same result, since both use Eq.2 to describe the boundary layer velocity profile. For  $M_\infty \geq 1.0$  the present method and that of Huang et al<sup>8</sup> which use Eq.6 for the velocity profile, generate almost identical results.

#### 5. Concluding Remarks

An algorithm for the prediction of mean velocity profile, skin friction coefficient and the shape parameter of the compressible two-dimensional turbulent boundary layers is presented. The prediction method relies on the transformed law of the wall and law of the wake for subsonic flows, the van Driest model for the complete inner region and the law of the wake for supersonic flows and a correlation between the integral length scale Reynolds number and the momentum thickness Reynolds number. The agreement between the prediction and a wide range of experimental data for zero pressure gradient turbulent boundary layers is very satisfactory. The predicted skin friction shows good agreement with some of the available methods for the estimation of skin friction, in particular with the van Driest II theory<sup>16</sup> and the method of Spalding & Chi<sup>17</sup>. For most of the subsonic and transonic-low supersonic data examined here the present method predicts the skin friction coefficient better than that of Huang et al<sup>8</sup>, with the exception of subsonic flows at  $Re_0$  greater than about  $1.6 \times 10^5$ . The accuracy of both methods at supersonic flows varies for different sets of experimental data and no preference can be given to either methods. In most cases and at any flow Mach number considered here, of the existing methods for the prediction of skin friction, that of von

Karman et al<sup>18,19</sup> gives the least accurate results particularly at supersonic speeds. For subsonic flows and outside the viscous sub-layer the present method, the Huang et al<sup>8</sup> and the modified Huang et al provide similar results for the velocity profile, and their accuracy is not Reynolds number dependent. In contrast, for high speed flows ( i.e.  $M_\infty > 1.0$  ) although the present method and Huang et al<sup>8</sup> produce similar results for the velocity profile, their accuracy depends on the Reynolds number based on the momentum thickness of the boundary layer. This suggests that at least for this flow regime, the expression used for the transformed velocity profile (i.e. Eq.2 or 6) does not sufficiently represent all the physical aspects of the mean flow distribution in a compressible turbulent boundary layer and should not be considered as universal. Extra information<sup>22</sup> , or perhaps a more physical approach to the formulation of the mean structure of compressible turbulent boundary layers, is required in order to achieve complete (physical and mathematical) convergence when it is applied in a prediction method. The boundary layer shape parameter as calculated by the three methods is generally  $\pm 2\%$  of the experimental values and its percent error depends mainly on the expression by which the boundary layer velocity profile is described.

## 6. References

- 1 Schlichting, H. "Boundary-Layer Theory," 7th ed., McGraw-Hill Book Company, New-York, 1979, pp. 587-589.
- 2 Fernholz, H.H., "A Critical Commentary on Mean Flow Data for Two-Dimensional Compressible Turbulent Boundary Layers," AGARDograph No.253, May 1980.
- 3 van Driest, E.R., "Turbulent Boundary Layer in Compressible Fluids," J. of Aeronautical Sciences, Vol.18, No.5, March 1951, pp. 145-160
- 4 van Driest, E.R., "Turbulent Flows with Heat Transfer," C.C.Lin ed., Princeton University Press, Princeton, N.J., 1959, pp. 339-427.
- 5 Coles,D.E., "The Turbulent Boundary Layer in Compressible Fluid," Rand Corp., Report R-403-PR, Santa Monica, Sept. 1962.
- 6 Coles, D.E., "The Law of the Wake in the Turbulent Boundary Layers," J. of Fluid Mechanics, Vol.1, Pt.2, July 1956, pp. 191-226.
- 7 Cebeci,T., and Smith, A.M.O., "Analysis of Turbulent Boundary Layers," 1st ed., Academic Press Inc., New York, 1974, pp. 146-148.
- 8 Huang P.G., Bradshaw P. and Coakley T.J., "Skin Friction and Velocity Profile Family for Compressible Turbulent Boundary Layers," AIAA J., Vol.31, No.9, Sept.1993, pp.1600-1604.
- 9 van Driest, E.R., "On Turbulent Flow Near a Wall," Journal of Aerospace Sciences, vol.23, 1956, pp.1007-1012.
- 10 Fernholz, H.H., private communication, Technische Universitat Berlin, Hermann-Fottinger-Institut fur Thermo-und Fluiddynamik, Berlin, Germany, Nov. 1991.
- 11 Motallebi, F., "Experimental Investigation of the Flow Quality in the GLT20 Subsonic-Transonic Boundary Layer Wind Tunnel," Faculty of Aerospace Engineering, Delft University of Technology, Report LR-720, Delft, The Netherlands, April 1993.
- 12 Motallebi, F., "Mean Flow Study of 2-D Subsonic Turbulent Boundary Layers," AIAA J., Vol.32, No.11, Nov.1994, pp.2153-2161.
- 13 Winter, K.G., and Gaudet, L., "Turbulent Boundary Layer Studies at High Reynolds Numbers at Mach Numbers Between 0.2 and 2.8," Aeronautical Research Council, ARC R.& M. No.3712, London, United Kingdom, Dec. 1970.
- 14 Gaudet, L. "Experimental Investigation of the Turbulent Boundary Layer at High Reynolds Numbers and a Mach Number of 0.8," Royal Aircraft Establishment, RAE Report, TR-84094, Bedford, United Kingdom, Sept. 1984.
- 15 Collins, Donald J., Coles, D.E. and Hicks John W., "Measurements in the Turbulent

Boundary Layer at Constant Pressure in Subsonic and Supersonic Flow, Part I: Mean Flow," Jet Propulsion Laboratory, California Institute of Technology, AEDC-TR-78-21, Pasadena, California, May 1978.

<sup>16</sup> van Driest, E.R., "Problem of Aerodynamic Heating," Aeronautical Engineering Review, Vol.15, No.10, Oct.1956, pp.26-41.

<sup>17</sup> Spalding, D.B. and Chi, S.W., "The Drag of a Compressible Boundary Layer on a Smooth Flat Plate With and Without Heat Transfer," Journal of Fluid Mechanics, Vol.8, Part I, Jan.1964, pp. 117-143.

<sup>18</sup> von Karman, T., "Turbulence and Skin Friction," Journal of the Aeronautical Sciences, Vol.1, No.1, Jan.1934, pp.1-20.

<sup>19</sup> Schoenherr, K.E., "Resistance of Flat Surfaces Moving Through a Fluid," Transaction of Society of Naval Architects and Marine Engineers, Vol.40, 1932, pp. 279-313.

<sup>20</sup> Gad-el-Hak, M. and Bandyopadhyay, Promode R., "Reynolds Number Effects in Wall-Bounded Turbulent Flows," ASME J. of Applied Mechanic Review, Vol.47, No.8, Aug.1994, pp.307-365.

<sup>21</sup> Gad-el-Hak, M., "Does a Turbulent Boundary Layer Ever Achieve Self-Preservation," Lecture given at the Department of Aerospace Engineering, Delft University of Technology, Delft, The Netherlands, June 1994.

<sup>22</sup> Motallebi, F. "Comments on Skin Friction and Velocity Profile Family for Compressible Turbulent Boundary Layers," AIAA J., Vol.32, No.9, pp.1938, Sept.1994.

<sup>23</sup> Fernholz, H.H. and Finley, P.J., "A Critical Compilation of Compressible Boundary Layer Data," AGARDograph No. 223, June, 1977.

<sup>24</sup> Fernholz, H.H. and Finley, P.J., "A Further Compilation of Compressible Boundary Layer Data with a Survey of Turbulence Data," AGARDograph No. 263, Nov. 1981.

**Table 1 Percent error in the prediction of skin friction coefficient  $\Delta C_f$ ,  
subsonic data ( $M_\delta < 1.0$ )**

Profile	Re	Present	$\Delta C_f = (1 - C_{f,cal}/C_{f,exp}) \times 100, \%$						$Re_\delta$	$M_\delta$
			van Driest II f.		von Karman et al		Spalding & Chi		Huang Modified	
			(Ref.16)	(Ref.18,19)	(Ref.17)	Hunag	(Ref.8)			
1	14	3.4	.7	-4.4	.8	3.7	3.9	23246	0.746	
2	14	2.5	.3	-5.4	.4	2.8	2.9	42939	0.782	
3	14	3.9	1.8	-3.8	2.0	4.0	4.2	57330	0.782	
4	14	3.6	1.8	-4.0	1.9	3.6	3.7	93366	0.784	
5	14	3.6	2.1	-3.7	2.2	3.6	3.8	140528	0.784	
6	14	3.9	2.4	-3.3	2.6	3.9	4.0	170284	0.784	
7	14	3.7	2.3	-3.5	2.4	3.7	3.6	200696	0.784	
8	14	4.4	3.1	-2.7	3.2	4.3	3.6	254272	0.784	
9	14	4.2	2.9	-2.8	3.1	4.1	3.1	275845	0.785	
10	14	3.6	2.3	-3.5	2.4	3.5	2.5	276588	0.784	
11	14	4.2	2.9	-2.9	3.1	4.1	2.9	289059	0.784	
12	14	4.3	3.1	-2.7	3.2	4.2	2.9	305741	0.784	
13	14	4.5	3.3	-2.5	3.4	4.4	3.0	310974	0.784	
1	13	3.1	.4	0.0	.4	3.0	3.2	55982	0.199	
2	13	1.1	-1.4	-1.7	-1.3	.9	1.1	96184	0.200	
3	13	3.3	1.1	.7	1.1	3.0	3.1	167496	0.200	
4	13	2.9	.8	.4	.8	2.6	2.1	210673	0.200	
5	13	1.1	-1.3	-2.8	-1.2	1.0	1.2	86628	0.398	
6	13	1.4	-.7	-4.2	-.7	1.4	1.5	85550	0.595	
7	13	1.6	-.3	-6.3	-.2	1.7	1.8	81004	0.790	
8	13	2.1	.5	-5.5	.6	2.2	2.3	120366	0.793	
9	13	1.7	.2	-5.9	.3	1.7	1.9	157450	0.793	
27	13	3.3	.0	-.4	.0	3.4	3.6	22432	0.204	
28	13	4.4	1.4	1.0	1.4	4.5	4.6	31900	0.198	
29	13	4.5	1.6	1.3	1.7	4.5	4.6	41861	0.202	
30	13	3.6	.8	.4	.8	3.6	3.7	46054	0.200	

**Table 1 \Continued**

$$\Delta C_f = (1 - C_{f, \text{cal}} / C_{f, \text{exp}}) \times 100, \%$$

Profile	Re	Present	van	von Karman	Spalding	Huang		$Re_\theta$	$M_\delta$
			Driest II	et al	& Chi	Modified	et al		
31	13	3.2	.5	.1	.5	3.2	3.3	54462	0.201
32	13	4.2	1.7	1.3	1.7	4.1	4.2	76500	0.205
33	13	4.3	1.9	1.5	1.9	4.1	4.2	95655	0.201
34	13	3.9	1.6	1.2	1.6	3.7	3.8	116552	0.201
35	13	4.3	2.1	1.7	2.1	4.1	4.2	135341	0.202
36	13	3.2	1.1	.7	1.1	3.0	3.0	166596	0.200
37	13	2.8	.7	.3	.7	2.5	2.0	209352	0.200
38	13	1.8	-.3	-.7	-.3	1.5	1.0	212689	0.201
JPL-A44	15	.5	-4.2	-4.3	-4.2	.9	1.1	5930	0.106
JPL-A45	15	1.2	-3.4	-3.5	-3.4	1.6	1.8	6183	0.107
JPL-A46	15	1.9	-2.6	-2.7	-2.6	2.3	2.5	6824	0.103
JPL-A47	15	.6	-4.1	-4.2	-4.1	.8	1.0	7202	0.104
JPL-A48	15	1.3	-3.3	-3.4	-3.3	1.6	1.7	7494	0.105
JPL-A49	15	2.0	-2.4	-2.5	-2.4	2.3	2.5	8038	0.107
JPL-A51	15	-1.4	-4.7	-8.1	-4.6	-1.1	-.9	18579	0.593
JPL-A52	15	1.1	-2.0	-5.4	-1.9	1.5	1.6	20333	0.593
JPL-A53	15	2.2	-.8	-4.2	-.7	2.5	2.7	21978	0.599
JPL-A54	15	2.9	-.2	-3.6	-.1	3.1	3.3	22636	0.602
JPL-A55	15	2.8	-.1	-3.4	.0	3.2	3.3	22995	0.596
JPL-A61	15	2.6	-.1	-3.5	-.1	2.8	3.0	30560	0.597
JPL-A62	15	2.7	.1	-3.3	.2	3.0	3.1	34081	0.596
JPL-A63	15	3.7	1.0	-2.3	1.1	3.8	4.0	36160	0.595
JPL-A64	15	4.1	1.5	-1.8	1.6	4.3	4.4	36348	0.593
JPL-A65	15	3.5	1.0	-2.3	1.1	3.7	3.9	37775	0.593
JPL-A71	15	-.3	-3.3	-9.4	-3.2	.1	.2	19466	0.796
JPL-A72	15	.4	-2.3	-8.3	-2.2	.9	1.0	22244	0.788
JPL-A73	15	2.7	.0	-6.0	.2	3.1	3.2	23622	0.805
JPL-A74	15	2.3	-.4	-6.4	-.2	2.6	2.8	23901	0.802

Table 1 \Continued.

$\Delta C_f = (1 - C_{f,cal}/C_{f,exp}) \times 100, \%$										
Profile	Re	Present	van	von Karman	Spalding			Huang	$Re_\theta$	$M_\infty$
			Driest II	et al	& Chi	Modified	et al			
f.	(Ref.16)	(Ref.18,19)	(Ref.17)	Hunag	(Ref.8)					
JPL-A75	15	2.1	-.5	-6.5	-.4	2.4	2.5	24738	0.799	
JPL-A81	15	2.1	-.3	-6.3	-.1	2.4	2.6	33449	0.798	
JPL-A82	15	3.2	.8	-5.0	1.0	3.5	3.6	37264	0.794	
JPL-A83	15	4.0	1.7	-4.2	1.8	4.1	4.3	39950	0.794	
JPL-A84	15	3.8	1.7	-4.1	1.8	4.1	4.3	41099	0.792	
JPL-A85	15	3.2	1.0	-4.8	1.1	3.5	3.6	42672	0.792	
JPL-A91	15	-.1	-2.8	-11.6	-2.6	.3	.4	18741	0.966	
JPL-A92	15	.2	-2.3	-11.1	-2.1	.8	.9	21631	0.967	
JPL-A93	15	2.4	.0	-8.7	.2	3.0	3.1	22473	0.972	
JPL-A94	15	2.0	-.4	-9.1	-.2	2.5	2.6	23025	0.967	
JPL-A95	15	2.0	-.3	-9.0	-.1	2.5	2.7	24062	0.965	
JPL-A101	15	1.9	-.1	-8.8	.1	2.5	2.7	32263	0.965	
JPL-A102	15	2.3	.3	-8.3	.5	2.8	2.9	36385	0.963	
JPL-A103	15	4.0	1.9	-6.6	2.1	4.3	4.5	38579	0.961	
JPL-A104	15	3.1	1.1	-7.5	1.3	3.5	3.6	39981	0.964	
JPL-A105	15	3.2	1.2	-7.3	1.4	3.5	3.6	42153	0.961	

**Table 2 Percent error in the prediction of skin friction coefficient  $C_f$ ,  
transonic and low supersonic data ( $1.0 \leq M_\infty \leq 2.0$ )**

Profile	Re	Present	$\Delta C_f, \%$						
			van Driest II	Von Karman et al	Spalding & Chi	Huang Modified	Huang et al	$Re_\theta$	$M_\infty$
			f.	(Ref.16)	(Refs.18,19)	(Ref.17)	Hunag		
58060101	24	.4	-1.2	-28.6	-.1	.8	.9	17585	1.77
10	13	.0	-2.7	-20.4	-2.1	.0	.2	17914	1.394
11	13	1.6	-.3	-17.9	.3	1.6	1.7	39333	1.395
12	13	2.0	.4	-17.4	.9	1.9	2.0	60234	1.400
13	13	2.0	.9	-17.0	1.4	1.9	2.0	113948	1.400
14	13	2.3	1.2	-16.5	1.7	2.1	2.2	128035	1.400
15	13	.8	-.3	-23.1	.4	.9	1.0	56479	1.597
16	13	.3	-.4	-28.9	.6	.6	.8	53671	1.800
17	13	-1.2	-1.4	-36.3	-.2	-.7	-.5	50860	2.000
JPL-A112	15	1.9	-.8	-16.4	-.3	1.8	2.0	19880	1.314
JPL-A113	15	2.2	-.3	-16.1	.1	2.2	2.3	21236	1.321
JPL-A114	15	2.8	.3	-15.4	.7	2.7	2.9	21971	1.320
JPL-A115	15	2.5	.1	-15.4	.5	2.5	2.6	23580	1.315
JPL-A122	15	2.7	.6	-14.9	1.0	2.6	2.7	34560	1.308
JPL-A123	15	4.6	2.4	-13.0	2.8	4.3	4.4	36689	1.317
JPL-A124	15	1.1	-1.0	-16.9	-.6	1.1	1.1	37659	1.312
JPL-A125	15	4.2	2.3	-13.1	2.6	4.1	4.2	39569	1.313

**Table 3 Percent error in the prediction of skin friction coefficient  $C_f$ ,  
supersonic data ( $M_\delta > 2.0$ )**

Profile	Re	Present f.	$\Delta C_f, \%$						$Re_9$	$M_\delta$	
			van Driest II		von Karman et al (Refs.18,19)		Spalding & Chi (Ref.17)		Huang Hunag (Ref.8)		
			Present	(Ref.16)	et al	(Refs.18,19)	& Chi	Modified	Hunag	(Ref.8)	
65020101	23	1.3	3.8	-61.3	6.0	1.9	2.0	427861	2.831		
65020102	23	-3.0	.2	-65.9	2.3	-1.9	-2.1	532000	2.787		
65020103	23	-1.0	3.2	-56.5	5.1	1.2	-.2	737157	2.669		
65020201	23	5.0	7.3	-55.6	9.6	5.5	5.6	366755	2.843		
65020202	23	-2.0	.7	-65.9	2.8	-1.3	-1.2	431247	2.809		
65020203	23	.7	4.2	-55.5	6.2	2.3	1.6	602895	2.693		
65020301	23	2.2	4.3	-60.8	6.8	2.7	2.8	225909	2.865		
65020401	23	1.7	3.7	-62.5	6.4	2.2	2.3	167222	2.897		
65020501	23	2.3	3.3	-61.8	6.2	2.7	2.8	50857	2.908		
65020601	23	2.8	3.7	-61.3	6.5	3.1	3.2	49261	2.910		
55010501	23	-1.5	-5.1	-47.9	-3.3	-2.9	-2.8	6030	2.908		
55010502	23	-3.6	-8.9	-53.5	-7.1	-7.0	-6.8	8214	2.242		
55010503	23	-5.2	-9.4	-54.4	-7.7	-7.6	-7.5	10863	2.236		
55010504	23	1.6	-0.1	-42.4	1.3	.9	1.1	20718	2.244		
74021801	23	-6.5	-5.7	-143.2	2.7	-5.7	-5.4	10134	4.517		
74021802	23	-8.3	-6.2	-147.1	1.8	-7.3	-7.2	15882	4.510		
74021803	23	-6.5	-4.7	-145.3	2.9	-5.9	-5.8	19789	4.510		
74021804	23	-7.0	-4.7	-145.9	2.9	-6.4	-6.1	25001	4.500		
74021805	23	-8.5	-5.6	-148.8	1.8	-7.5	-7.5	28447	4.493		
77010301	24	18.8	15.5	-53.0	20.1	16.3	16.6	2871	3.480		
77010801	24	-22.4	-24.5	-143.8	-14.7	-27.9	-27.4	1456	4.000		
58020201	23	10.3	7.3	-42.1	10.7	7.5	7.7	2011	2.735		
58020203	23	7.3	3.3	-49.9	6.5	5.2	5.4	3834	2.731		
58020207	23	-3.5	-5.9	-67.5	-2.9	-5.3	-5.2	12228	2.739		
58020301	23	6.7	4.4	-78.3	10.7	4.3	4.5	2186	3.684		
58020304	23	.5	-.2	-94.5	5.3	.0	.1	12174	3.667		
58020306	23	-8.4	-9.5	-112.7	-3.4	-9.2	-9.1	10822	3.681		
18	13	-1.1	-4.2	-44.5	-2.4	-2.5	-2.3	14640	2.186		

Table 3 \Continued.

$$\Delta C_f = (1 - C_{f,cal}/C_{f,exp}) \times 100, \%$$

Profile	Re	Present f.	van Driest II	von Karman et al	Spalding & Chi	Huang Modified	Huang et al	$Re_\theta$	$M_\delta$
			(Ref.16)	(Ref.18,19)	(Ref.17)	Hunag	(Ref.8)		
19	13	-1.7	-3.4	-45.0	-1.7	-2.4	-2.3	30865	2.197
20	13	-2.2	-3.3	-45.4	-1.7	-2.8	-2.7	48223	2.201
21	13	-.3	-.6	-42.4	.9	-.6	-.5	88907	2.206
22	13	-2.2	-2.8	-51.6	-.9	-2.5	-2.4	42743	2.402
23	13	-2.9	-3.1	-59.2	-.7	-3.0	-2.9	41902	2.599
24	13	-2.2	-4.2	-65.6	-1.1	-3.0	-2.8	12330	2.789
25	13	-4.9	-5.5	-69.5	-2.5	-5.1	-5.0	25028	2.797
26	13	-5.8	-5.7	-70.8	-2.8	-5.8	-5.7	40239	2.799
39	13	-1.1	-3.5	-44.5	-1.7	-2.1	-1.9	19939	2.198
40	13	-1.8	-3.8	-45.3	-2.1	-2.6	-2.5	24993	2.199
41	13	-2.0	-3.7	-45.4	-2.0	-2.7	-2.5	30300	2.200
42	13	-1.7	-3.1	-44.9	-1.5	-2.3	-2.2	35014	2.201
43	13	-1.6	-2.9	-44.8	-1.3	-2.3	-2.1	39867	2.202
44	13	-1.9	-3.0	-45.0	-1.4	-2.4	-2.3	46899	2.204
45	13	-1.2	-2.0	-43.9	-.5	-1.6	-1.5	53841	2.205
46	13	-1.5	-2.2	-44.4	-.7	-1.9	-1.8	63569	2.206
47	13	-.9	-1.4	-43.4	.1	-1.2	-1.1	73310	2.207
48	13	-.3	-.6	-42.5	.9	-.6	-.4	84259	2.208
JPL-A132	15	4.2	2.3	-36.2	3.7	3.4	3.5	23938	2.172
JPL-A133	15	4.0	2.1	-36.3	3.5	3.2	3.3	24409	2.166
JPL-A134	15	4.0	2.0	-36.3	3.4	3.1	3.2	25782	2.164
JPL-A135	15	3.5	1.7	-37.0	3.1	2.9	3.0	25891	2.172
JPL-A142	15	4.9	3.7	-34.9	5.0	4.2	4.4	40005	2.181
JPL-A143	15	5.1	3.8	-34.5	5.1	4.3	4.4	41312	2.173
JPL-A144	15	5.5	4.4	-34.2	5.6	4.9	5.1	42380	2.182
JPL-A145	15	4.8	3.7	-35.1	5.0	4.3	4.5	44136	2.180

Fig. 1 Percent error in skin friction coefficient  $\Delta C_f = (1 - C_{f,cal}/C_{f,exp}) \times 100\%$ .  
 Experimental data from Gaudet <sup>14</sup>,  $M_6 = 0.784$

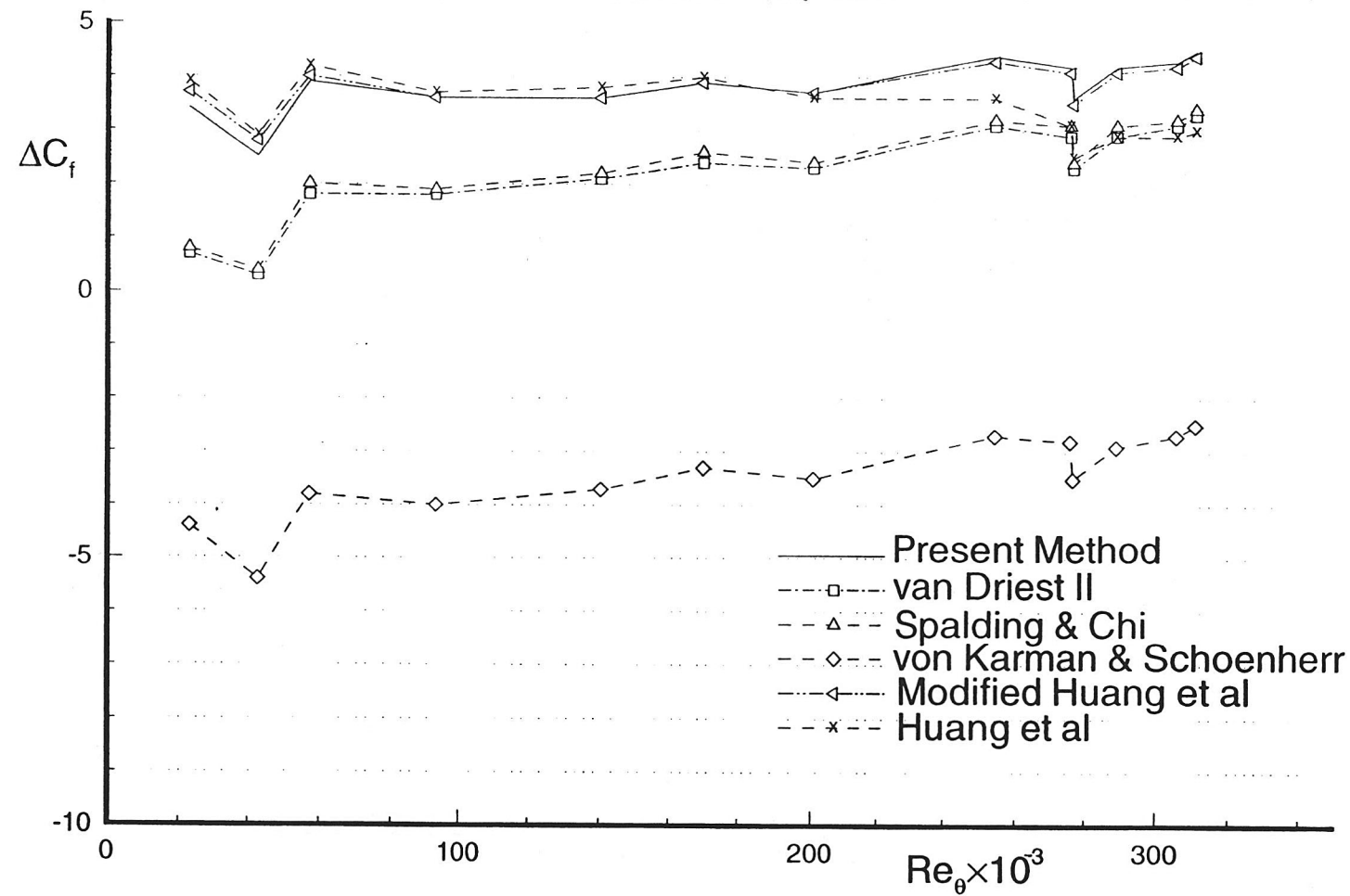


Fig. 2

Percent error in skin friction coefficient  $\Delta C_f = (1 - C_{f,cat}/C_{f,exp}) \times 100\%$ .  
 Experimental data from Winter & Gaudet<sup>13</sup>,  $M_6 = 0.20$

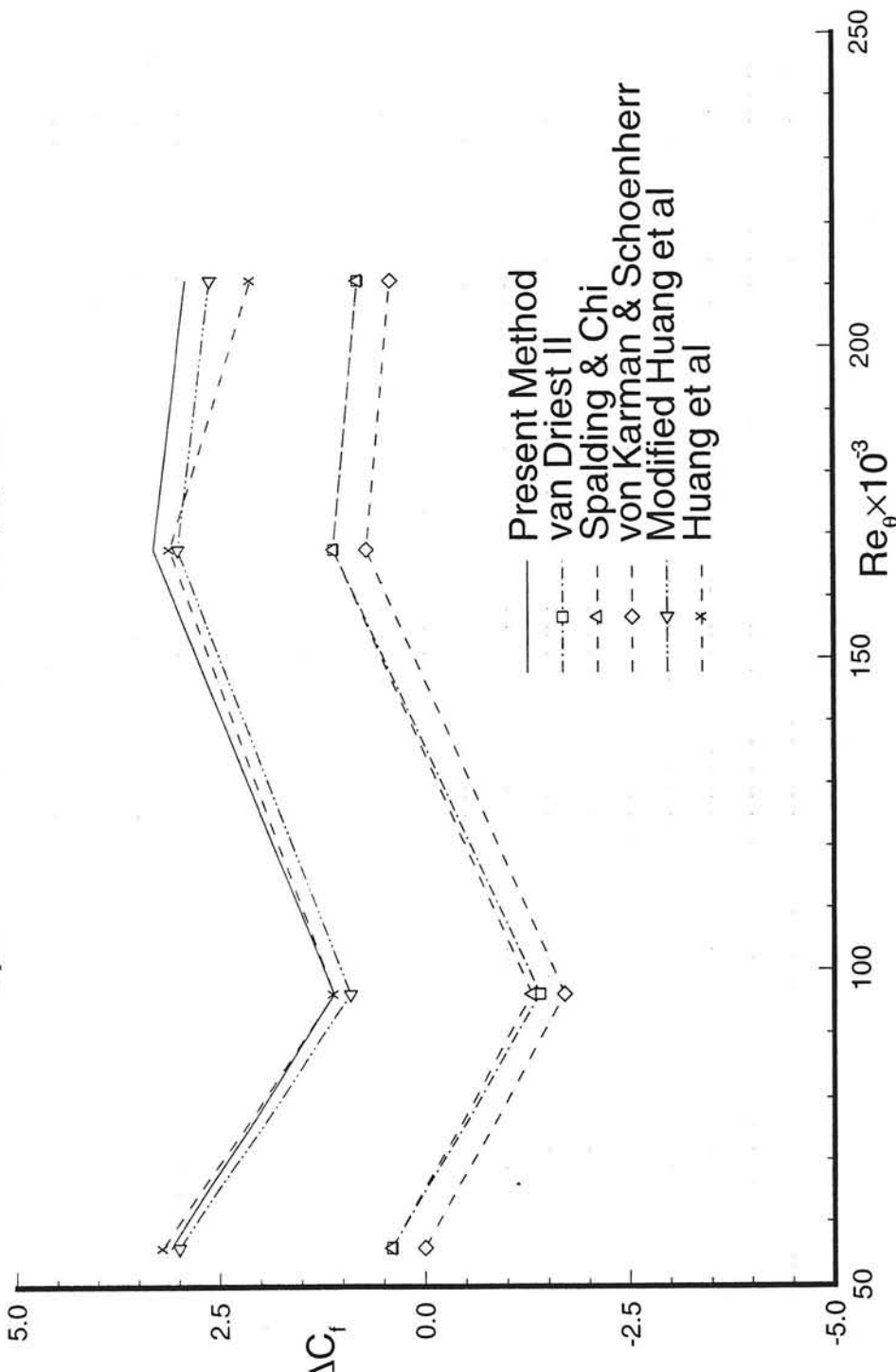


Fig. 3 Percent error in skin friction coefficient  $\Delta C_f = (1 - C_{f,cal}/C_{f,exp}) \times 100\%$ .  
Experimental data from Gaudet<sup>14</sup>,  $M_\infty = 0.79$

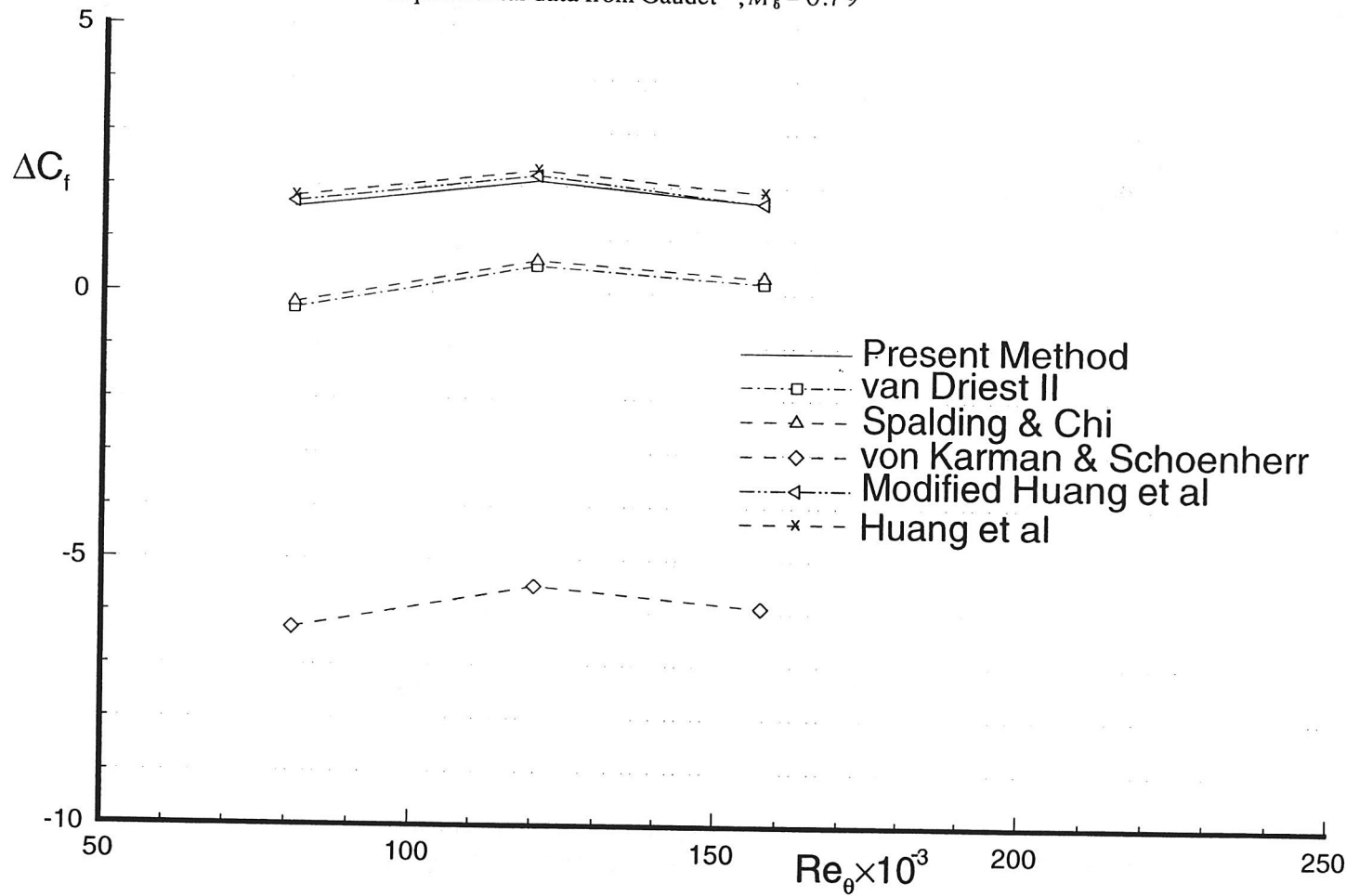


Fig. 4 Percent error in skin friction coefficient  $\Delta C_f = (1 - C_{f, \text{cal}}/C_{f, \text{exp}}) \times 100\%$ .  
 Experimental data from Collins et al<sup>15</sup>,  $M_b = 0.59$

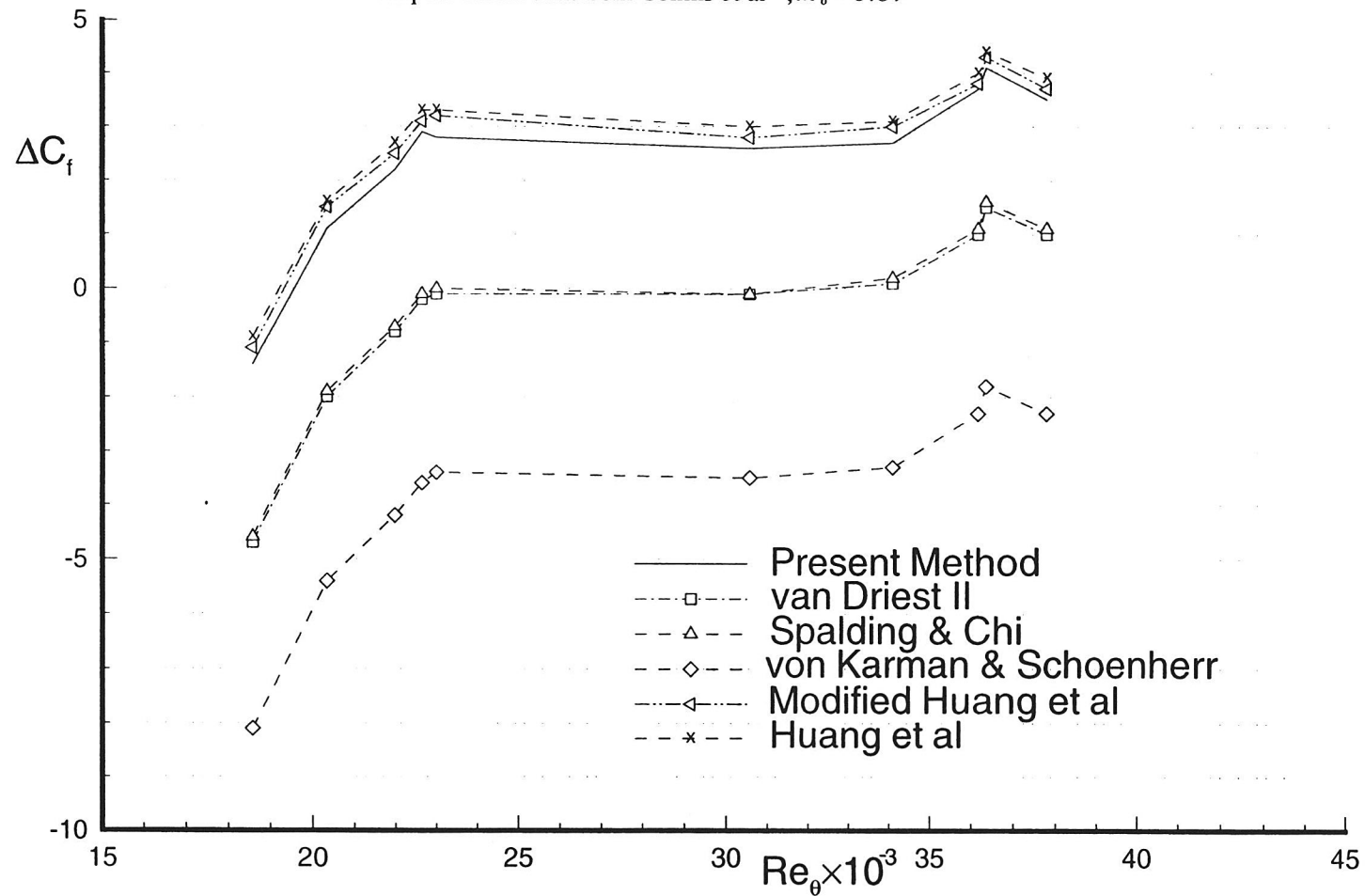


Fig. 5 Percent error in skin friction coefficient  $\Delta C_f = (1 - C_{f, \text{cal}}/C_{f, \text{exp}}) \times 100\%$ .  
Experimental data from Collins et al<sup>15</sup>,  $M_\infty = 0.79$

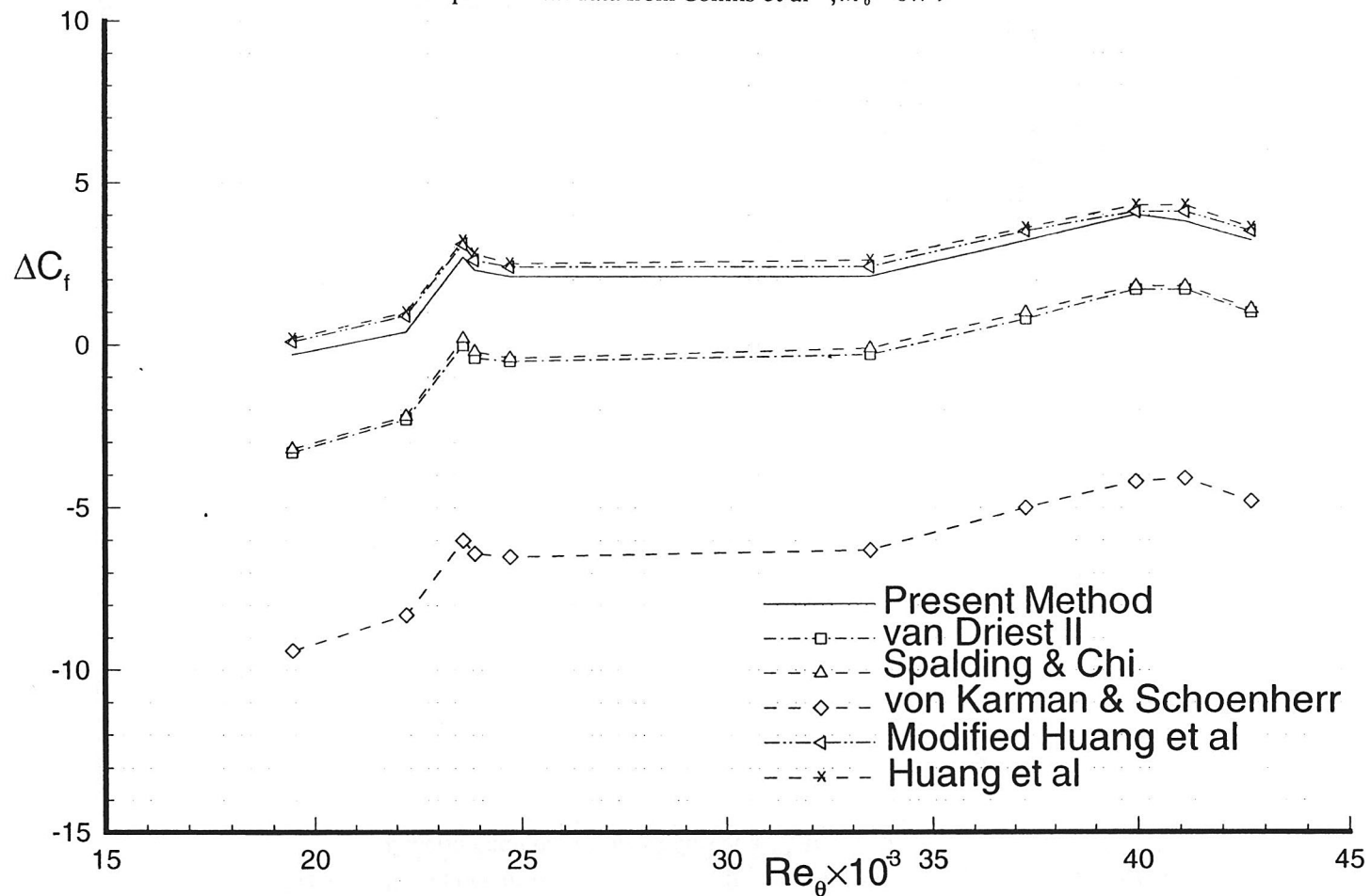
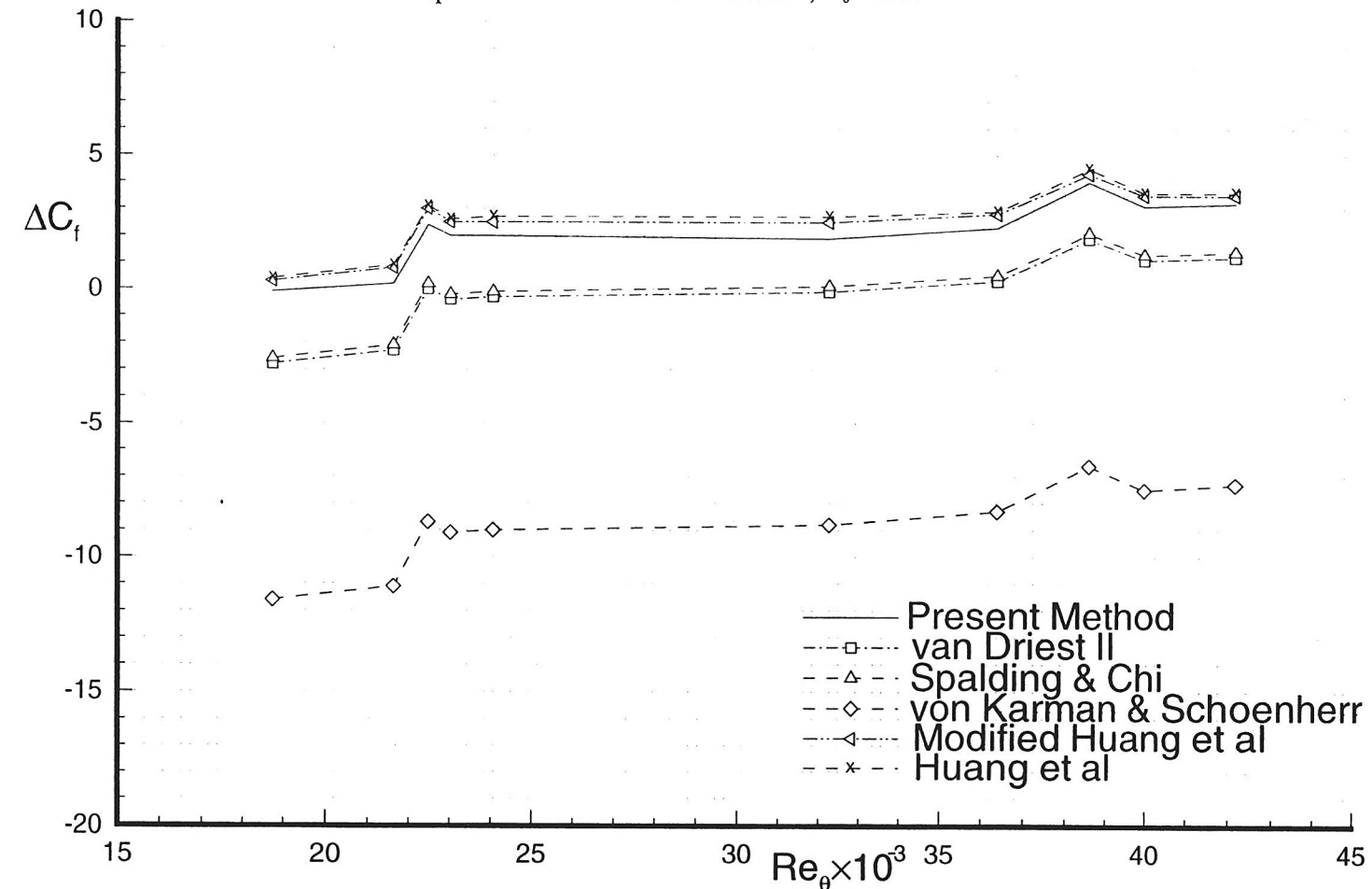


Fig. 6 Percent error in skin friction coefficient  $\Delta C_f = (1 - C_{f, \text{cal}}/C_{f, \text{exp}}) \times 100\%$ .  
 Experimental data from Collins et al<sup>15</sup>,  $M_6 = 0.97$



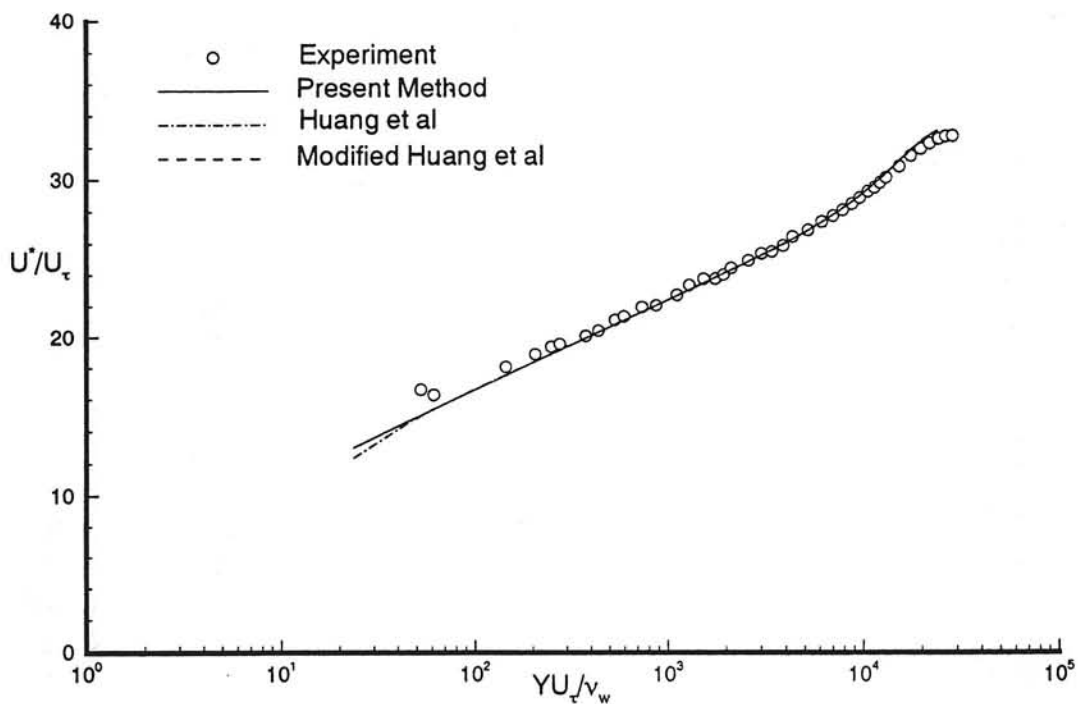


Fig. 7a Transformed velocity profile in semi-logarithmic coordinates. Experimental data from Winter & Gaudet<sup>13</sup>,  $M_\infty = 0.20$ ,  $Re_\infty = 55982$ , profile 1.

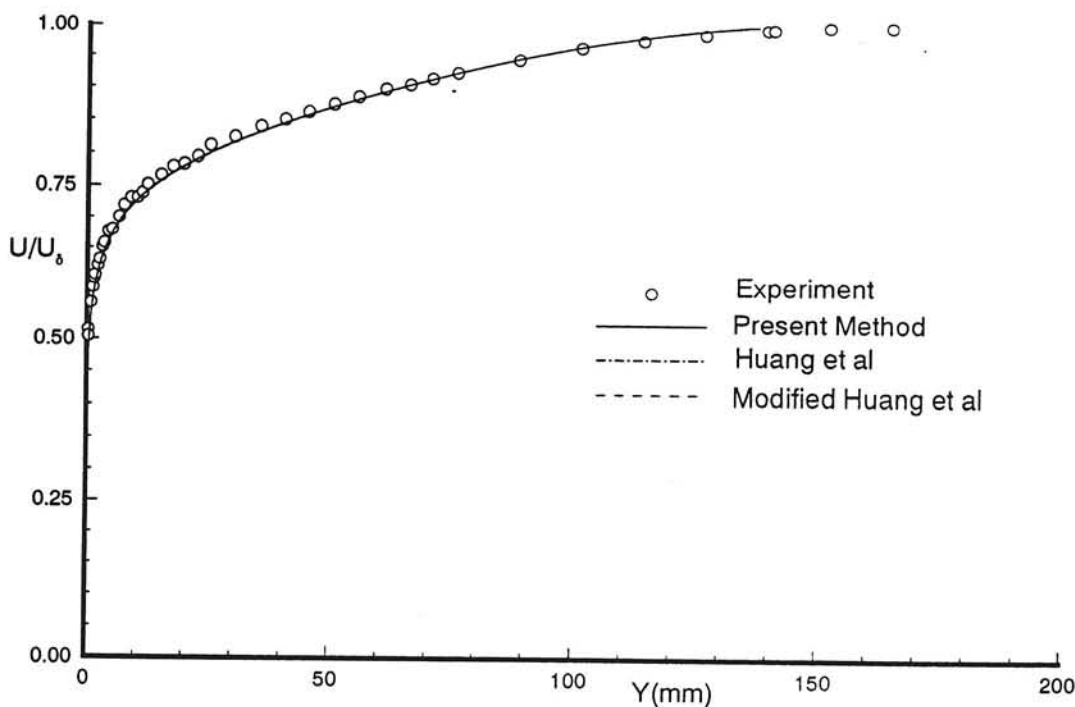


Fig. 7b Untransformed velocity profile in normal coordinates. Experimental data from Winter & Gaudet<sup>13</sup>,  $M_\delta = 0.20$ ,  $R\alpha_0 = 55982$ , profile 1.

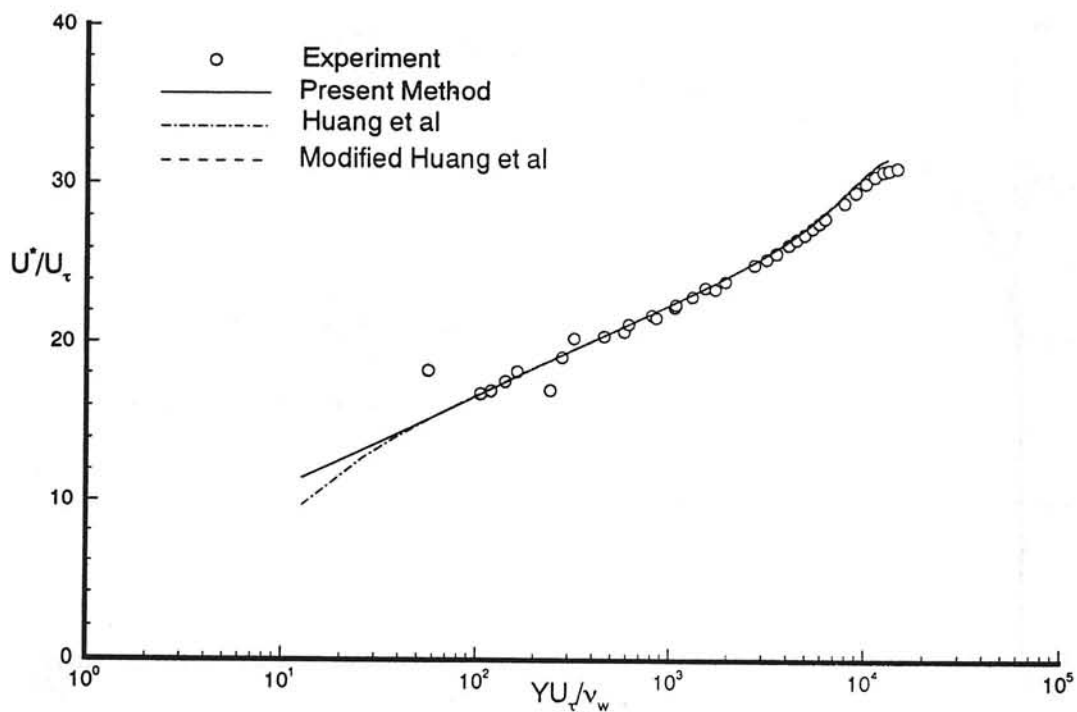


Fig. 8a Transformed velocity profile in semi-logarithmic coordinates. Experimental data from Gaudet<sup>14</sup>,  $M_b = 0.7824$ ,  $Re_0 = 42939$ , profile 2.

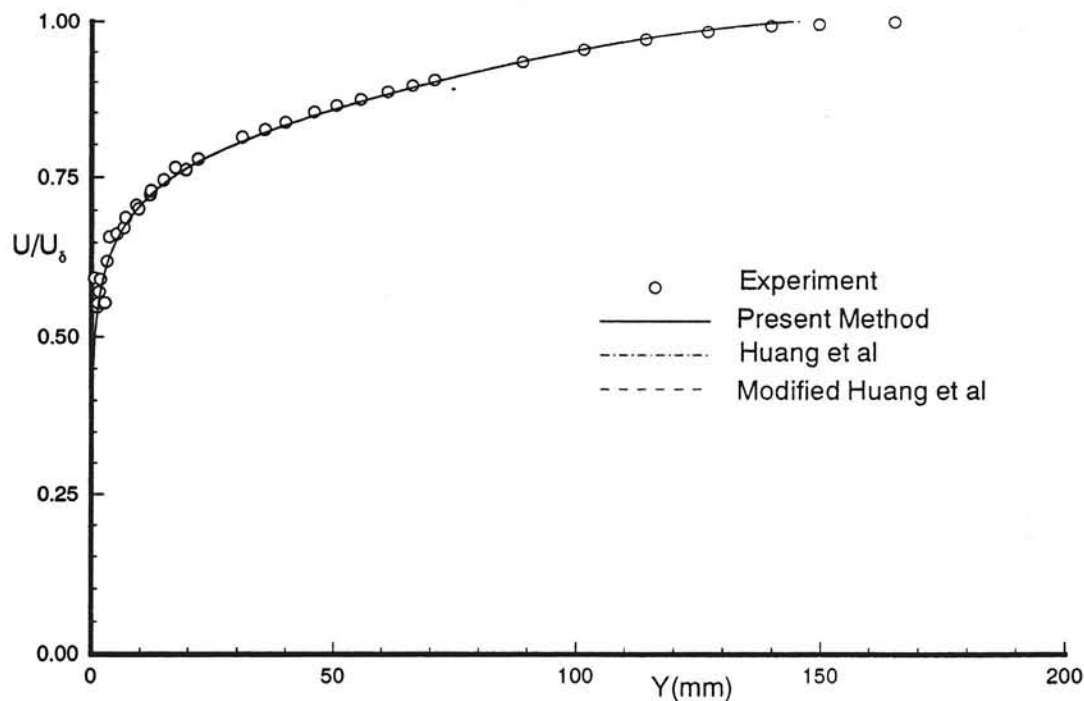


Fig. 8b Untransformed velocity profile in normal coordinates. Experimental data from Gaudet<sup>14</sup>,  $M_\delta = 0.7824$ ,  $Re_\delta = 42939$ , profile 2.

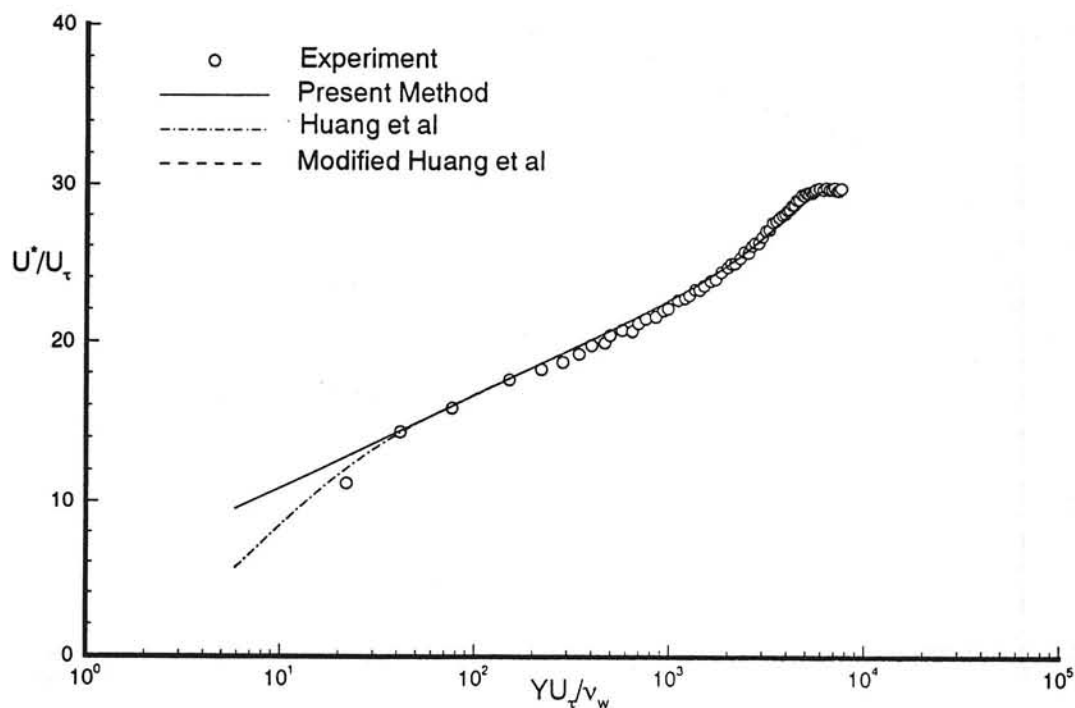


Fig. 9a Transformed velocity profile in semi-logarithmic coordinates. Experimental data from Collins et al<sup>15</sup>,  $M_\infty = 0.5927$ ,  $Re_\theta = 18870$ , profile JPL-A-51.

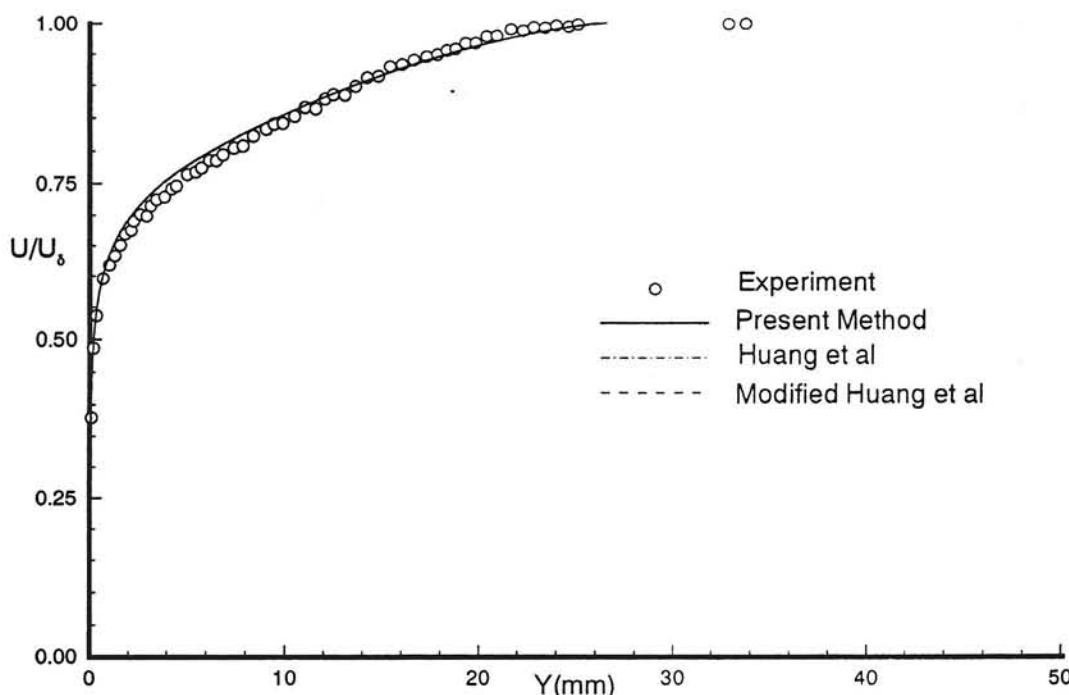


Fig. 9b Untransformed velocity profile in normal coordinates. Experimental data from Collins et al<sup>15</sup>,  $M_\delta = 0.5927$ ,  $Re_\delta = 18870$ , profile JPL-A-51.

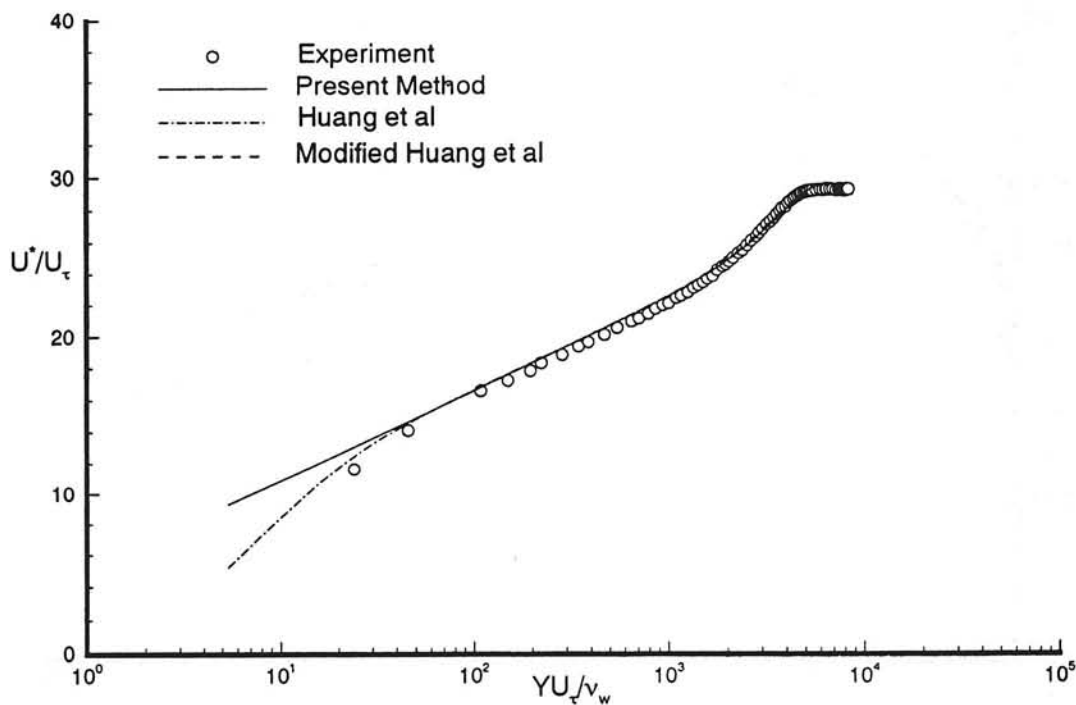


Fig. 10a Transformed velocity profile in semi-logarithmic coordinates. Experimental data from Collins et al<sup>15</sup>,  $M_\infty = 0.9664$ ,  $Re_\infty = 18650$ , profile JPL-A-91.

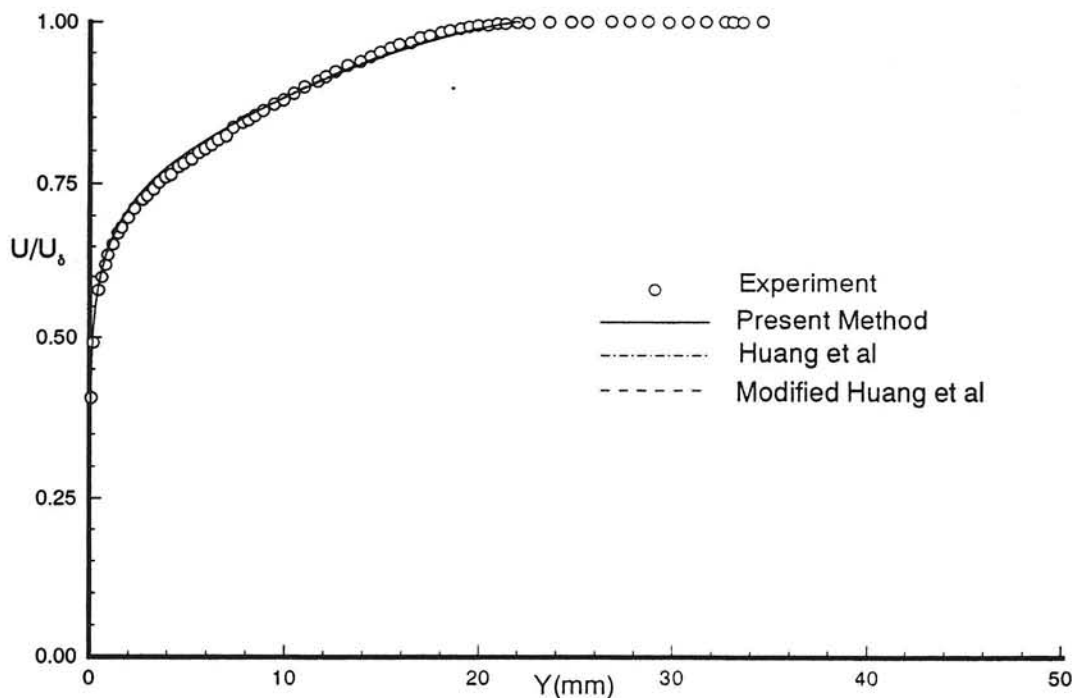


Fig. 10b Untransformed velocity profile in normal coordinates. Experimental data from Collins et al<sup>15</sup>,  $M_\delta = 0.9664$ ,  $Re_\delta = 18650$ , profile JPL-A-91.

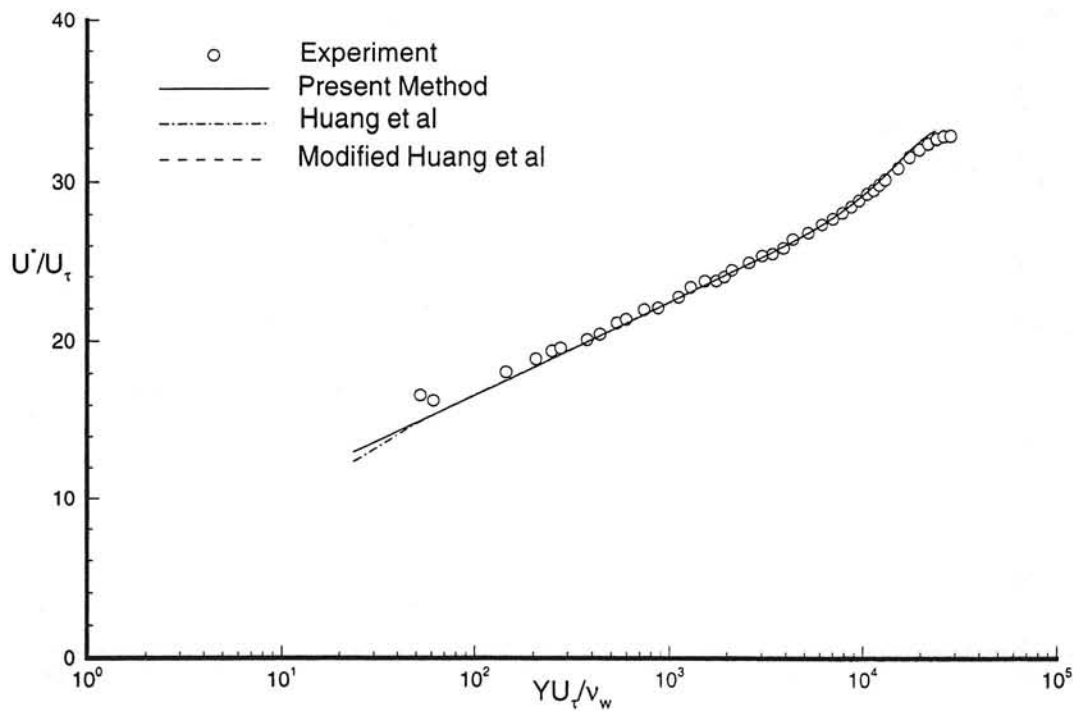


Fig. 11a Transformed velocity profile in semi-logarithmic coordinates. Experimental data from Winter & Gaudet<sup>13</sup>,  $M_\infty = 0.7904$ ,  $Re_\theta = 81000$ , profile 7.

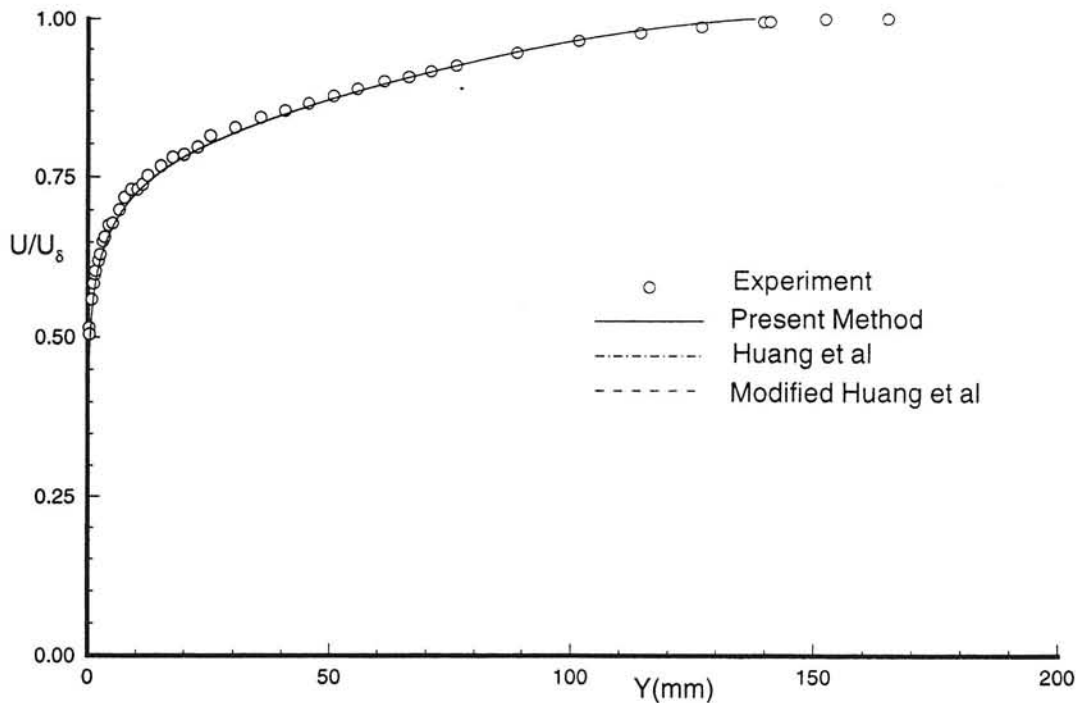


Fig. 11b Untransformed velocity profile in normal coordinates. Experimental data from Winter & Gaudet<sup>13</sup>,  $M_\delta = 0.7904$ ,  $Re_\delta = 81000$ , profile 7.

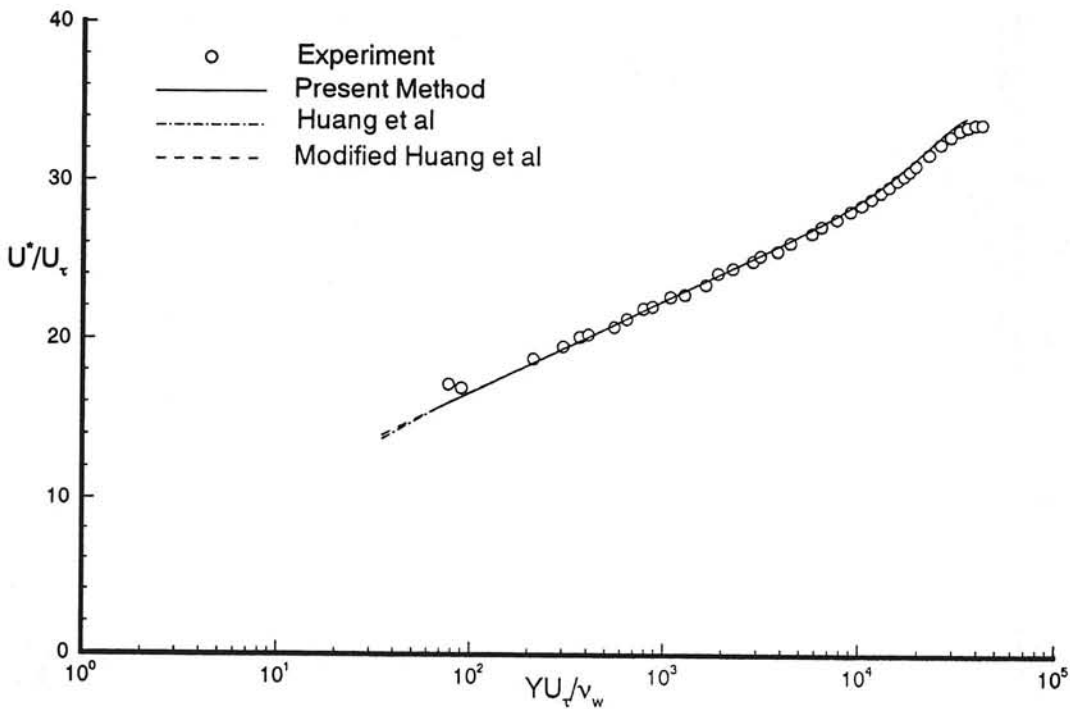


Fig. 12a Transformed velocity profile in semi-logarithmic coordinates. Experimental data from Winter & Gaudet<sup>13</sup>,  $M_\delta = 0.7930$ ,  $Re_\delta = 120366$ , profile 8.

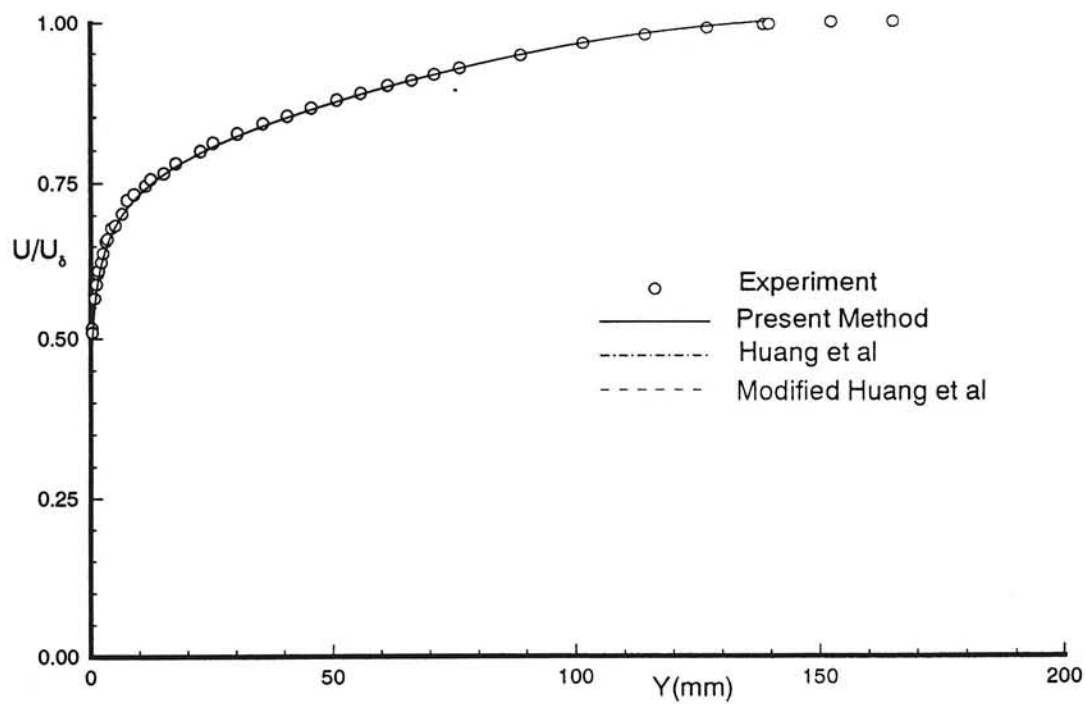


Fig. 12b Untransformed velocity profile in normal coordinates. Experimental data from Winter & Gaudet<sup>13</sup>,  $M_\delta = 0.7930$ ,  $Re_\delta = 120366$ , profile 8.

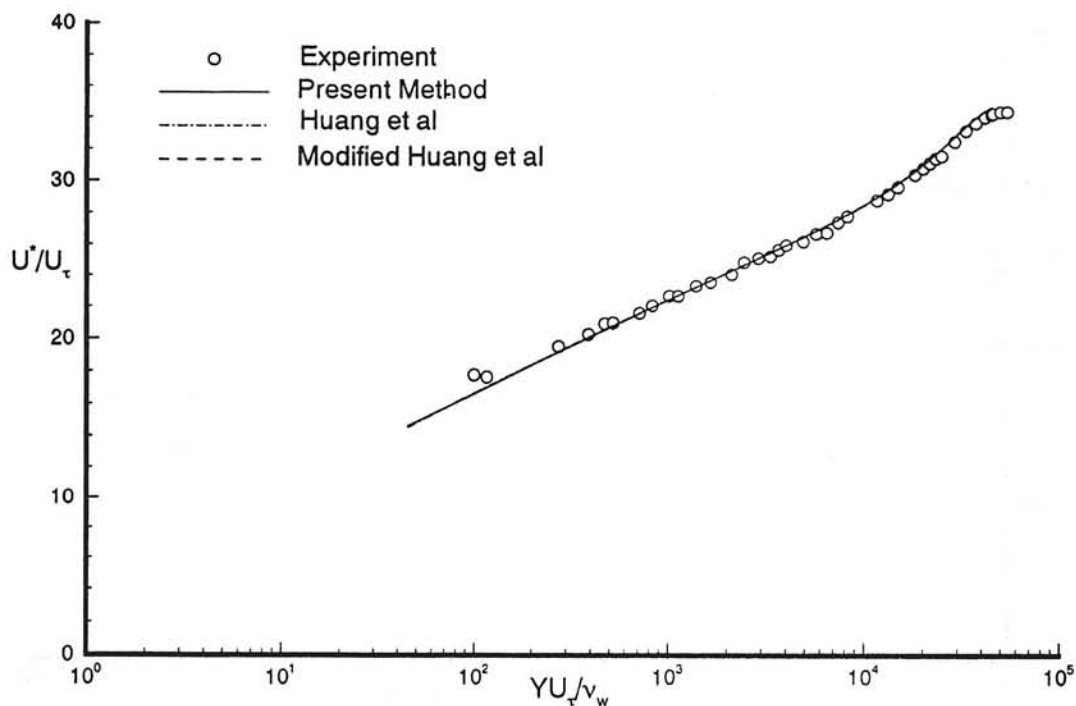


Fig. 13a Transformed velocity profile in semi-logarithmic coordinates. Experimental data from Winter & Gaudet<sup>13</sup>,  $M_\infty = 0.7933$ ,  $Rho_0 = 157450$ , profile 9.

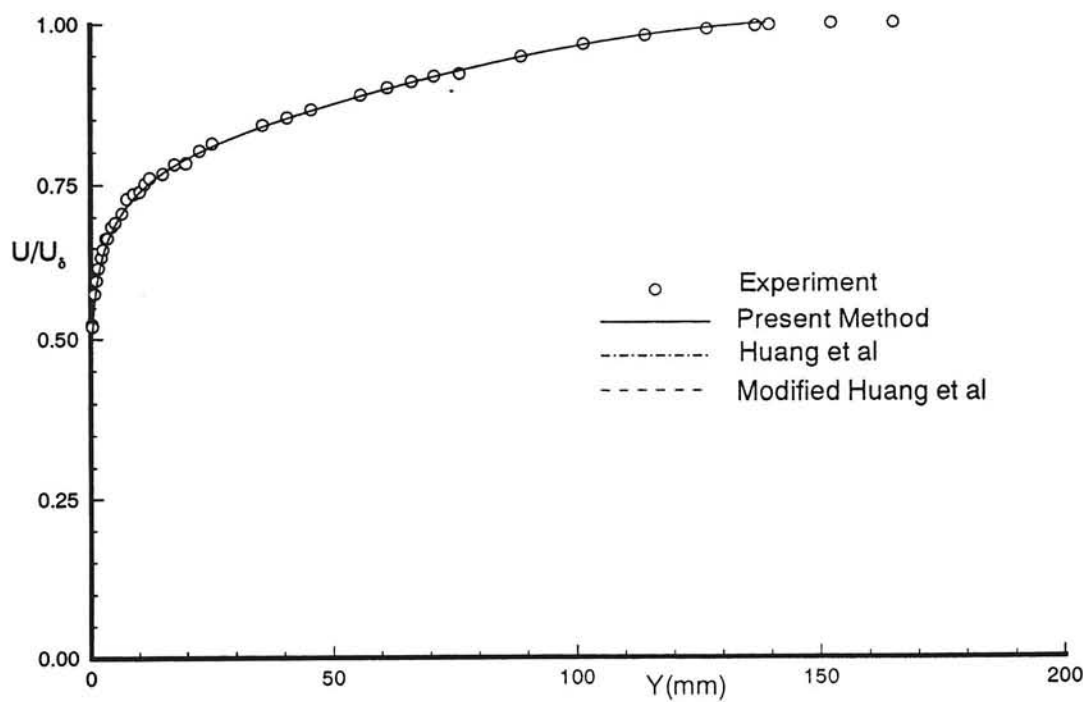


Fig. 13b Untransformed velocity profile in normal coordinates. Experimental data from Winter & Gaudet<sup>13</sup>,  $M_\delta = 0.7933$ ,  $Re_\delta = 157450$ , profile 9.

Fig. 14 Percent error in skin friction coefficient  $\Delta C_f = (1 - C_{f, \text{cal}}/C_{f, \text{exp}}) \times 100\%$ .  
Experimental data from Winter & Gaudet <sup>13</sup>,  $M_6 = 1.40$ .

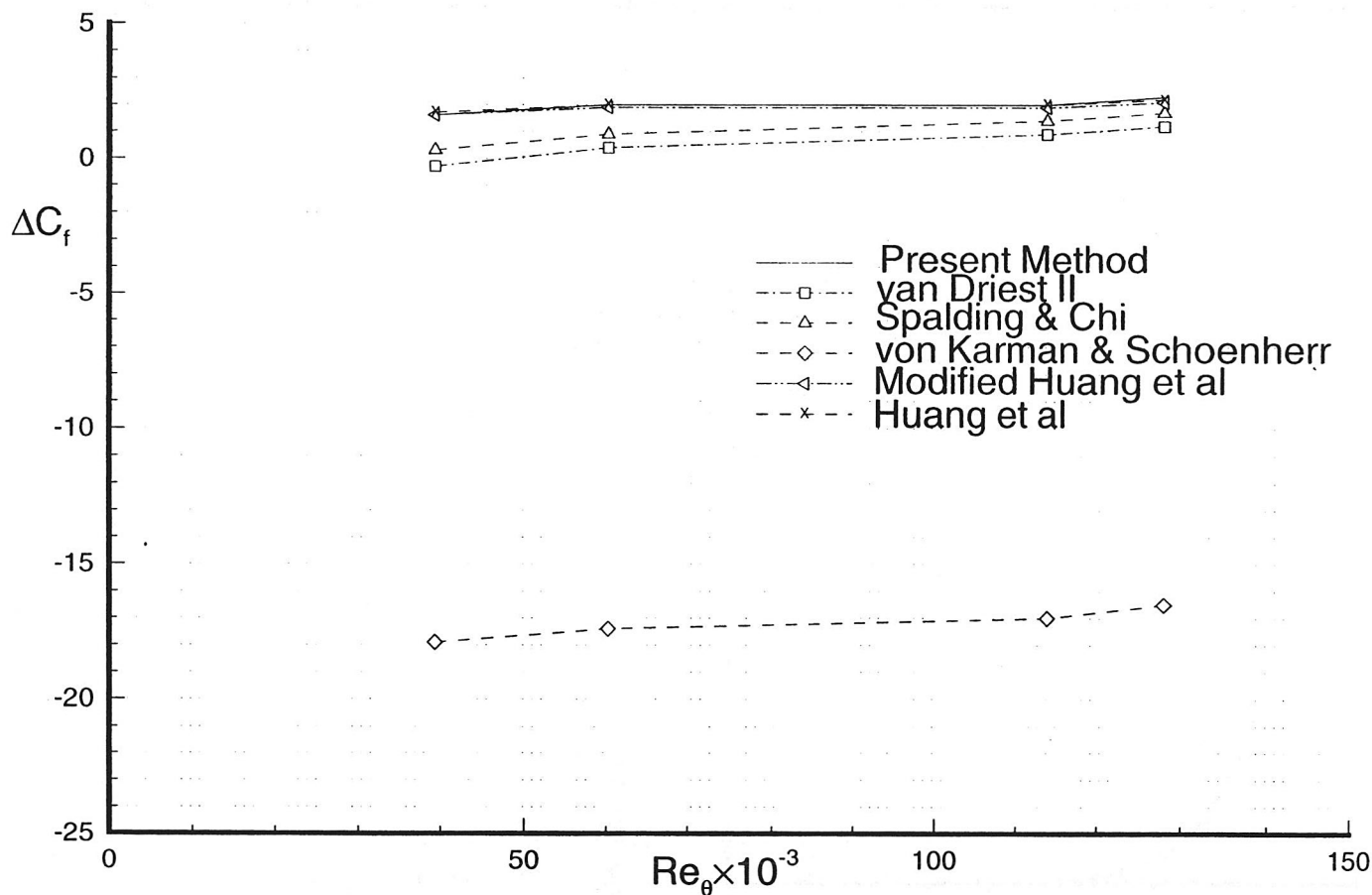
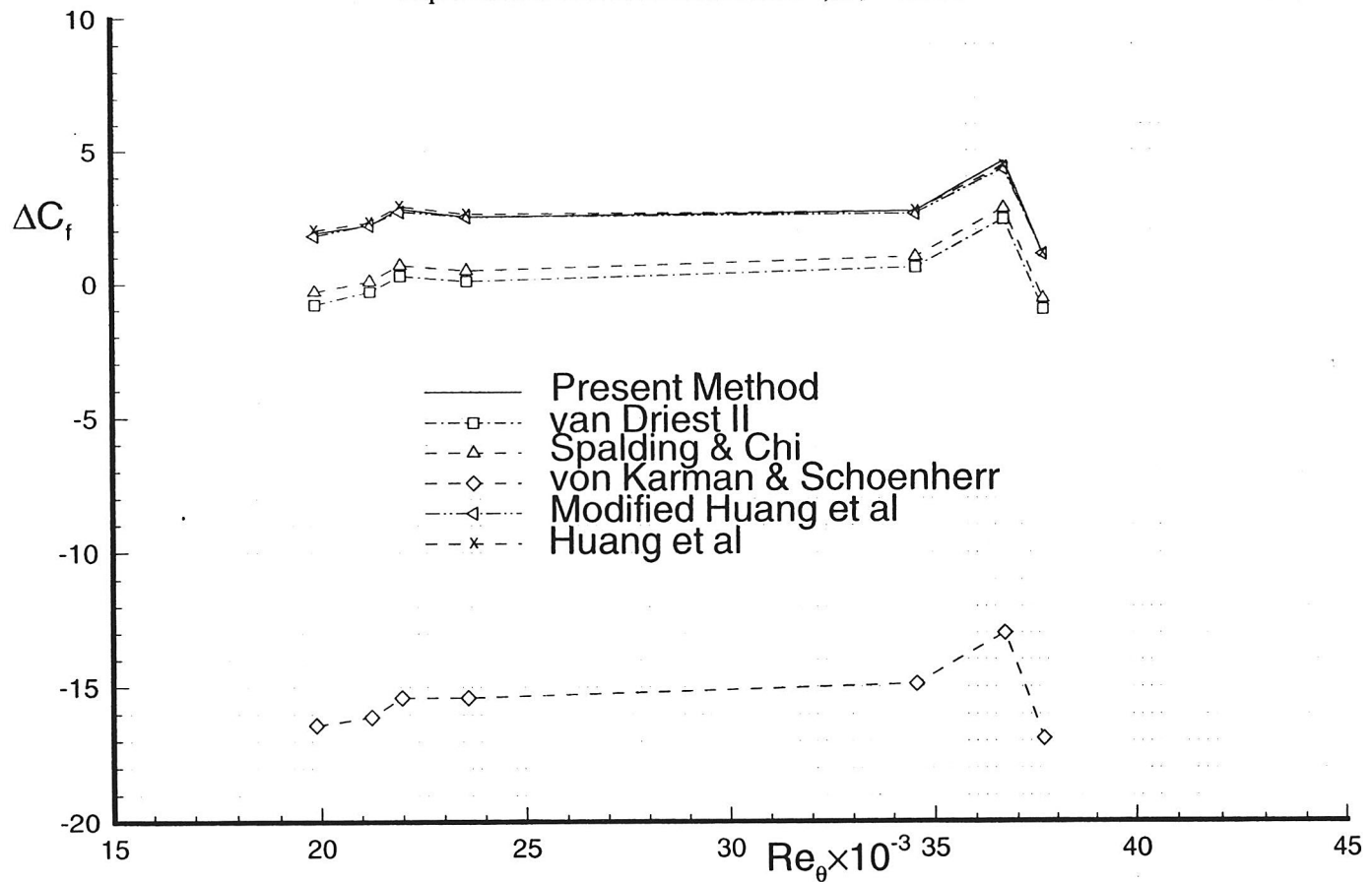


Fig. 15 Percent error in skin friction coefficient  $\Delta C_f = (1 - C_{f,cal}/C_{f,exp}) \times 100\%$ .  
 Experimental data from Collins et al<sup>15</sup>,  $M_\infty = 1.31$ .



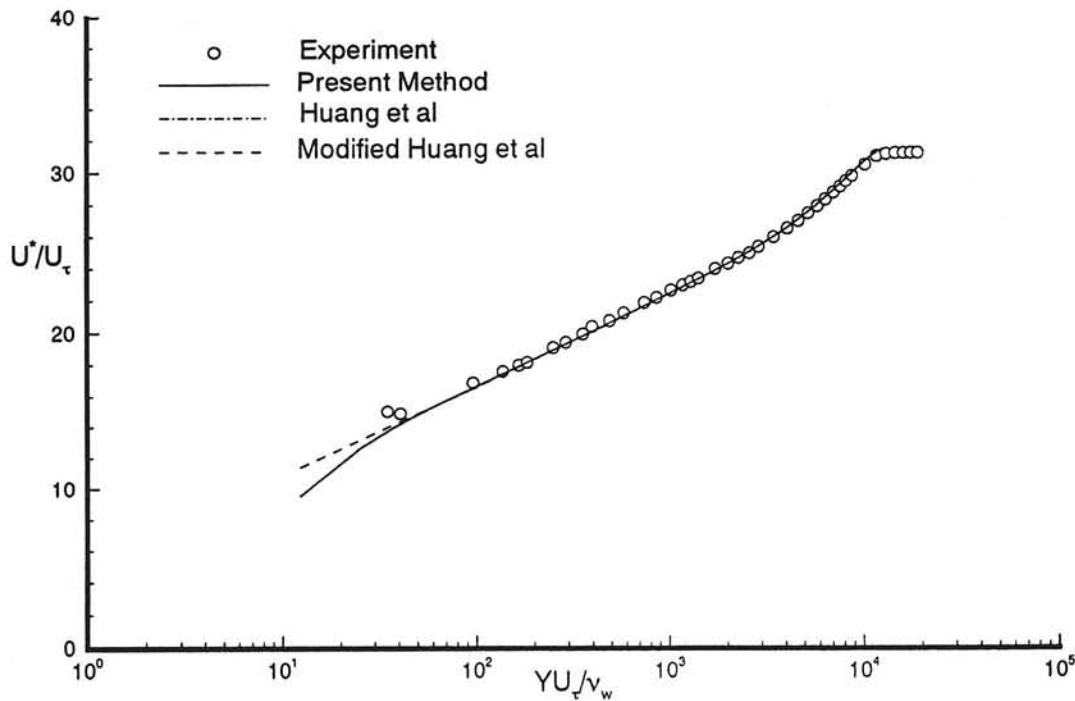


Fig. 16a Transformed velocity profile in semi-logarithmic coordinates. Experimental data from Winter & Gaudet<sup>13</sup>,  $M_\infty = 1.5970$ ,  $Re_0 = 56479$ , profile 15.

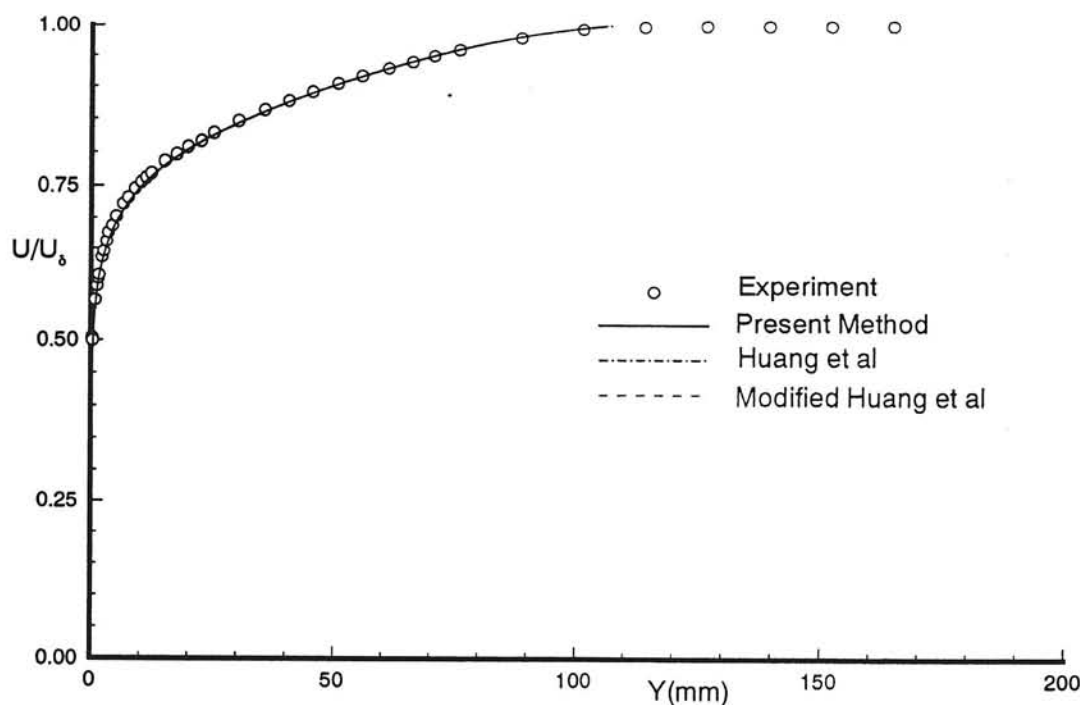


Fig. 16b Untransformed velocity profile in normal coordinates. Experimental data from Winter & Gaudet<sup>13</sup>,  $M_\delta = 1.5970$ ,  $Re_0 = 56479$ , profile 15.

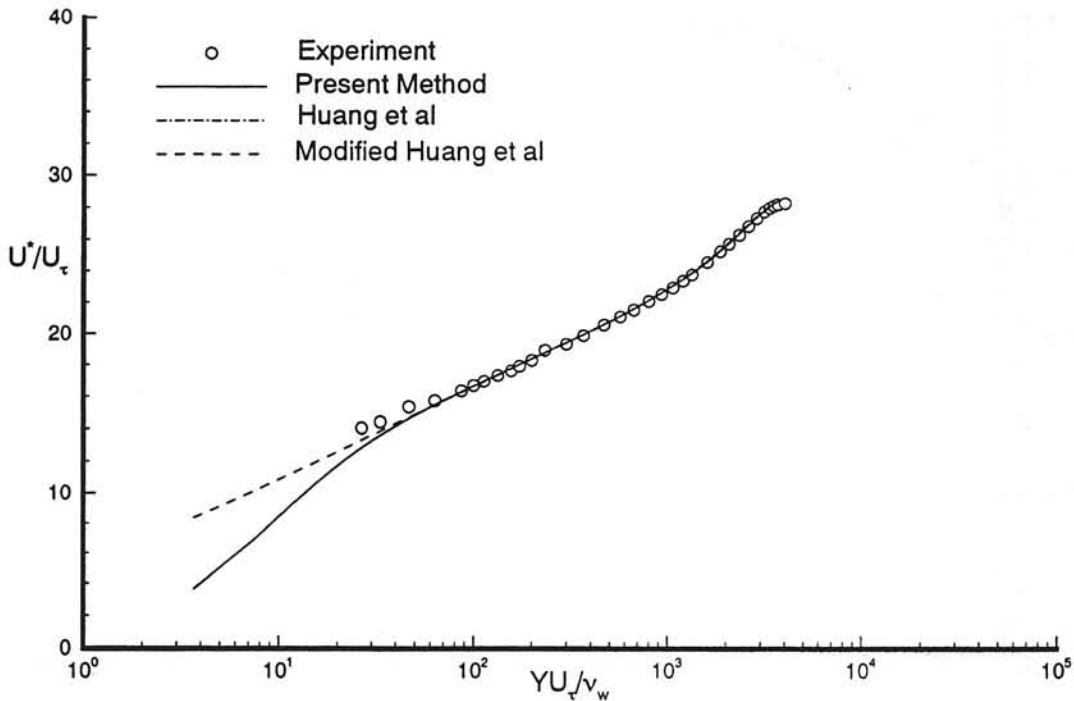


Fig. 17a Transformed velocity profile in semi-logarithmic coordinates. Experimental data from Morkovin & Phinney<sup>24</sup>,  $M_\delta = 1.770$ ,  $Re_\theta = 17672$ , case 58060101.

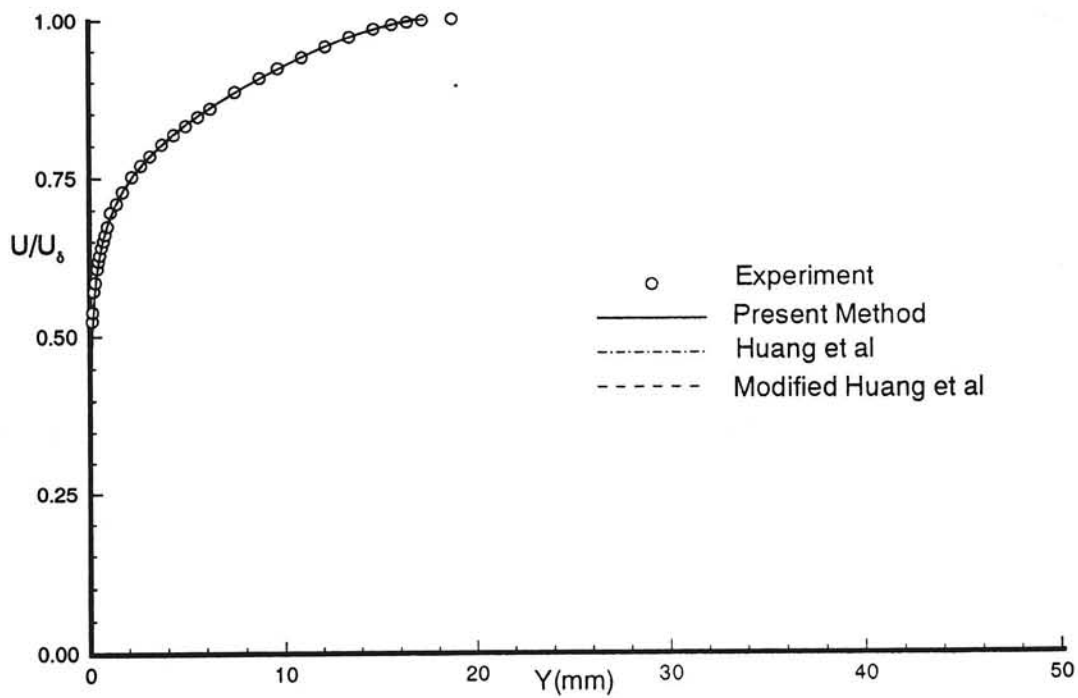


Fig. 17b Untransformed velocity profile in normal coordinates. Experimental data from Morkovin<sup>24</sup>,  $M_\delta = 1.770$ ,  $Re_\delta = 17672$ , case 58060101.

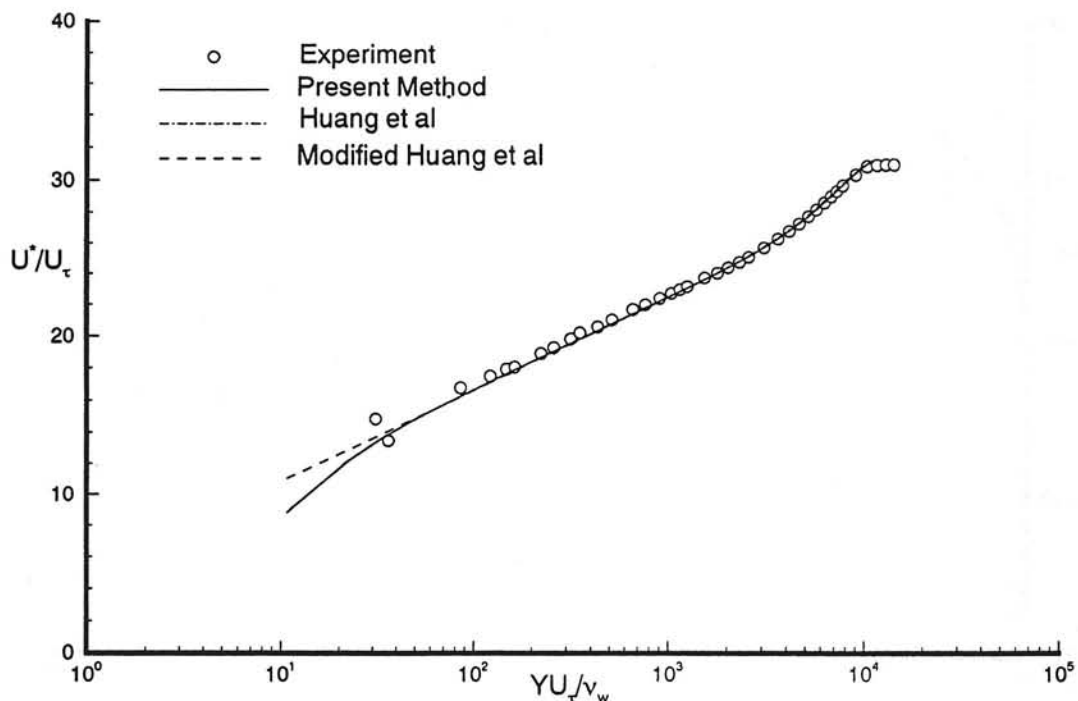


Fig. 18a Transformed velocity profile in semi-logarithmic coordinates. Experimental data from Winter & Gaudet<sup>13</sup>,  $M_\infty = 1.8002$ ,  $Re_\delta = 53671$ , profile 16.

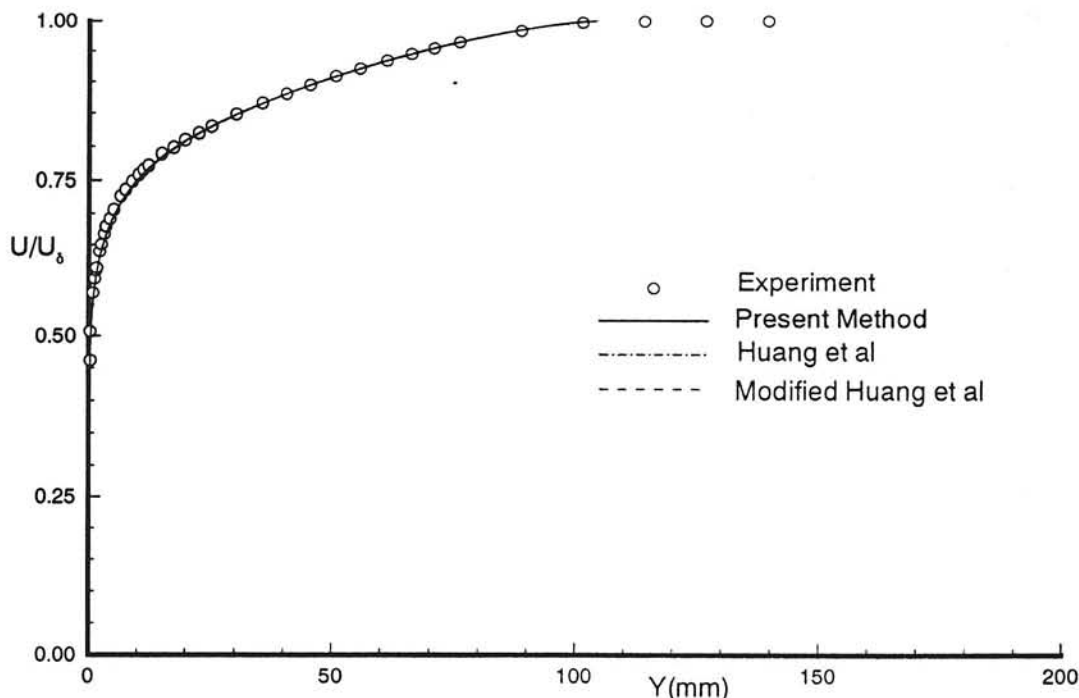


Fig. 18b Untransformed velocity profile in normal coordinates. Experimental data from Winter & Gaudet<sup>13</sup>,  $M_\delta = 1.5970$ ,  $R\delta_0 = 56479$ , profile 16.

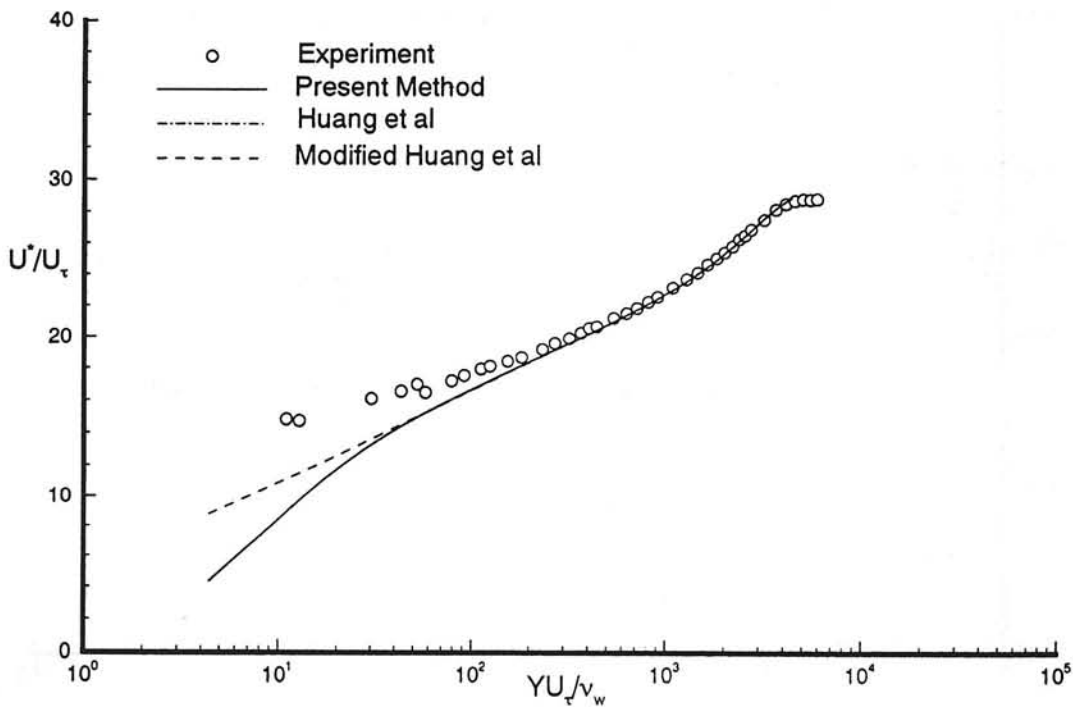


Fig. 19a Transformed velocity profile in semi-logarithmic coordinates. Experimental data from Winter & Gaudet<sup>13</sup>,  $M_\infty = 1.3943$ ,  $Re_0 = 17914$ , profile 10.

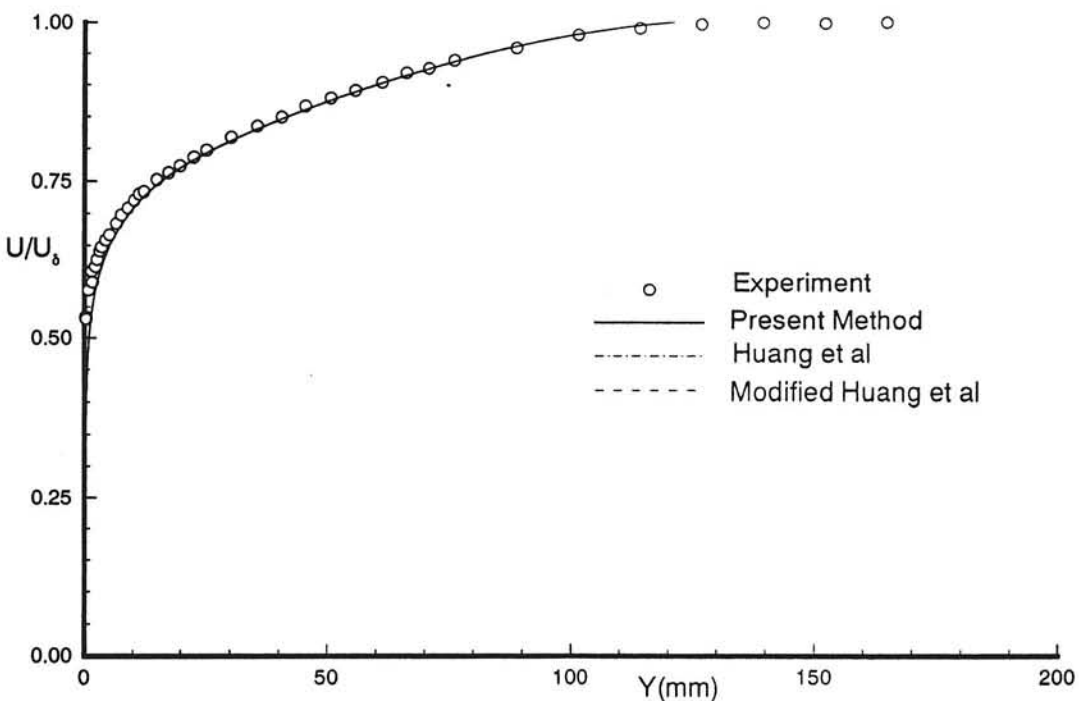


Fig. 19b Untransformed velocity profile in normal coordinates. Experimental data from Winter & Gaudet<sup>13</sup>,  $M_\delta = 1.3943$ ,  $Re_\delta = 17914$ , profile 10.

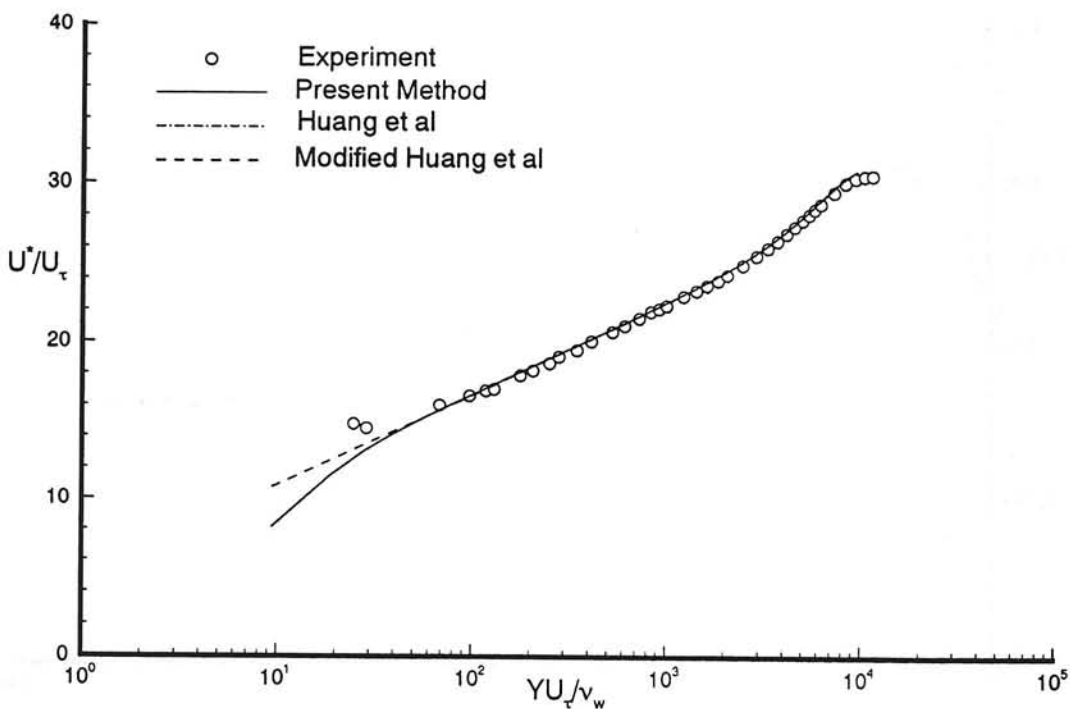


Fig. 20a Transformed velocity profile in semi-logarithmic coordinates. Experimental data from Winter & Gaudet<sup>13</sup>,  $M_\infty = 1.3951$ ,  $Re_\infty = 39333$ , profile 11.

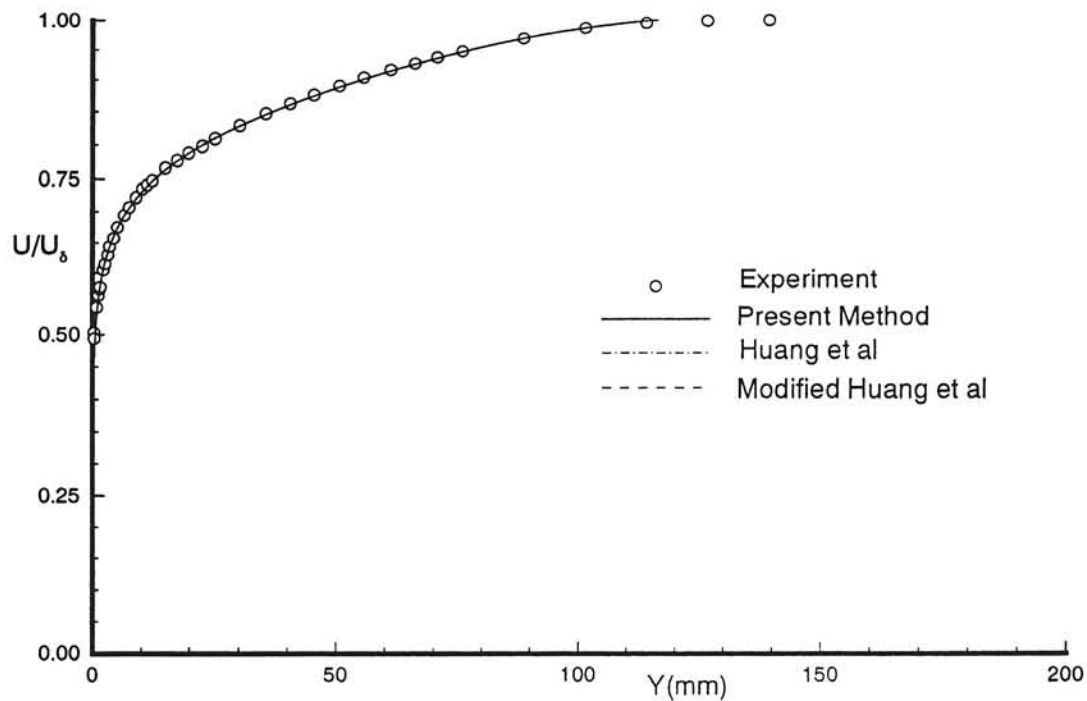


Fig. 20b Untransformed velocity profile in normal coordinates. Experimental data from Winter & Gaudet<sup>13</sup>,  $M_\delta = 1.3951$ ,  $Re_\delta = 39333$ , profile 11.

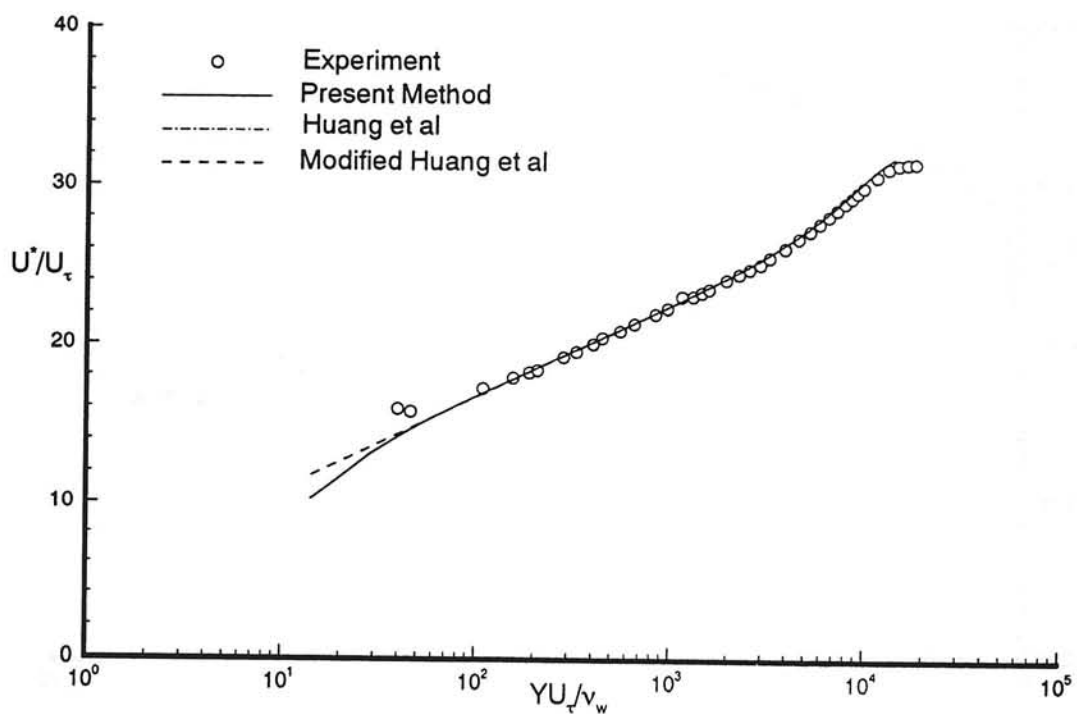


Fig. 21a Transformed velocity profile in semi-logarithmic coordinates. Experimental data from Winter & Gaudet<sup>13</sup>,  $M_\infty = 1.4003$ ,  $Re_\infty = 60234$ , profile 12.

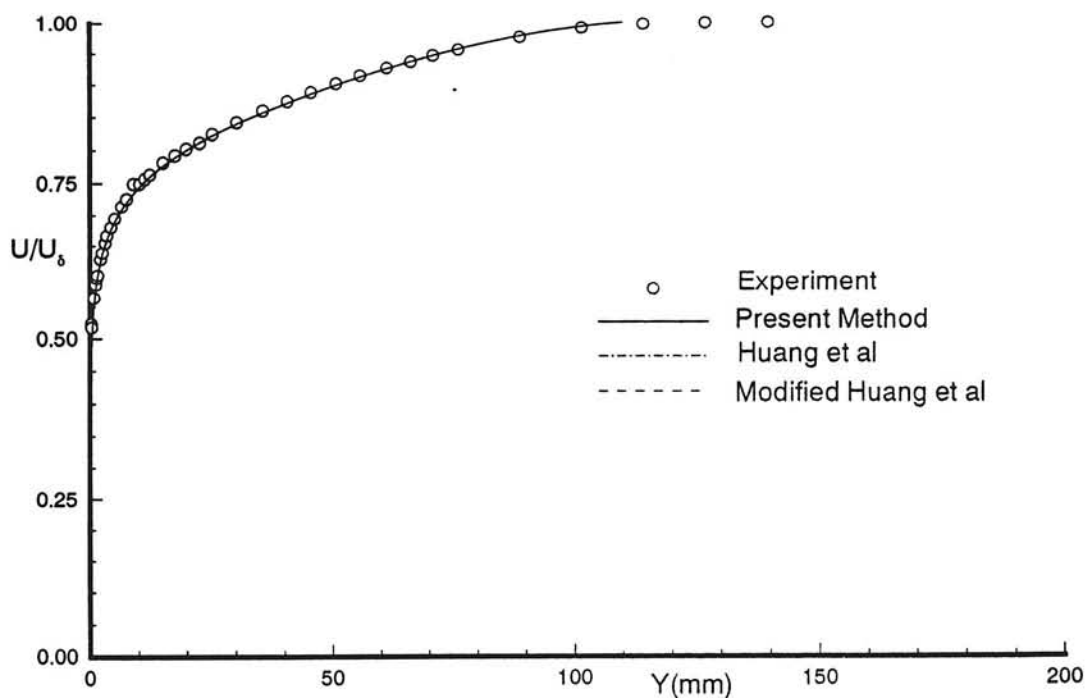


Fig. 21b Untransformed velocity profile in normal coordinates. Experimental data from Winter & Gaudet<sup>13</sup>,  $M_b = 1.4003$ ,  $R\alpha_0 = 60234$ , profile 12.

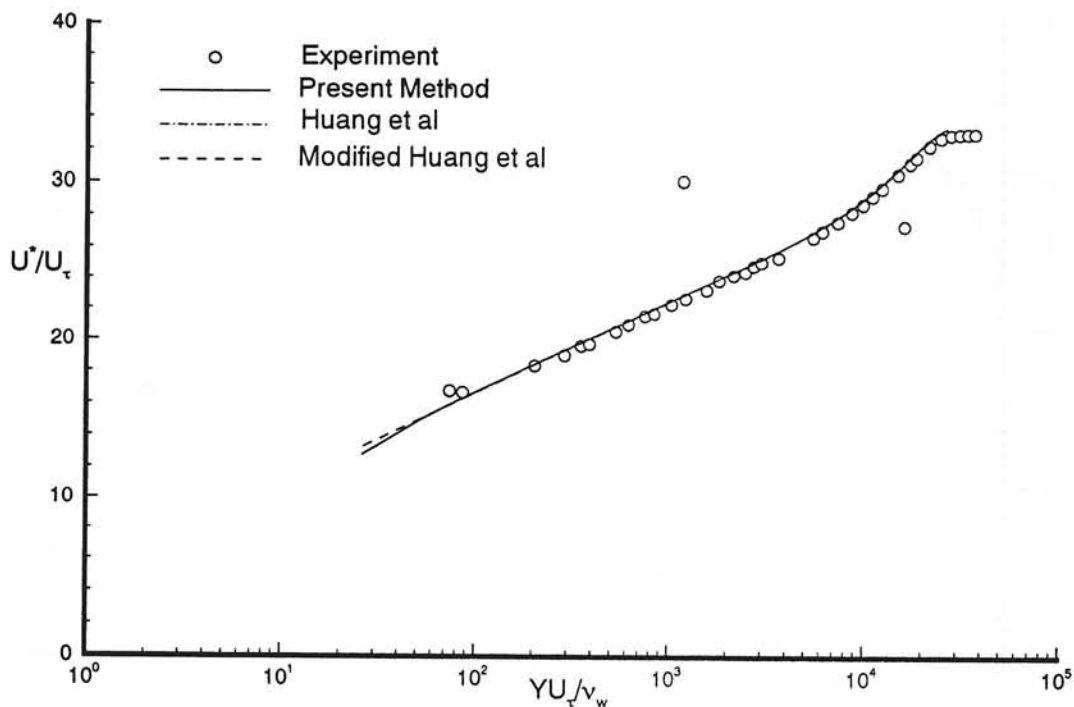


Fig. 22a Transformed velocity profile in semi-logarithmic coordinates. Experimental data from Winter & Gaudet<sup>13</sup>,  $M_\delta = 1.3999$ ,  $Re_\delta = 113948$ , profile 13.

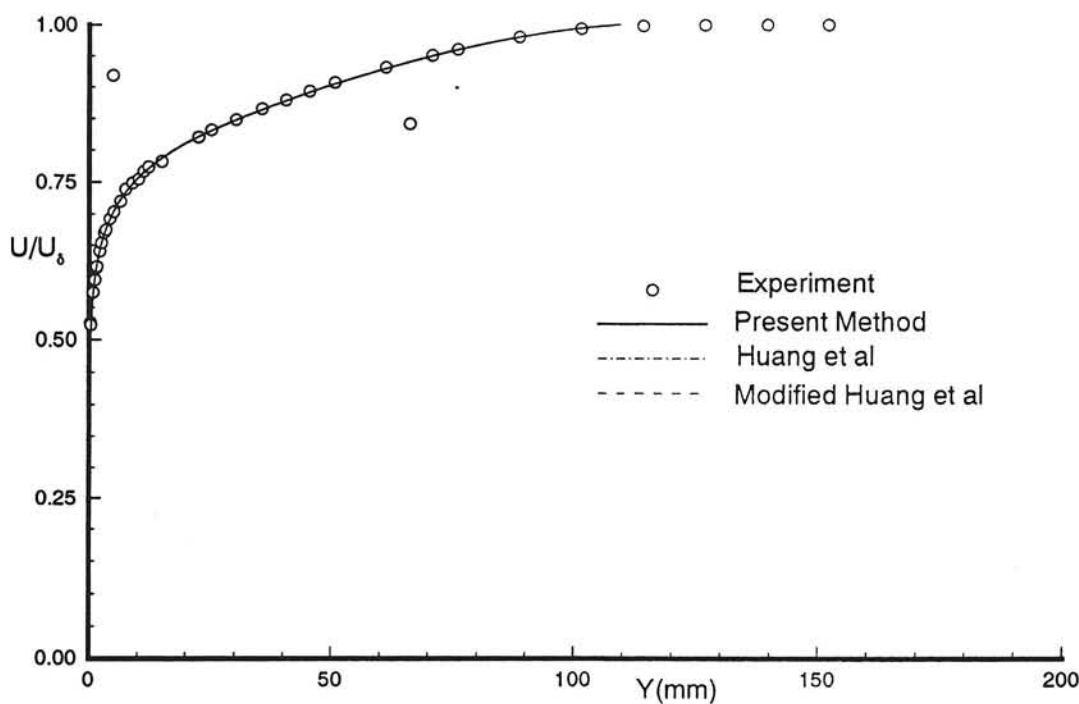


Fig. 22b Untransformed velocity profile in normal coordinates. Experimental data from Winter & Gaudet<sup>13</sup>,  $M_\delta = 1.3999$ ,  $Re_\delta = 113948$ , profile 13.

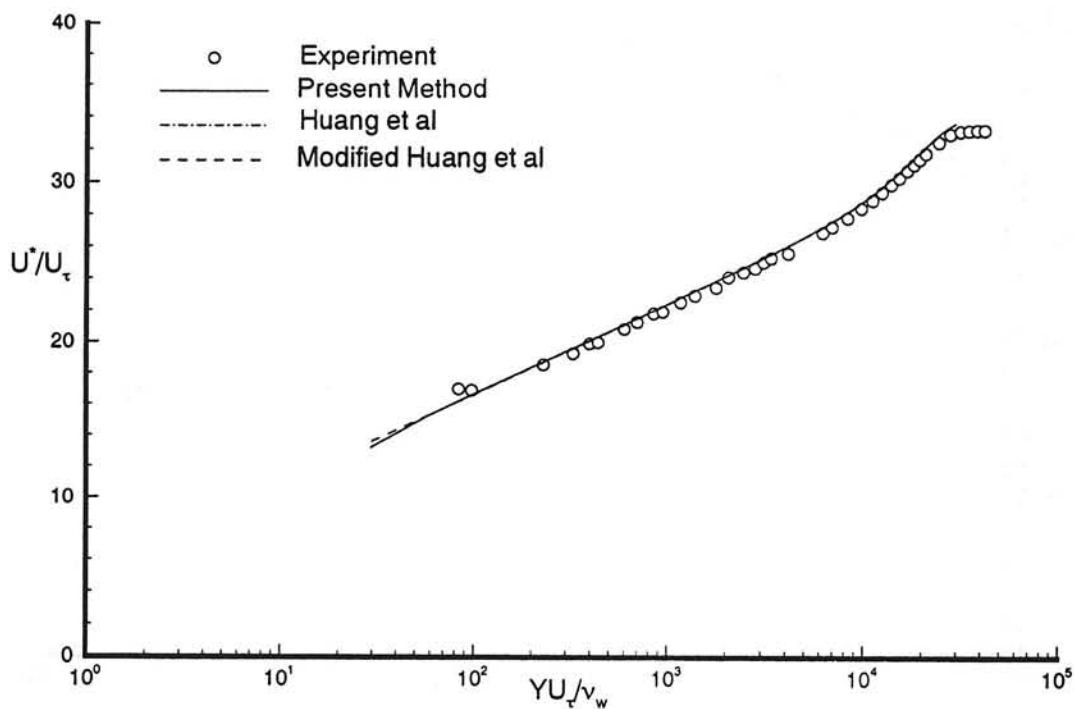


Fig. 23a Transformed velocity profile in semi-logarithmic coordinates. Experimental data from Winter & Gaudet<sup>13</sup>,  $M_b = 1.4003$ ,  $Re_b = 128035$ , profile 14.

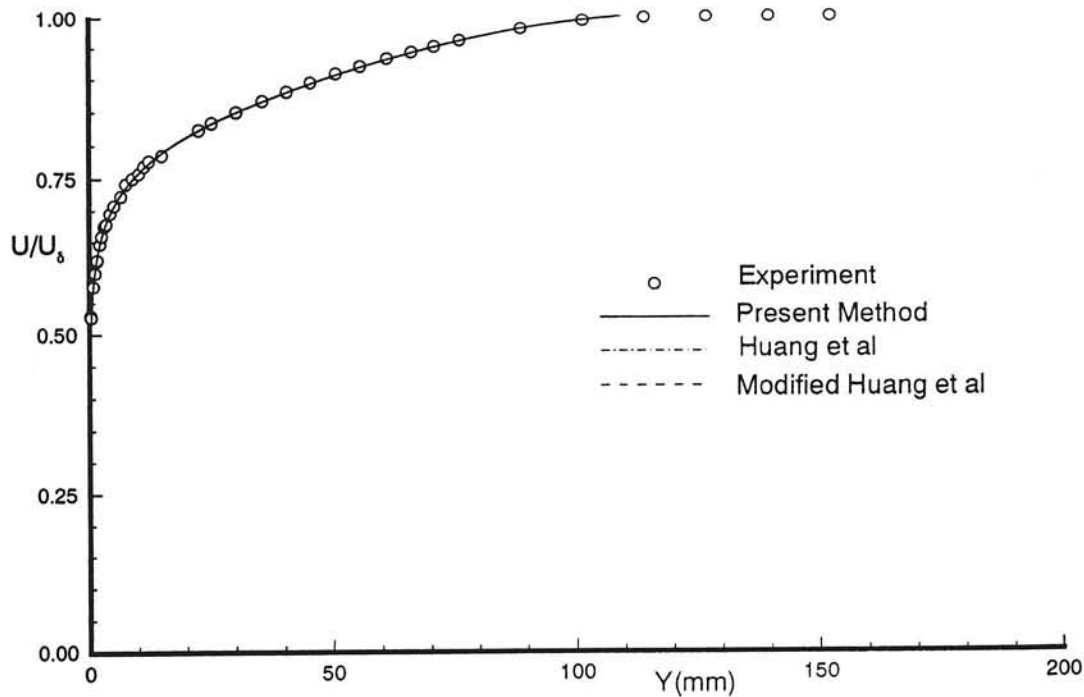


Fig. 23b Untransformed velocity profile in normal coordinates. Experimental data from Winter & Gaudet<sup>13</sup>,  $M_\delta = 1.4003$ ,  $Re_\delta = 128035$ , profile 14.

Fig. 24 Percent error in skin friction coefficient  $\Delta C_f = (1 - C_{f, \text{cal}} / C_{f, \text{exp}}) \times 100\%$ . Experimental data from Winter & Gaudet<sup>13</sup>,  $M_\infty = 2.20$ , profiles 18 to 21.

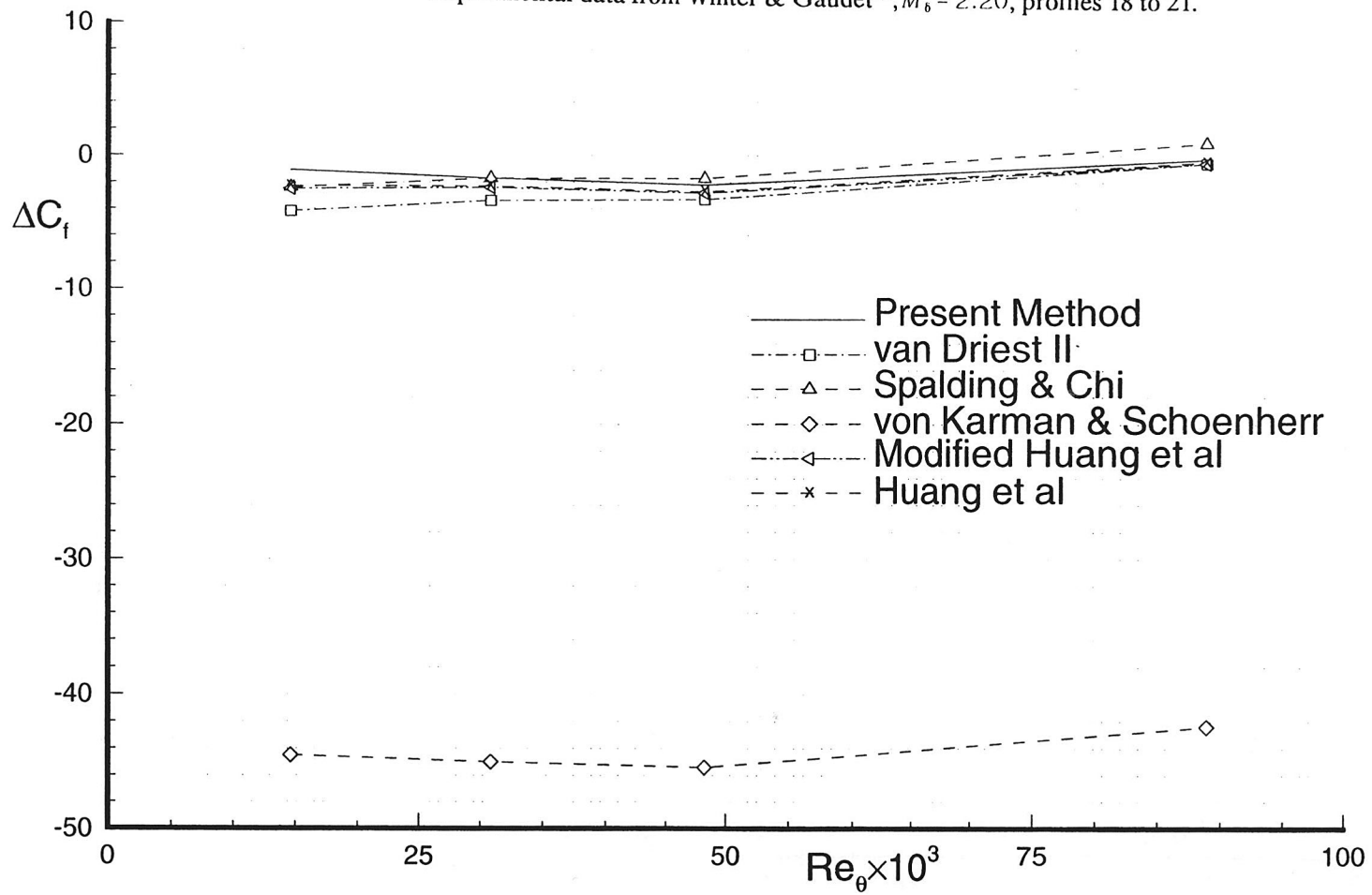


Fig. 25 Percent error in skin friction coefficient  $\Delta C_f = (1 - C_{f,cal}/C_{f,exp}) \times 100\%$ .  
 Experimental data from Moore & Harkness<sup>23</sup>,  $M_\infty = 2.90$ , case 6502.

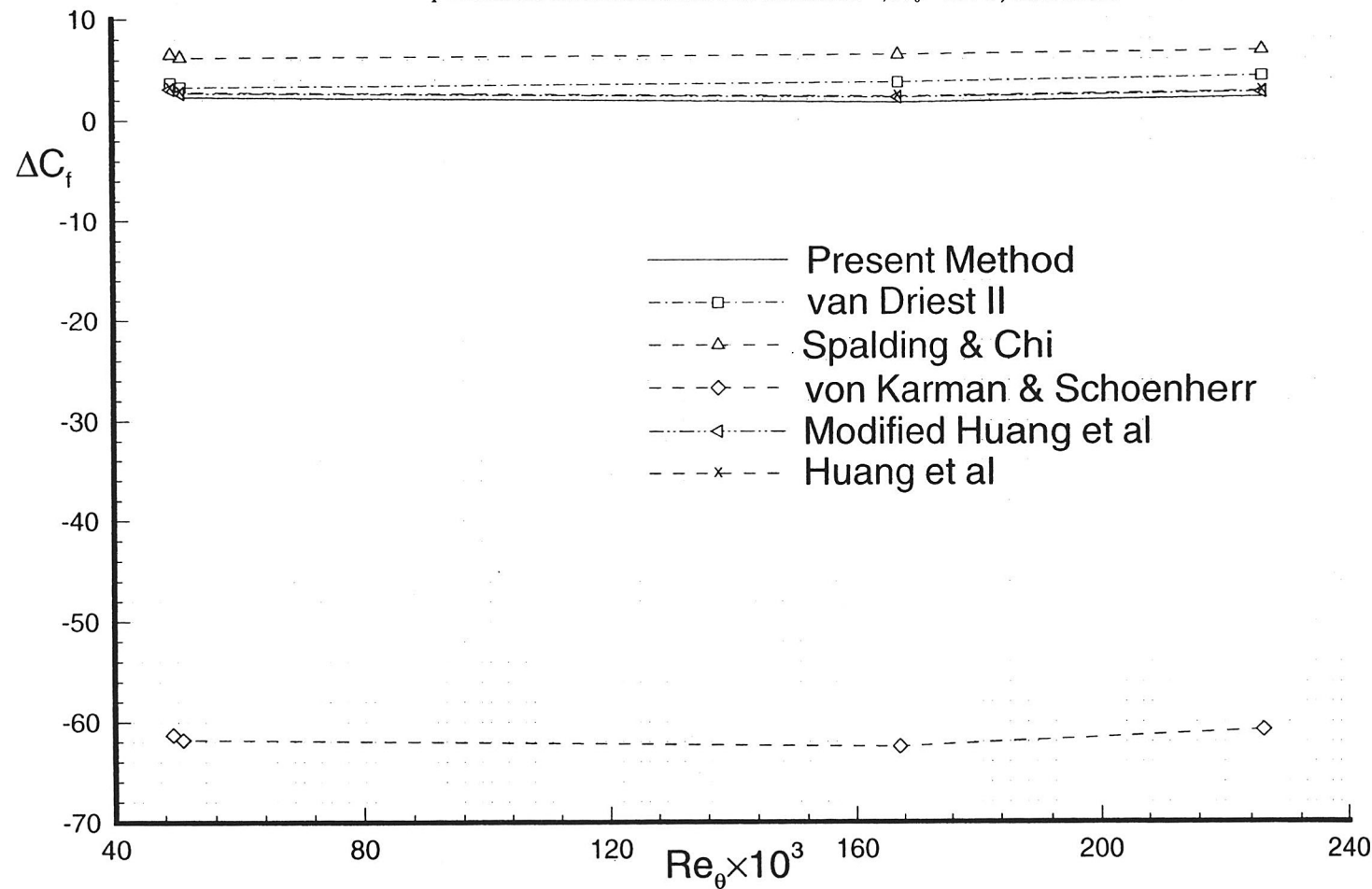
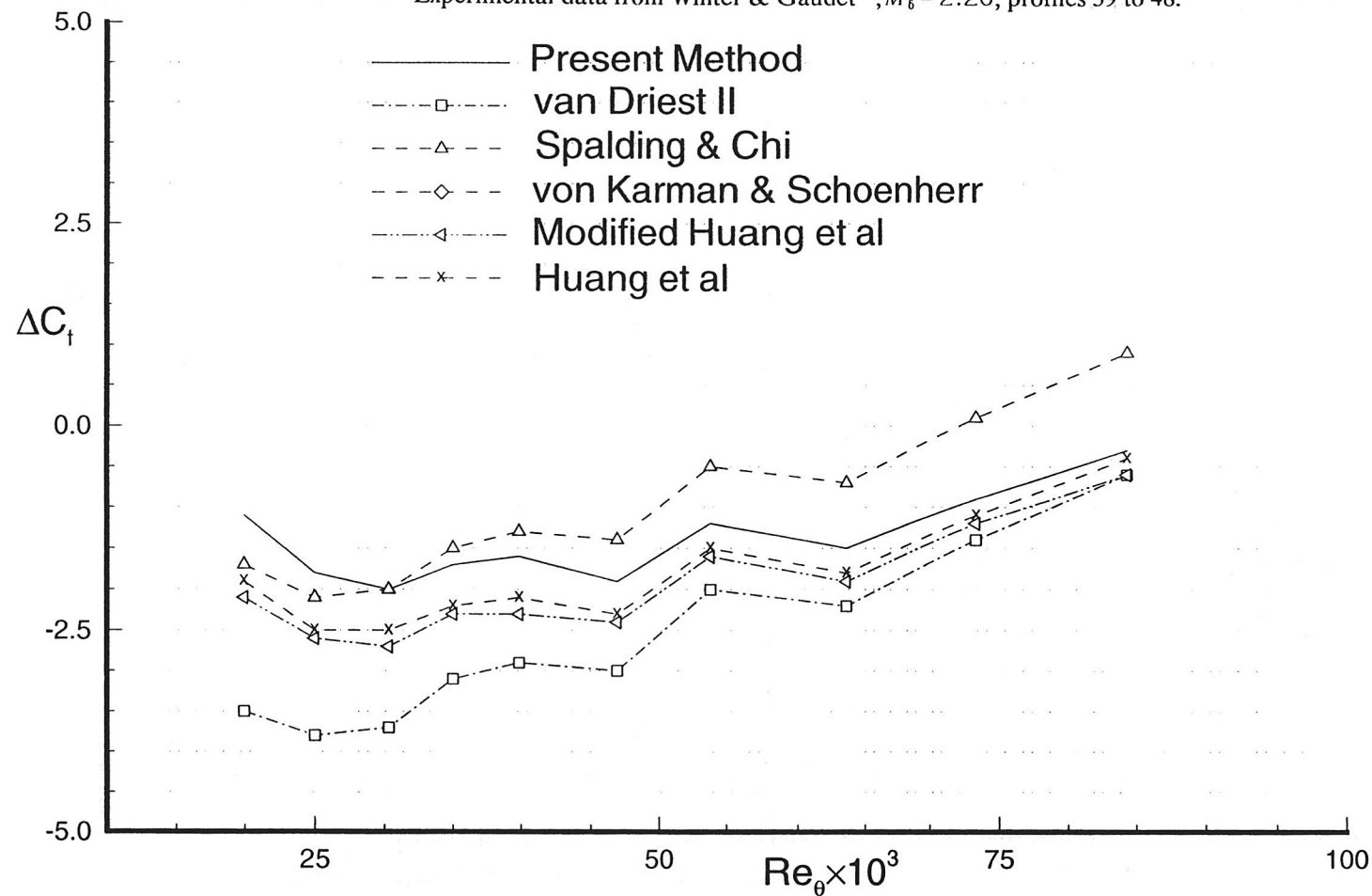


Fig. 26 Percent error in skin friction coefficient  $\Delta C_f = (1 - C_{f,cal}/C_{f,exp}) \times 100\%$ .  
 Experimental data from Winter & Gaudet<sup>13</sup>,  $M_\infty = 2.20$ , profiles 39 to 48.



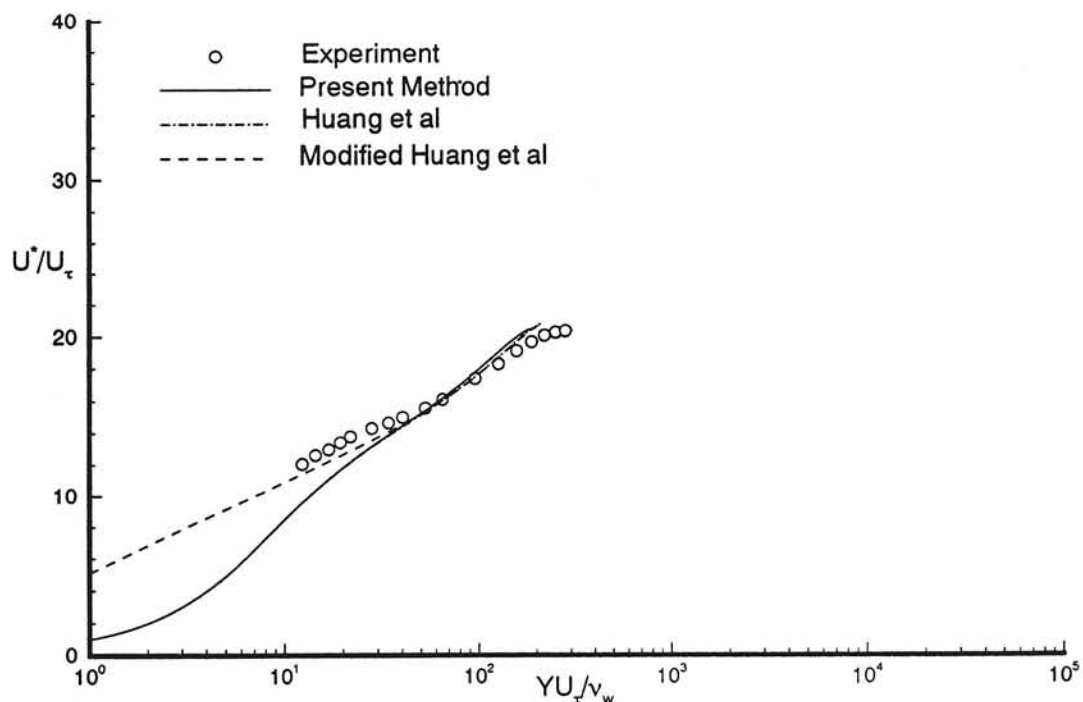


Fig. 27a Transformed velocity profile in semi-logarithmic coordinates. Experimental data from Stalmach<sup>23</sup>,  $M_\delta = 3.6840$ ,  $Re_\delta = 2115.3$ , case 58020301.

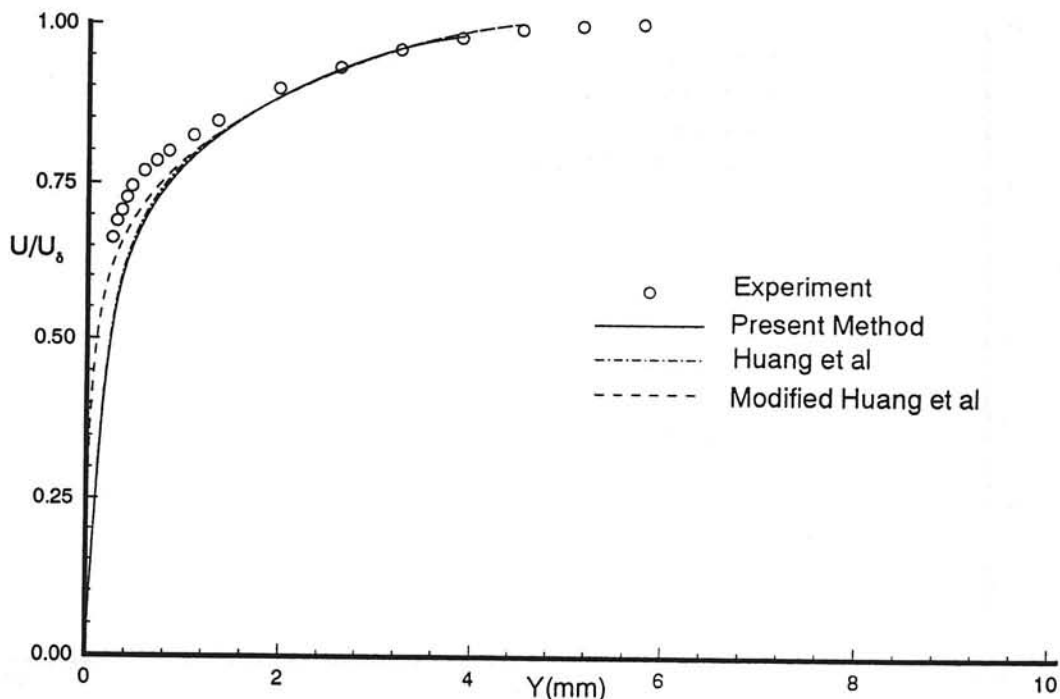


Fig. 27b Untransformed velocity profile in normal coordinates. Experimental data from Stalmach<sup>23</sup>,  $M_\delta = 3.6840$ ,  $Re_\delta = 2115.3$ , case 58020301.

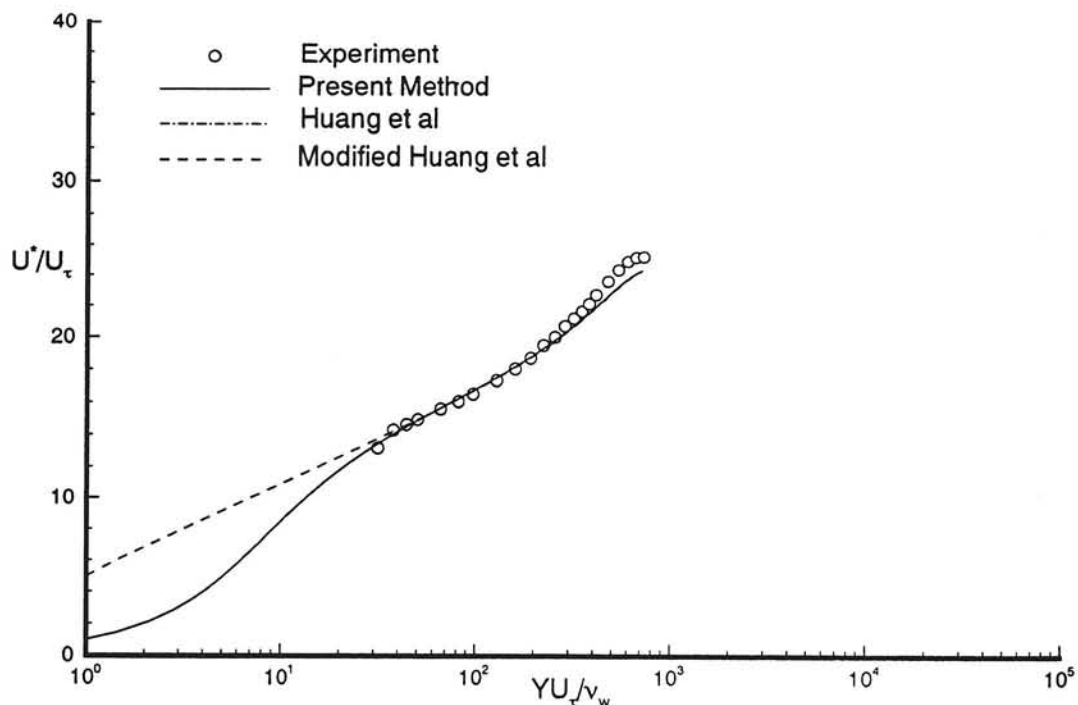


Fig. 28a Transformed velocity profile in semi-logarithmic coordinates. Experimental data from Stalmach<sup>23</sup>,  $M_\infty = 3.6670$ ,  $Re_\infty = 8134.9$ , case 58020304.

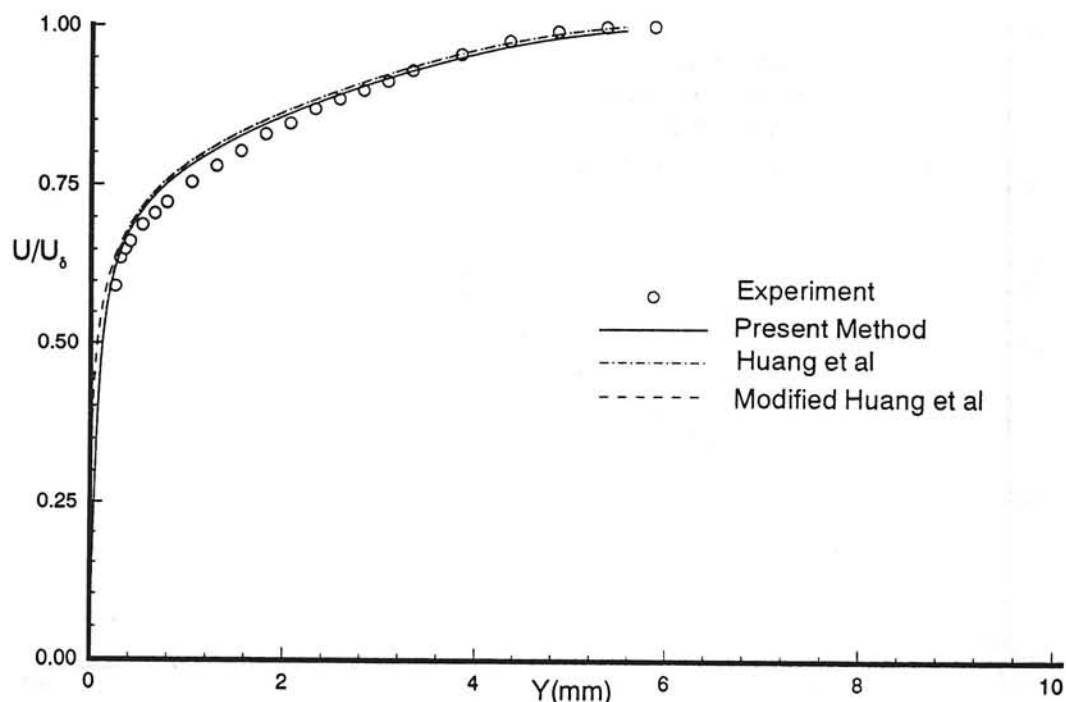


Fig. 28b Untransformed velocity profile in normal coordinates. Experimental data from Stalmach<sup>23</sup>,  $M_\delta = 3.6670$ ,  $Re_\delta = 8134.9$ , case 58020304.

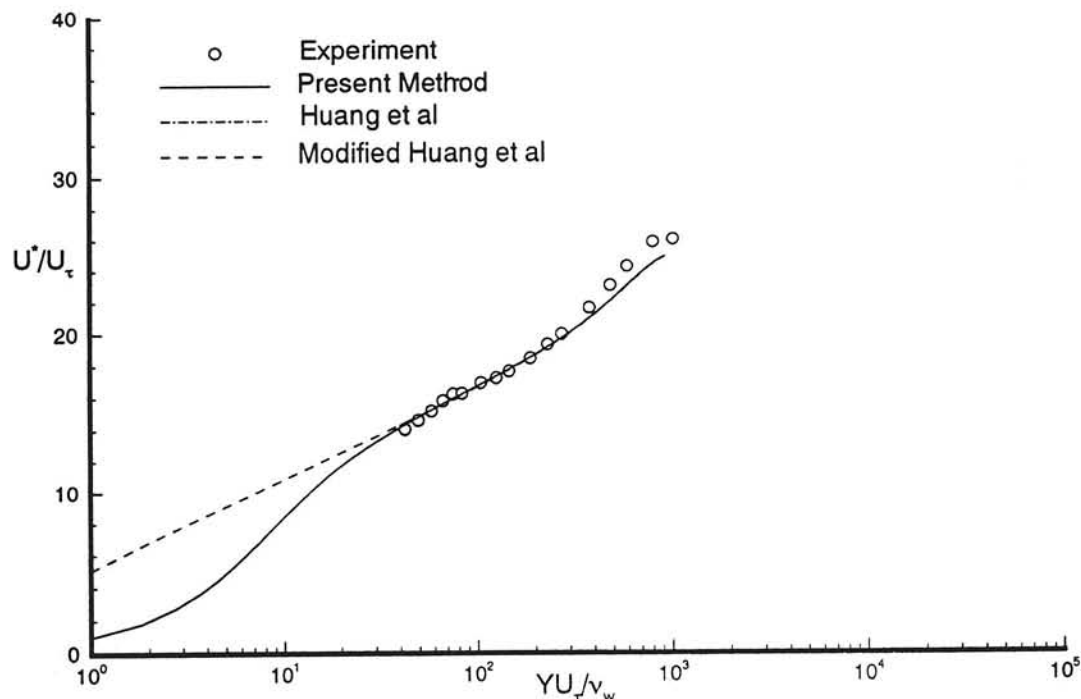


Fig. 29a Transformed velocity profile in semi-logarithmic coordinates. Experimental data from Stalmach<sup>23</sup>,  $M_\infty = 3.681$ ,  $Re_\infty = 10484$ , case 58020306.

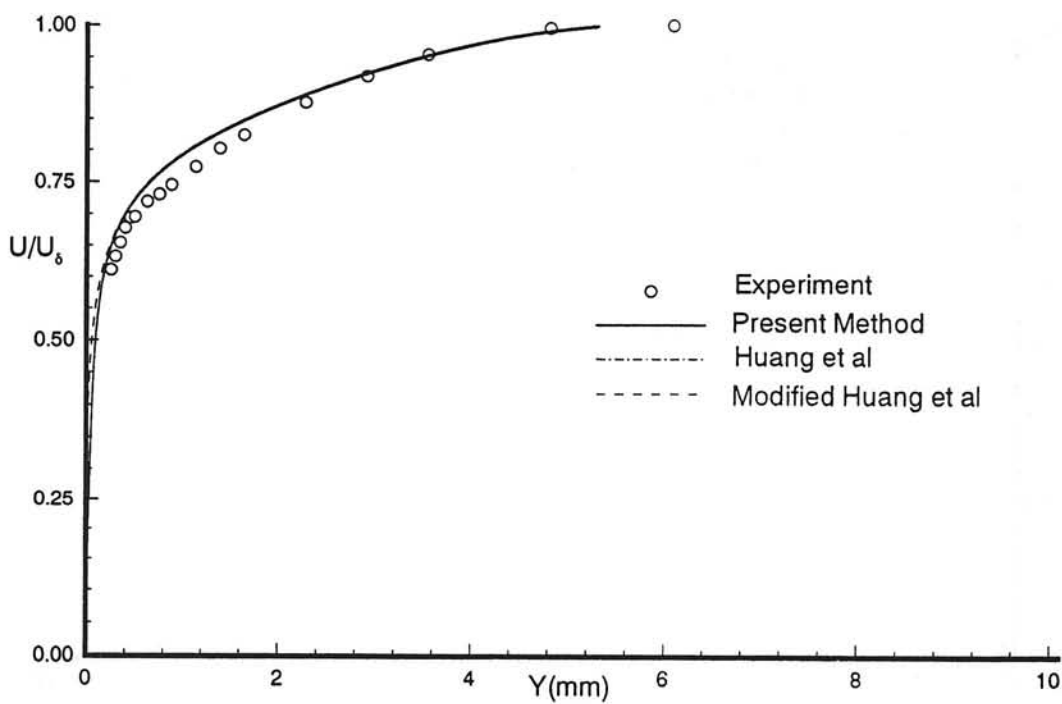


Fig. 29b Untransformed velocity profile in normal coordinates. Experimental data from Stalmach<sup>23</sup>,  $M_\delta = 3.681$ ,  $Re_\delta = 10484$ , case 58020306.

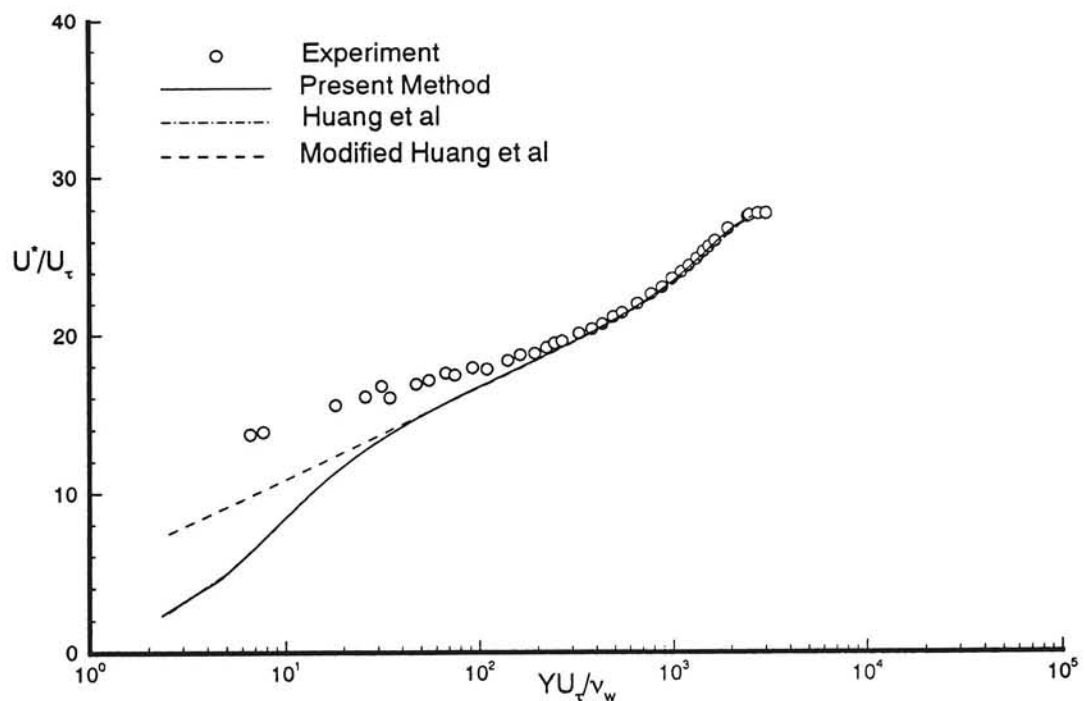


Fig. 30a Transformed velocity profile in semi-logarithmic coordinates. Experimental data from Winter & Gaudet<sup>13</sup>,  $M_\infty = 2.1865$ ,  $Re_\infty = 14640$ , profile 18.

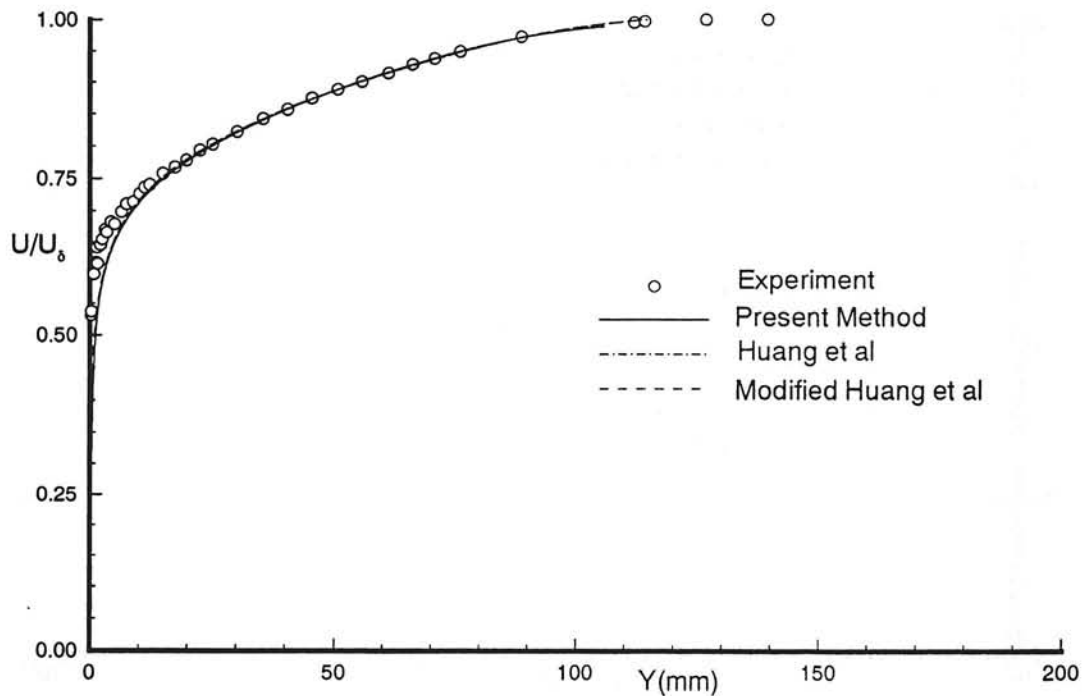


Fig. 30b Untransformed velocity profile in normal coordinates. Experimental data from Winter & Gaudet<sup>13</sup>,  $M_\infty = 2.1865$ ,  $Re_\delta = 14640$ , profile 18.

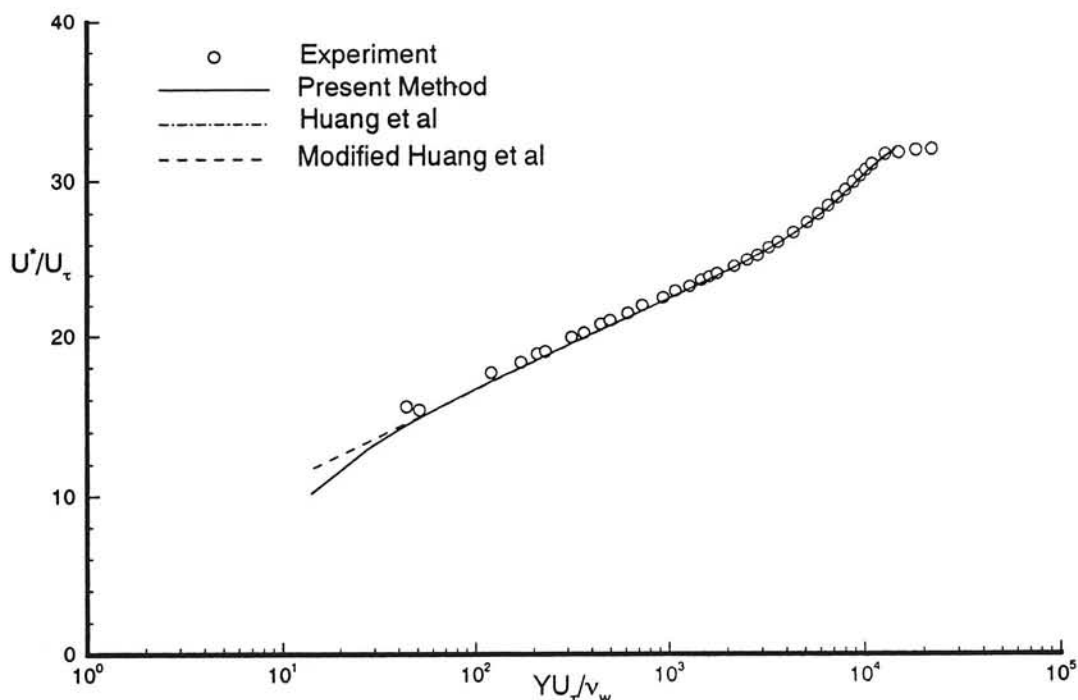


Fig. 31a Transformed velocity profile in semi-logarithmic coordinates. Experimental data from Winter & Gaudet<sup>13</sup>,  $M_\infty = 2.2064$ ,  $Re_\theta = 88907$ , profile 21.

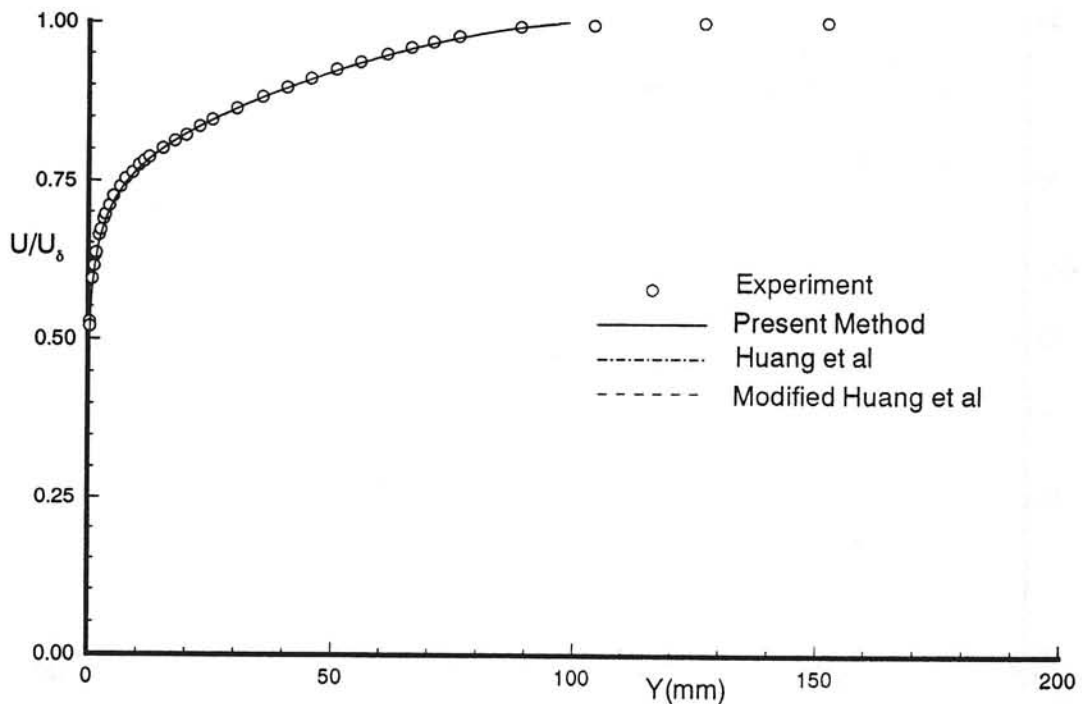


Fig. 31b Untransformed velocity profile in normal coordinates. Experimental data from Winter & Gaudet<sup>13</sup>,  $M_\infty = 2.2064$ ,  $R\delta_0 = 88907$ , profile 21.

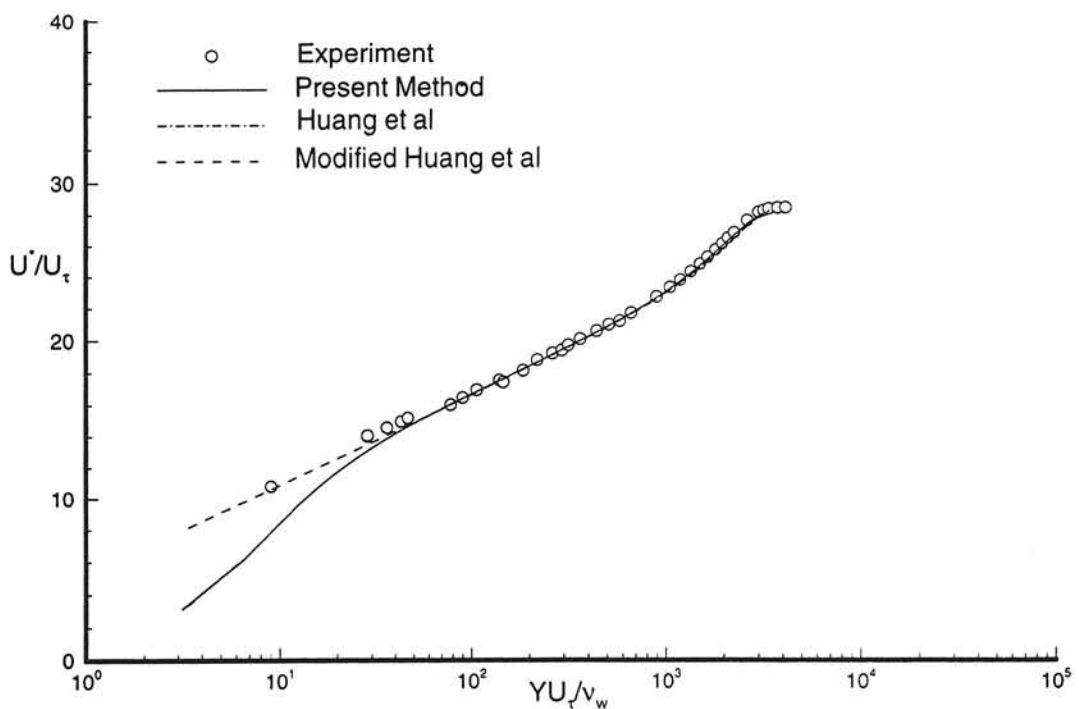


Fig. 32a Transformed velocity profile in semi-logarithmic coordinates. Experimental data from Winter & Gaudet <sup>13</sup>,  $M_\infty = 2.1984$ ,  $Re_0 = 19939$ , profile 39.

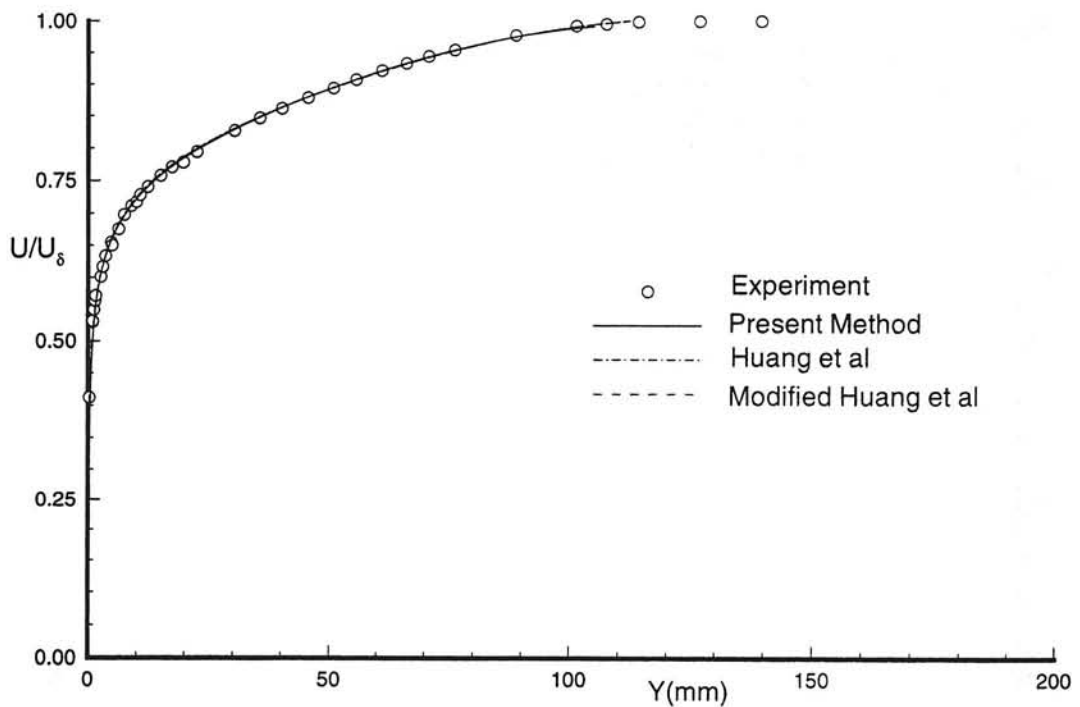


Fig. 32b Untransformed velocity profile in normal coordinates. Experimental data from Winter & Gaudet <sup>13</sup>,  $M_\infty = 2.1984$ ,  $Re_\infty = 19939$ , profile 39.

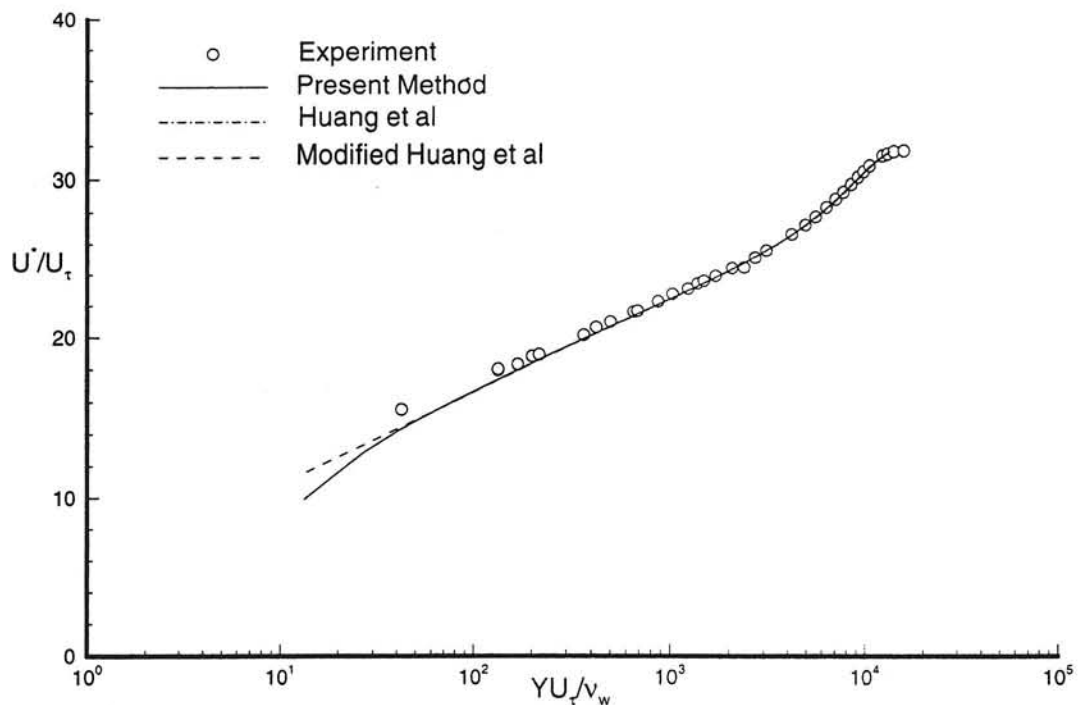


Fig. 33a Transformed velocity profile in semi-logarithmic coordinates. Experimental data from Winter & Gaudet <sup>13</sup>,  $M_\delta = 2.2082$ ,  $Re_\delta = 84259$ , profile 48.

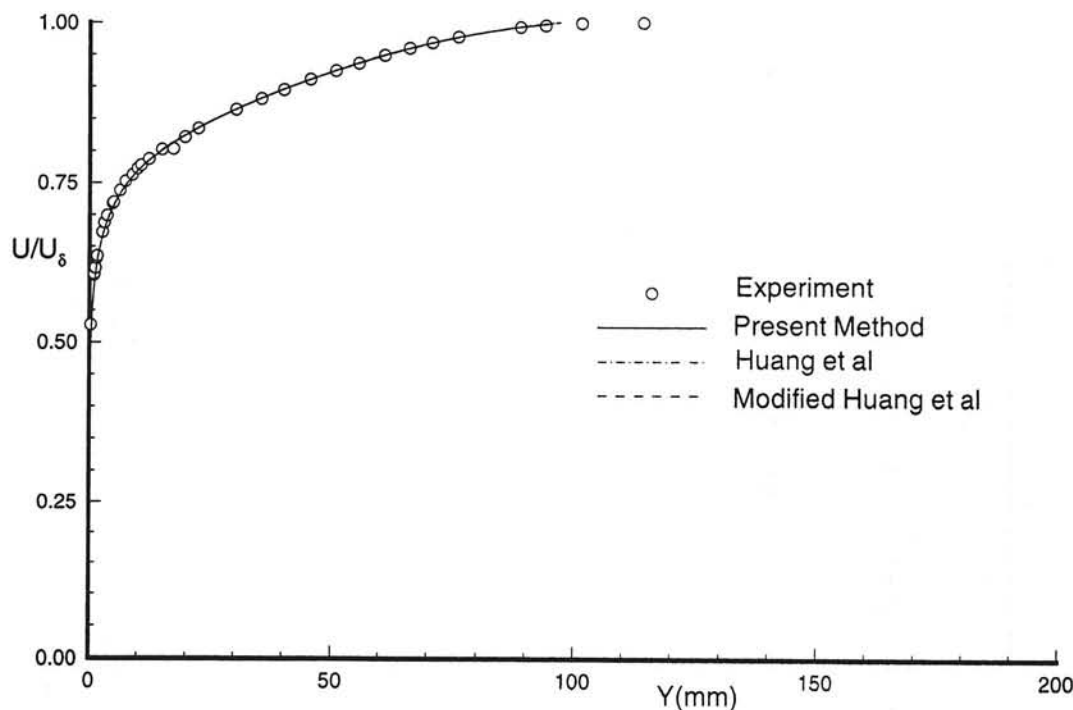


Fig. 33b Untransformed velocity profile in normal coordinates. Experimental data from Winter & Gaudet <sup>13</sup>,  $M_\delta = 2.2082$ ,  $R\delta = 8.1259$ , profile 48.

Fig. 34 Percent error in shape parameter  $\Delta H = (1 - H_{cal}/H_{exp}) \times 100\%$ . Experimental data from Collins et al<sup>15</sup>,  $M_b = 0.59$ .

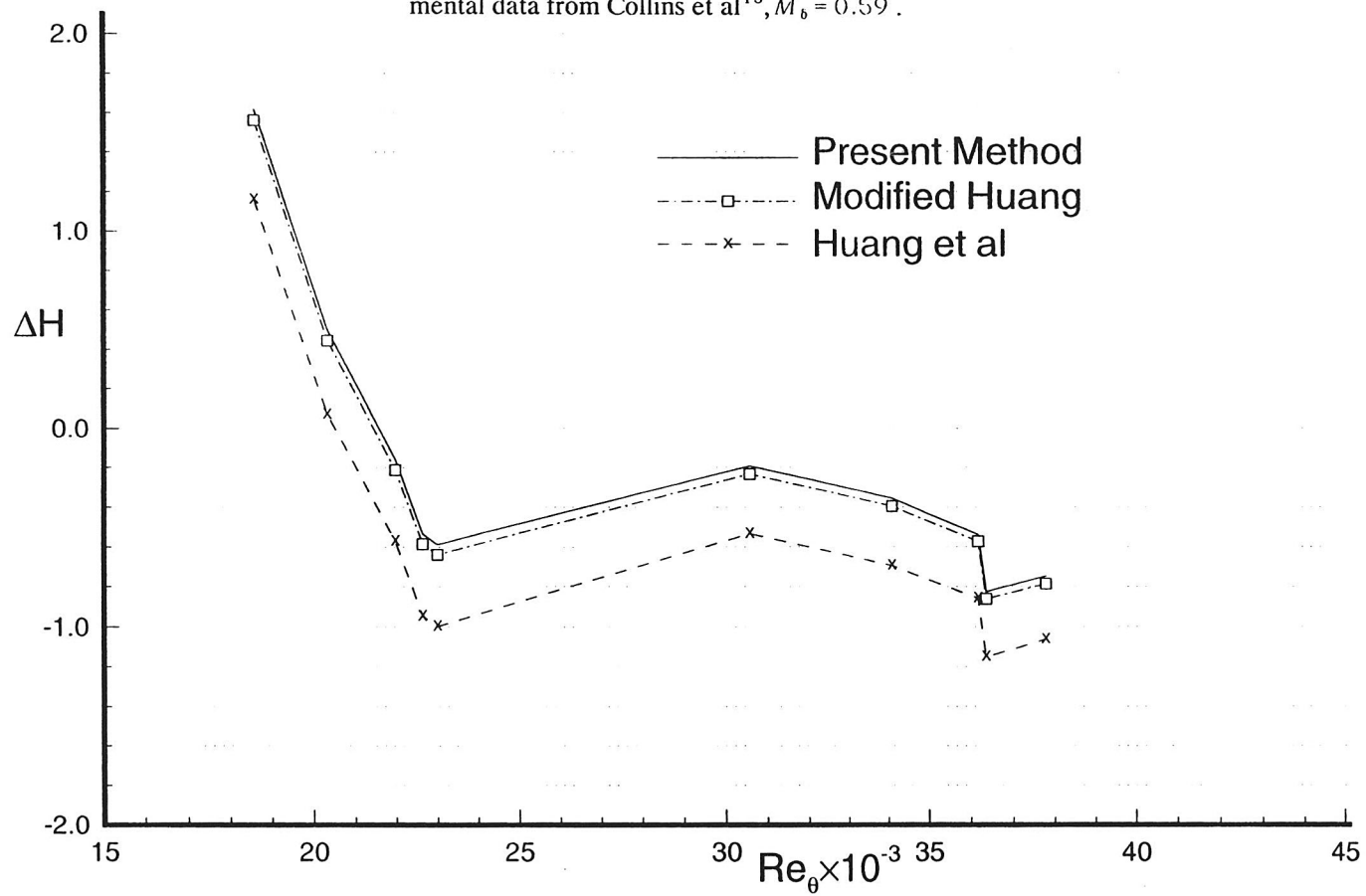


Fig. 35 Percent error in shape parameter  $\Delta H = (1 - H_{cal}/H_{exp}) \times 100\%$ . Experimental data from Collins et al<sup>15</sup>,  $M_b = 0.79$ .

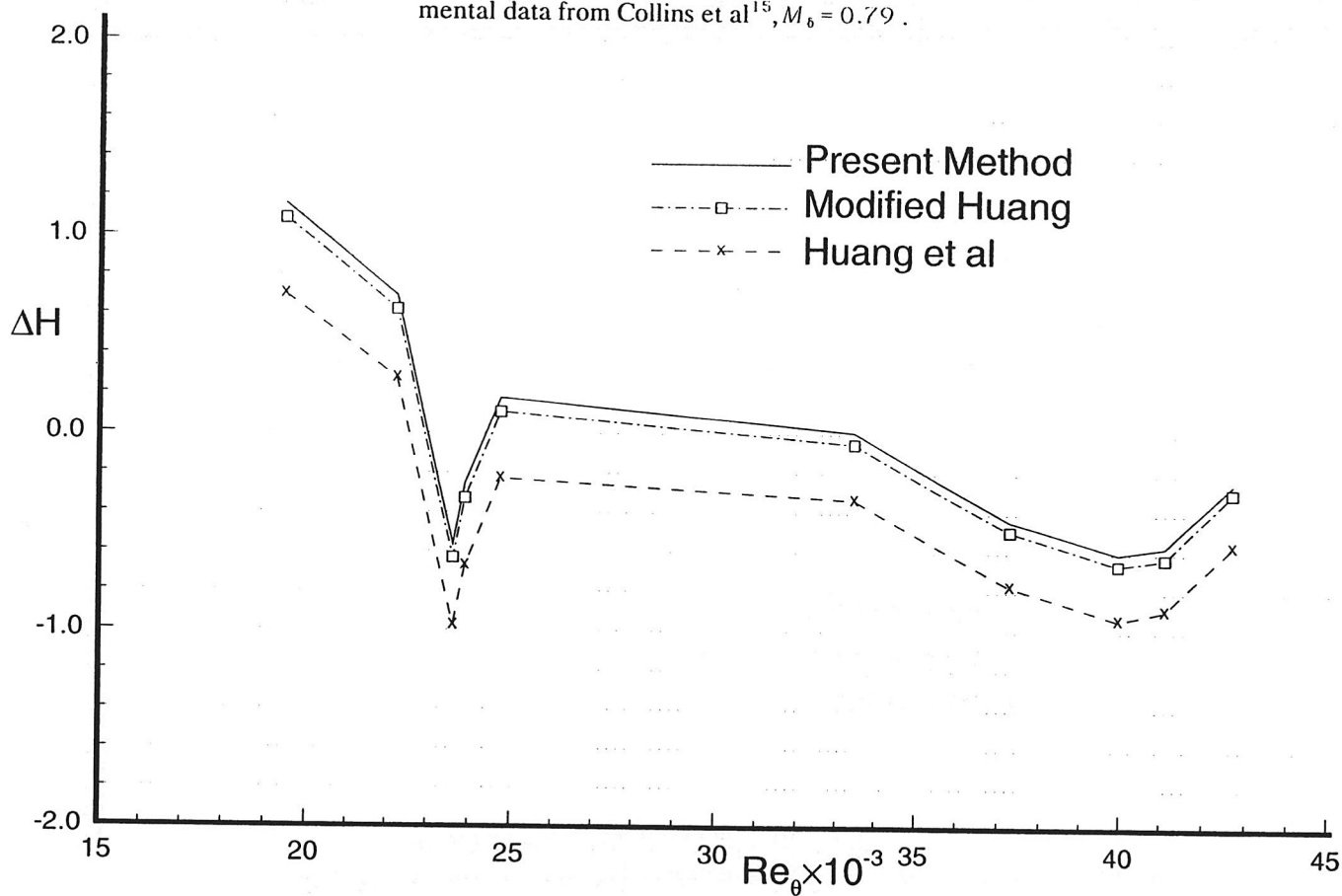


Fig. 36 Percent error in shape parameter  $\Delta H = (1 - H_{\text{cal}}/H_{\text{exp}}) \times 100\%$ . Experimental data from Collins et al<sup>15</sup>,  $M_b = 0.97$ .

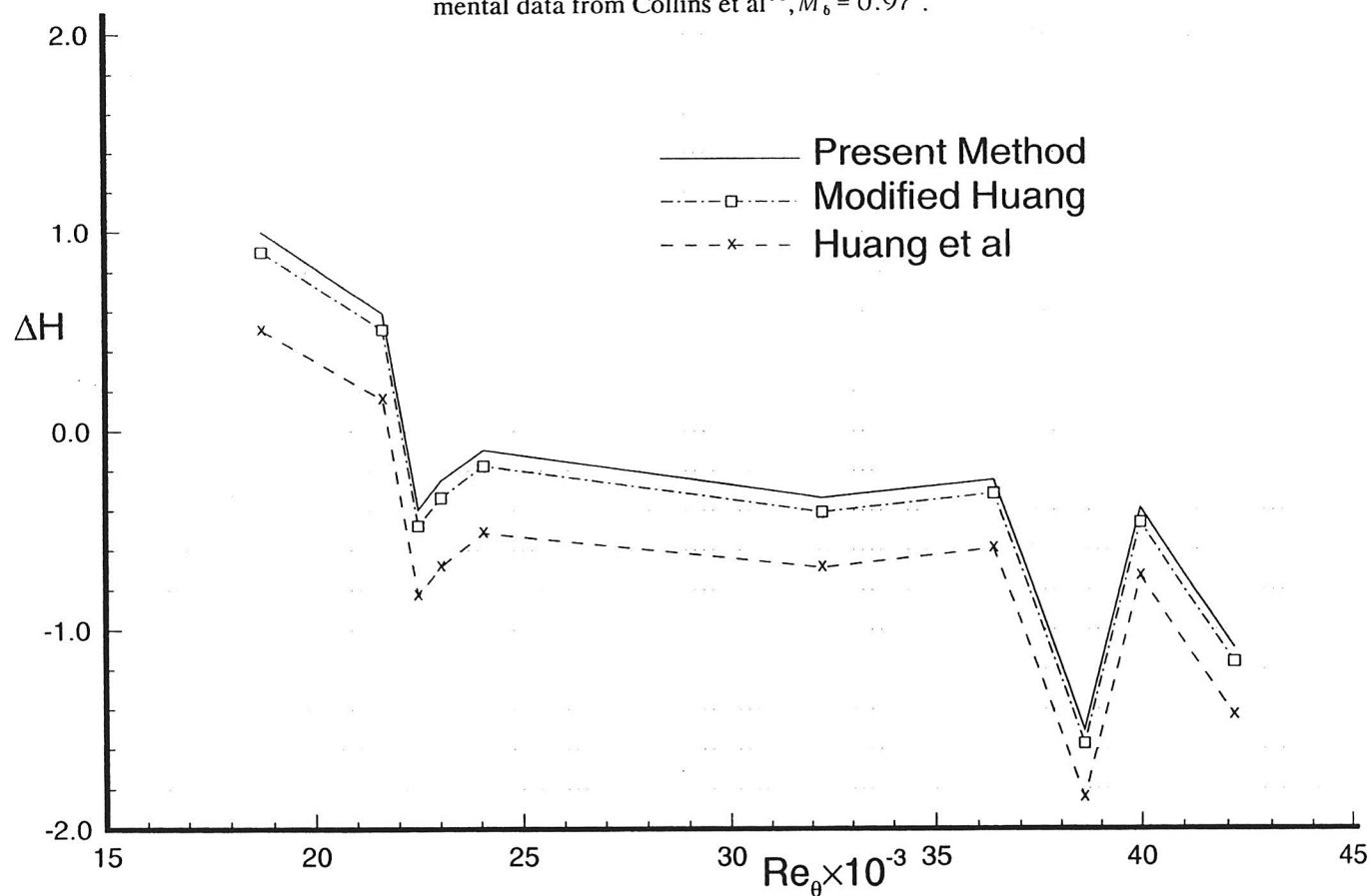


Fig. 37 Percent error in shape parameter  $\Delta H = (1 - H_{cal}/H_{exp}) \times 100\%$ . Experimental data from Winter & Gaudet<sup>13</sup>,  $M_6 = 0.20$ .

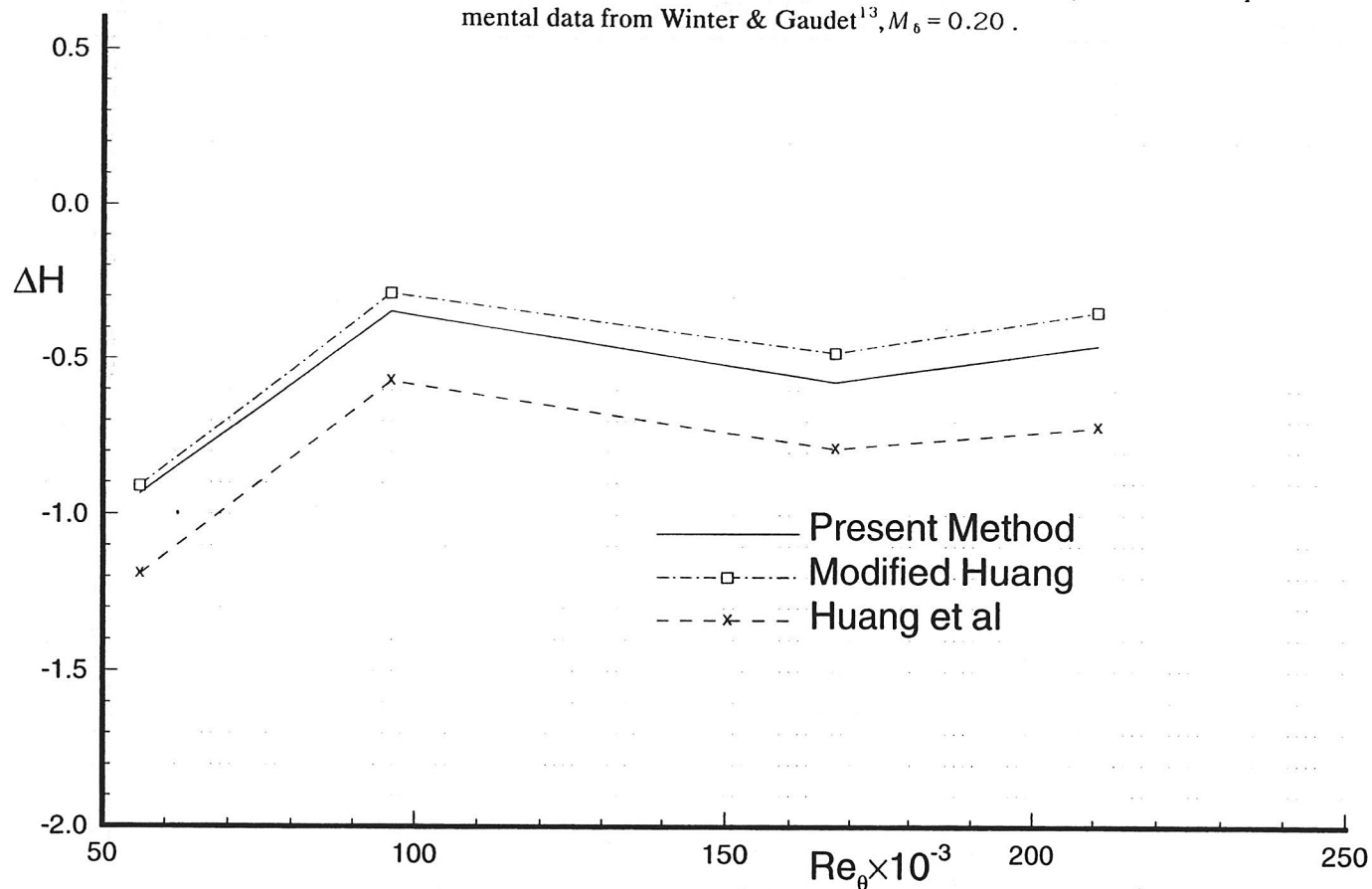


Fig. 38 Percent error in shape parameter  $\Delta H = (1 - H_{cal}/H_{exp}) \times 100\%$ . Experimental data from Winter & Gaudet<sup>13</sup>,  $M_6 = 0.79$ .

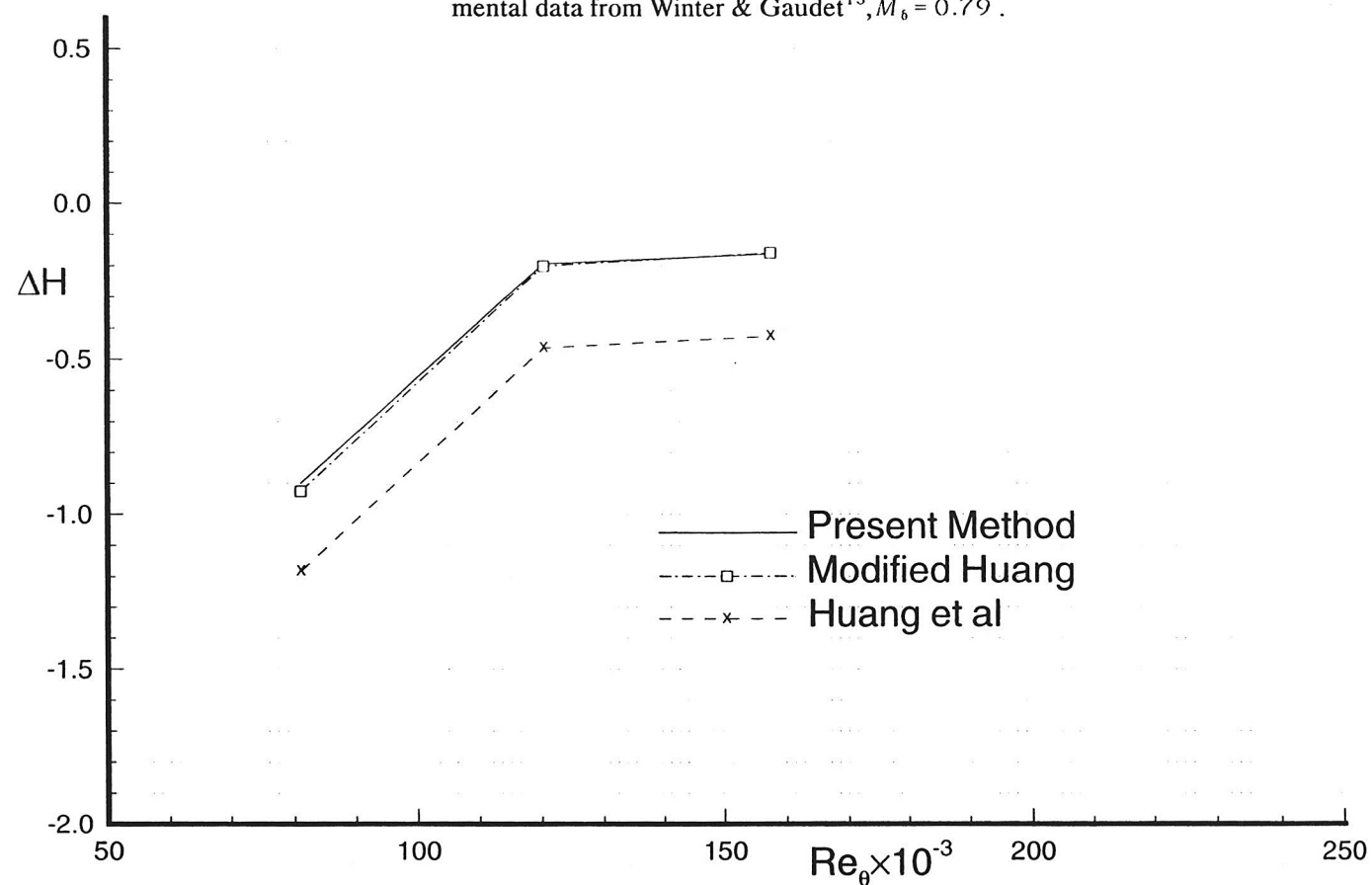


Fig. 39 Percent error in shape parameter  $\Delta H = (1 - H_{cal}/H_{exp}) \times 100\%$ . Experimental data from Gaudet<sup>13</sup>,  $M_\infty = 0.784$ .

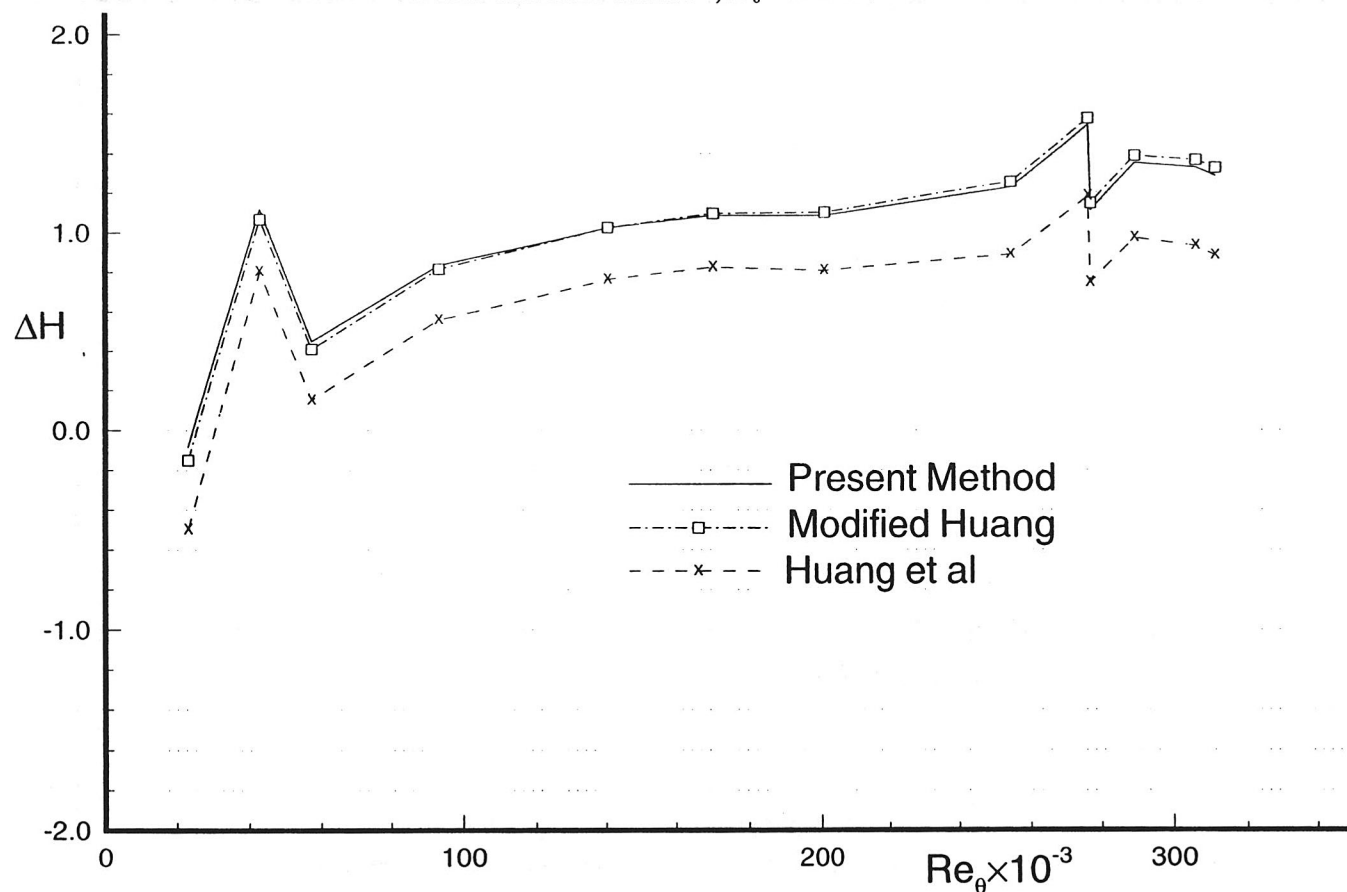


Fig. 40 Percent error in shape parameter  $\Delta H = (1 - H_{cal}/H_{exp}) \times 100\%$ . Experimental data from Collins et al<sup>15</sup>,  $M_\infty = 1.31$ .

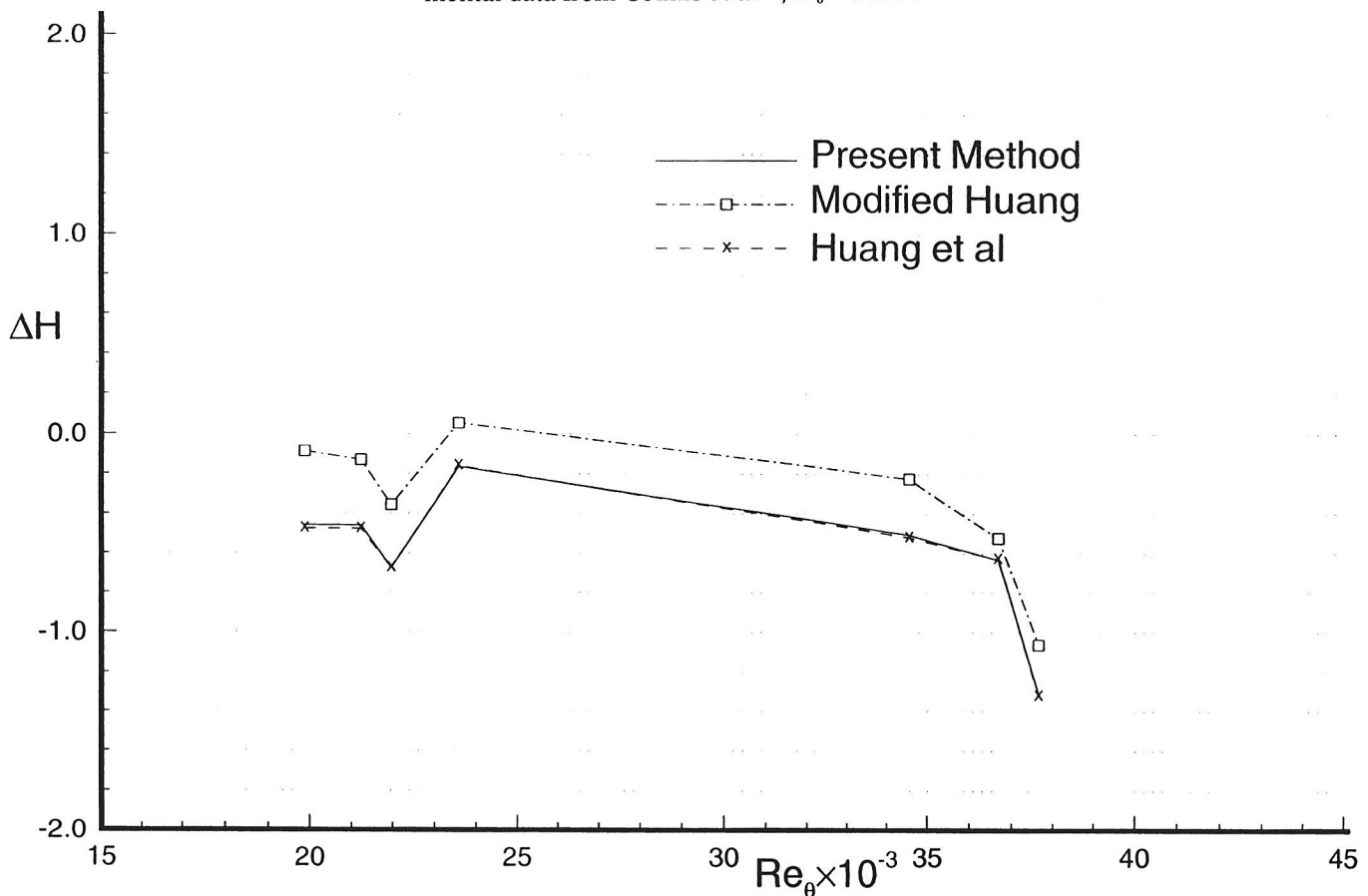


Fig. 41 Percent error in shape parameter  $\Delta H = (1 - H_{cal}/H_{exp}) \times 100\%$ . Experimental data from Collins et al<sup>15</sup>,  $M_\infty = 1.31$ .

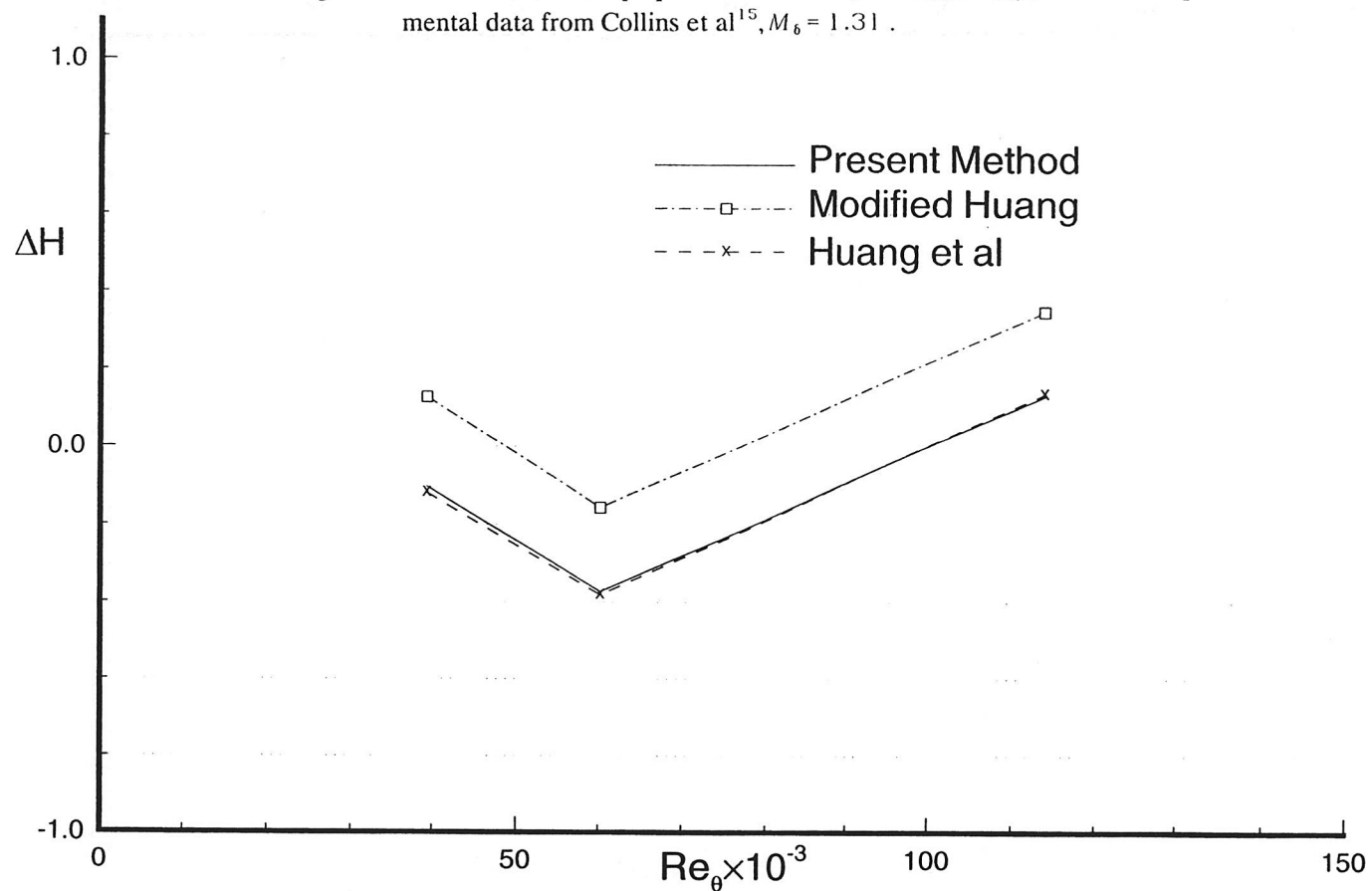


Fig. 42 Percent error in shape parameter  $\Delta H = (1 - H_{cal}/H_{exp}) \times 100\%$ . Experimental data from Winter & Gaudet<sup>13</sup>,  $M_6 = 2.2$ , profiles 18 to 21.

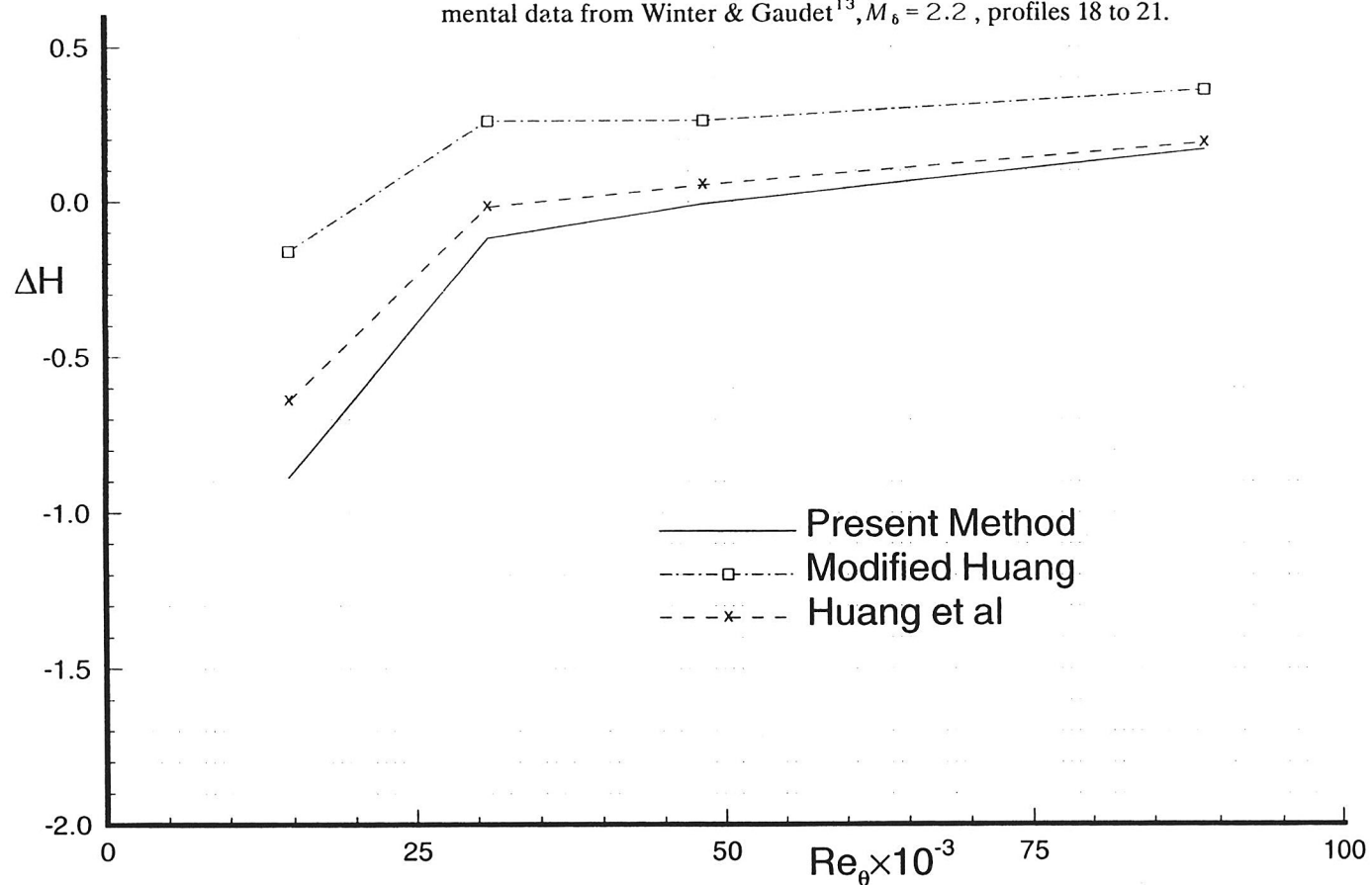


Fig. 43 Percent error in shape parameter  $\Delta H = (1 - H_{cal}/H_{exp}) \times 100\%$ . Experimental data from Winter & Gaudet<sup>13</sup>,  $M_b = 2.2$ , profiles 39 to 48.

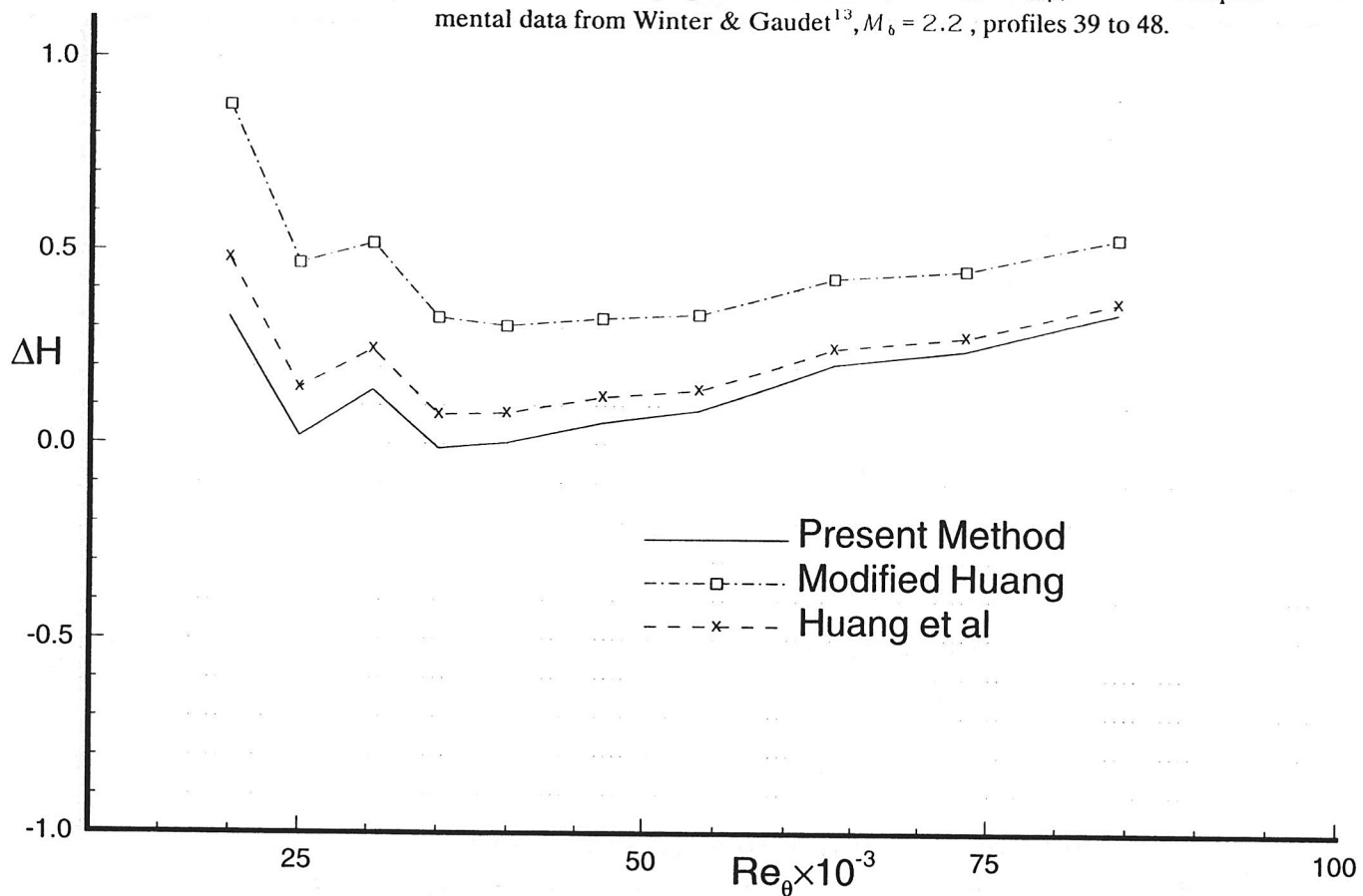
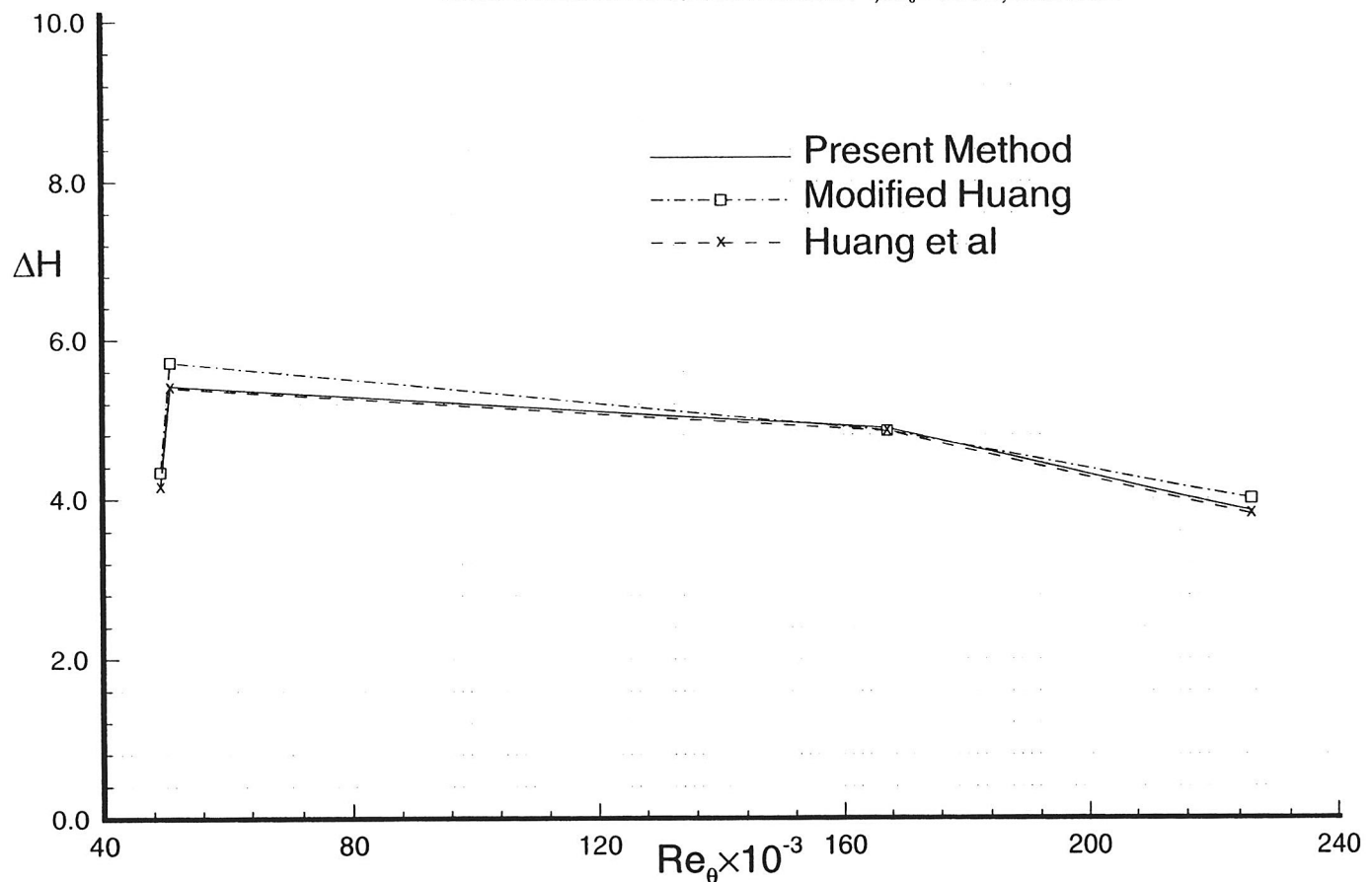


Fig. 44 Percent error in shape parameter  $\Delta H = (1 - H_{cal}/H_{exp}) \times 100\%$ . Experimental data from Moore & Harkness<sup>23</sup>,  $M_\infty = 2.90$ , case 6502.





## **Series 01: Aerodynamics**

01. F. Motallebi, 'Prediction of Mean Flow Data for Adiabatic 2-D Compressible Turbulent Boundary Layers'  
1997 / VI + 90 pages / ISBN 90-407-1564-5
02. P.E. Skåre, 'Flow Measurements for an Afterbody in a Vertical Wind Tunnel'  
1997 / XIV + 98 pages / ISBN 90-407-1565-3
03. B.W. van Oudheusden, 'Investigation of Large-Amplitude 1-DOF Rotational Galloping'  
1998 / IV + 100 pages / ISBN 90-407-1566-1
04. E.M. Houtman / W.J. Bannink / B.H. Timmerman, 'Experimental and Computational Study of a Blunt Cylinder-Flare Model in High Supersonic Flow'  
1998 / VIII + 40 pages / ISBN 90-407-1567-X
05. G.J.D. Zondervan, 'A Review of Propeller Modelling Techniques Based on Euler Methods'  
1998 / IV + 84 pages / ISBN 90-407-1568-8
06. M.J. Tummers / D.M. Passchier, 'Spectral Analysis of Individual Realization LDA Data'  
1998 / VIII + 36 pages / ISBN 90-407-1569-6
07. P.J.J. Moeleker, 'Linear Temporal Stability Analysis'  
1998 / VI + 74 pages / ISBN 90-407-1570-X
08. B.W. van Oudheusden, 'Galloping Behaviour of an Aeroelastic Oscillator with Two Degrees of Freedom'  
1998 / IV + 128 pages / ISBN 90-407-1571-8
09. R. Mayer, 'Orientation on Quantitative IR-thermography in Wall-shear Stress Measurements'  
1998 / XII + 108 pages / ISBN 90-407-1572-6
10. K.J.A. Westin / R.A.W.M. Henkes, 'Prediction of Bypass Transition with Differential Reynolds Stress Models'  
1998 / VI + 78 pages / ISBN 90-407-1573-4
11. J.L.M. Nijholt, 'Design of a Michelson Interferometer for Quantitative Refraction Index Profile Measurements'  
1998 / 60 pages / ISBN 90-407-1574-2
12. R.A.W.M. Henkes / J.L. van Ingen, 'Overview of Stability and Transition in External Aerodynamics'  
1998 / IV + 48 pages / ISBN 90-407-1575-0
13. R.A.W.M. Henkes, 'Overview of Turbulence Models for External Aerodynamics'  
1998 / IV + 40 pages / ISBN 90-407-1576-9

## **Series 02: Flight Mechanics**

01. E. Obert, 'A Method for the Determination of the Effect of Propeller Slip-stream on a Static Longitudinal Stability and Control of Multi-engined Aircraft'  
1997 / IV + 276 pages / ISBN 90-407-1577-7
02. C. Bill / F. van Dalen / A. Rothwell, 'Aircraft Design and Analysis System (ADAS)'  
1997 / X + 222 pages / ISBN 90-407-1578-5
03. E. Torenbeek, 'Optimum Cruise Performance of Subsonic Transport Aircraft'  
1998 / X + 66 pages / ISBN 90-407-1579-3

## **Series 03: Control and Simulation**

01. J.C. Gibson, 'The Definition, Understanding and Design of Aircraft Handling Qualities'  
1997 / X + 162 pages / ISBN 90-407-1580-7
02. E.A. Lomonova, 'A System Look at Electromechanical Actuation for Primary Flight Control'  
1997 / XIV + 110 pages / ISBN 90-407-1581-5
03. C.A.A.M. van der Linden, 'DASMAT-Delft University Aircraft Simulation Model and Analysis Tool. A Matlab/Simulink Environment for Flight Dynamics and Control Analysis'  
1998 / XII + 220 pages / ISBN 90-407-1582-3

## **Series 05: Aerospace Structures and Computational Mechanics**

01. A.J. van Eekelen, 'Review and Selection of Methods for Structural Reliability Analysis'  
1997 / XIV + 50 pages / ISBN 90-407-1583-1
02. M.E. Heerschap, 'User's Manual for the Computer Program Cufus. Quick Design Procedure for a CUT-out in a FUSElage version 1.0'  
1997 / VIII + 144 pages / ISBN 90-407-1584-X
03. C. Wohlever, 'A Preliminary Evaluation of the B2000 Nonlinear Shell Element Q8N.SM'  
1998 / IV + 44 pages / ISBN 90-407-1585-8
04. L. Gunawan, 'Imperfections Measurements of a Perfect Shell with Specially Designed Equipment (UNIVIMP)'  
1998 / VIII + 52 pages / ISBN 90-407-1586-6

## **Series 07: Aerospace Materials**

01. A. Vašek / J. Schijve, 'Residual Strength of Cracked 7075 T6 Al-alloy Sheets under High Loading Rates'  
1997 / VI + 70 pages / ISBN 90-407-1587-4
02. I. Kunes, 'FEM Modelling of Elastoplastic Stress and Strain Field in Centre-cracked Plate'  
1997 / IV + 32 pages / ISBN 90-407-1588-2
03. K. Verolme, 'The Initial Buckling Behavior of Flat and Curved Fiber Metal Laminate Panels'  
1998 / VIII + 60 pages / ISBN 90-407-1589-0
04. P.W.C. Provó Kluit, 'A New Method of Impregnating PEI Sheets for the *In-Situ* Foaming of Sandwiches'  
1998 / IV + 28 pages / ISBN 90-407-1590-4
05. A. Vlot / T. Soerjanto / I. Yeri / J.A. Schelling, 'Residual Thermal Stresses around Bonded Fibre Metal Laminate Repair Patches on an Aircraft Fuselage'  
1998 / IV + 24 pages / ISBN 90-407-1591-2
06. A. Vlot, 'High Strain Rate Tests on Fibre Metal Laminates'  
1998 / IV + 44 pages / ISBN 90-407-1592-0
07. S. Fawaz, 'Application of the Virtual Crack Closure Technique to Calculate Stress Intensity Factors for Through Cracks with an Oblique Elliptical Crack Front'  
1998 / VIII + 56 pages / ISBN 90-407-1593-9
08. J. Schijve, 'Fatigue Specimens for Sheet and Plate Material'  
1998 / VI + 18 pages / ISBN 90-407-1594-7

## **Series 08: Astrodynamics and Satellite Systems**

01. E. Mooij, 'The Motion of a Vehicle in a Planetary Atmosphere'  
1997 / XVI + 156 pages / ISBN 90-407-1595-5
02. G.A. Bartels, 'GPS-Antenna Phase Center Measurements Performed in an Anechoic Chamber'  
1997 / X + 70 pages / ISBN 90-407-1596-3
03. E. Mooij, 'Linear Quadratic Regulator Design for an Unpowered, Winged Re-entry Vehicle'  
1998 / X + 154 pages / ISBN 90-407-1597-1



3021884

This book presents a method for the prediction of mean flow data (i.e. skin friction, velocity profile and shape parameter) for adiabatic two-dimensional compressible turbulent boundary layers at zero pressure gradient. The transformed law of the wall, law of the lake, the van Driest model for the complete inner region and a correlation between the Reynolds number based on the boundary layer integral length scale and the Reynolds number based on the boundary layer momentum thickness were used to predict the mean flow quantities. The results for skin friction coefficient show good agreement with a number of existing theories including the van Driest II and the Huang et al. Comparison with a large number of experimental data suggests that at least for transonic and supersonic flows, the velocity profile as described by van Driest and Coles is Reynolds number dependent and should not be presumed universal. Extra information or perhaps a better physical approach to the formulation of the mean structure of compressible turbulent boundary layers even in zero pressure gradient and adiabatic condition, is required in order to achieve complete (physical and mathematical) convergence when it is applied in any prediction methods.

ISBN 90-407-1564-5



9 799040 715647

